FABRICATION AND EVALUATION OF SUSTAINED RELEASE HYDROGEL BEADS CONTAINING AMOXICILLIN TRIHYDRATE AND ACETAMINOPHEN FOR INFECTIOUS DISEASE

THESIS SUBMITTED IN THE PARTIAL FULFILLMENT OF THE REQUIREMENTS FOR THE DEGREE OF MASTER OF PHARMACY (PHARMACEUTICS)

IN THE FACULTY OF ENGINEERING AND TECHNOLOGY

JADAVPUR UNIVERSITY

BY

ADITI BALA

B. Pharm

Roll. No.: 002211402044

Registration No. 163685 of 2022-23

UNDER THE GUIDANCE OF

Dr. SANCHITA MANDAL

ASSISTANT PROFESSOR

DEPARTMENT OF PHARMACEUTICAL TECHNOLOGY

FACULTY OF ENGINEERING AND TECHNOLOGY

JADAVPUR UNIVERSITY

KOLKATA-700032

2024

CERTIFICATE OF APPROVAL

This is to certify that Ms. ADITI BALA (Class Roll No: 002211402044, and Registration No: 163685 of 2022-23) has carried out the research work on the subject entitled "FABRICATION AND EVALUATION OF SUSTAINED RELEASE HYDROGEL BEADS CONTAINING AMOXICILLIN TRIHYDRATE AND ACETAMINOPHEN FOR INFECTIOUS DISEASE" independently with proper care and attention under my supervision and guidance in the Pharmaceutics Research Laboratory in the Department of Pharmaceutical Technology, Jadavpur University. She has incorporated her findings into this thesis of the same title being submitted by her, in partial fulfilment of the requirements for the degree of Master of Pharmacy from Jadavpur University. I appreciate her endeavour to complete the project and her work has reached my gratification.

28/8/2024

Dr. Sanchita Mandal

Assistant Professor

Department of Pharmaceutical Technology

Jadavpur University

Assistant Professor
Dept. of Pharmaceutical Technology
Jadavpur University
Kolkata - 700 032, W.B. India

28/8/24

Prof. (Dr.) Amalesh Samanta

Head of the Department

Department of Pharmaceutical Technology

Jadavpur University

Head
Dept. of Pharmaceutical Technology
Jadavpur University
Kolkata - 700 032, W.B. India

Dipak Laha 28.8.24

Prof. Dipak Laha

Dean

Faculty of Engineering and Technology

Jadavpur University

DEAN
Faculty of Engineering & Technology
JADAVPUR UNIVERSITY

DECLARATION OF ORIGINALITY AND COMPLIANCE OF ACADEMIC ETHICS

I hereby declare that this thesis contains a literature survey and original research work by the undersigned candidate as part of her Master of Pharmaceutical Technology studies. All information in this document has been obtained and presented in accordance with academic rules and ethical conduct. I also declare that, as required by these rules and conduct, I have fully cited and referenced all materials and the results are original to this work.

Name: **Aditi Bala**

Roll no: **002211402044**

Registration number: **163685 of 2022-23**

Thesis Title: **Fabrication and evaluation of sustained release hydrogel beads containing Amoxicillin trihydrate and Acetaminophen for infectious disease**

Aditi Bala 28/08/2024

Signature with date

ACKNOWLEDGEMENT

I deem it a pleasure and privilege to work under the guidance of Dr. Sanchita Mandal, Assistant Professor, Department of Pharmaceutical Technology, Jadavpur University for her valuable guidance, encouragement, affection, inspiration and immense support throughout the work. Her valuable advice which is of paramount importance and help shall be responsible for the successful completion of this work.

I am thankful to the authority of Jadavpur University and the Head of the Department Prof. Dr. Amalesh Samanta for providing all the facilities to carry out this work. I would convey my regards and acknowledge to Instrument Room of Department of Pharmaceutical Technology, Departmental library of Pharmaceutical Technology, Department of Metallurgical Engineering, Jadavpur University, Kolkata, Eminent College of Pharmaceutical Technology for their assistance in providing me instrument facilities for the purpose of my research work.

I convey my regards and heartfelt thanks to my lab-mate Mr. Rahul Molla, my batchmates Ms. Pallabita Rakshit, Mr. Snehaneel Mitra, Mr. Sagar Roy, my respected seniors in the laboratory with special mention to Ms. Ushasi Das, Ms. Pallobi Dutta, Mr. Arnab Sarkar, Mr. Akash de, Ms. Ajeya Samanta and Mr. Pankaj Paul, and my dear juniors Ms. Shila Barman, Mr. Arindam Sarkar for their help and co-operation which made my work successful.

Last but not the least, I would like to express my gratitude towards my father Mr. Arun Kumar Bala, my mother Mrs. Dipa Bala for their kind co-operation and encouragement which has helped me in every step of my academic career.

Date:

Place: Jadavpur University

Department of Pharmaceutical Technology

Kolkata -700032.

Aditi Bala

Aditi Bala

Dedicated to my Parents

CONTENTS

Chapter 5-

[1] A. Bala, R. Molla, S. Panja, and S. Mandal, "A Review on Applications of Biosynthesised Silver Nanoparticles A Review on Applications of Biosynthesized Silver Nanoparticles INTRODUCTION- BIOSYNTHESIS OF SILVER NANOPARTICLES-," vol. 10, no. 7, pp. 1136–1147, 2023.

[2] R. Molla, A. Bala, G. Baidya, and S. Mandal, "A Detailed Discussion on Mucoadhesive Drug Delivery System," vol. 12, no. 5, pp. 30–40, 2023, doi: 10.35629/6718-12053040.

[3] U. Das, A. Bala, R. Molla, and S. Mandal, "Nanomedicine in infectious disease challenges and regulatory concerns," *Nanostructured Drug Deliv. Syst. Infect. Dis. Treat.*, pp. 237–259, Jan. 2024, doi: 10.1016/B978-0-443-13337-4.00012-4.

CHAPTER 1

INTRODUCTION

1. INTRODUCTION

Over the last few decades, advancements in novel drug delivery systems and polymer technology have revolutionized the pharmaceutical landscape. Centre of these advancements is the development of polymer technology, which has enabled the creation of sophisticated delivery mechanisms capable of controlled and targeted drug release. Polymers, with their versatile chemical properties, have played a crucial role in enhancing the efficacy, safety, and patient compliance of drug therapies. Polymers have been engineered to respond to various physiological stimuli, such as pH, temperature, or enzymes, allowing for precise delivery to specific sites within the body, thereby reducing side effects and improving patient compliance. Innovations like biodegradable polymers, nanoparticles, and hydrogels have further expanded the possibilities of drug delivery, offering platforms that can carry complex molecules, including proteins and nucleic acids, with high stability and bioavailability. These technologies have opened new avenues for the treatment of chronic diseases, cancer, and other conditions that require sustained or localized drug action, marking a significant leap forward in the capabilities of modern medicine [1].

1.1.Polymers-

Polymers, also known as macromolecules, are very large molecules consisting of many repeating units and are formed by a process called polymerization, which links together small molecules known as monomers [2]. The monomers can be linked together in various ways to give rise to linear polymers, branched polymers or crosslinked polymers etc. They are essential in various fields like plastics, rubber, fibres, and more. Due to their broad spectrum of properties, both synthetic and natural polymers play essential and ubiquitous roles in everyday life. Each type of polymer has its own unique properties and applications, making them indispensable in modern industries and everyday life. Polymers are large molecules composed of repeating structural units called monomers. They are classified into various types based on their structure, composition, and properties. Here are some common types of polymers [3]:

1.1.1. Classification of polymers by Structure:

1.1.1.1. Linear Polymers:

A linear polymer is made up of monomer units that are arranged in a long straight chain (fig-1). This type of polymer has no branching or cross linking. The long chains are typically held together by the weaker van der Waals or hydrogen bonding. Since these bonding types are relatively easy to break with heat, linear polymers are typically thermoplastic. Heat breaks the bonds between the long chains allowing the chains to flow past each other, allowing the material to be remoulded. Upon cooling the bonds between the long chains reform, i.e., the polymer hardens. Example- polyethylene, polypropylene, polyvinyl chloride [4].

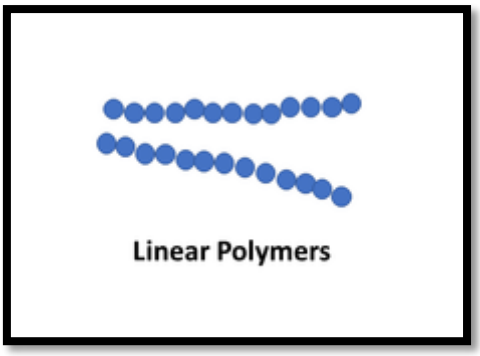

Fig 1- Linear polymers

1.1.1.2. Branched Polymers or Side chain polymers:

These polymers have monomer units attached to the main chain or backbone via side chains (fig-2). The side chains can affect the physical and chemical properties of the polymers. Since these shorter chains can interfere with efficient packing of the polymers, branched polymers tend to be less dense than similar linear polymers. The short chains do not bridge from one longer backbone to another, heat will typically break the bonds between the branched polymer chains and allow the polymer to be a thermoplastic, although there are some very complex branched polymers that resist this 'melting' and thus break up (becoming hard in the process) before softening, i.e., they are thermosetting. Example- polystyrene [5].

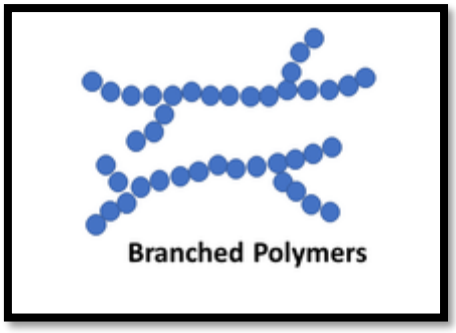

Fig 2- Branched polymers

1.1.1.3. Cross-linked Polymers:

In crosslinked polymer the individual polymer chains which have covalent bonds between polymer chains, forming a three-dimensional network structure (fig-3). This structure is typically achieved through the use of crosslinking agents which react with the polymer chains to form covalent bonds between them. These polymers are often used in applications where rigidity and toughness are required, such as in car tires and shoe soles. These types of polymers resemble ladders. The chains link from one backbone to another. So, unlike linear polymers which are held together by weaker van der Waals forces, crosslinked polymers are tied together via covalent bonding. This much stronger bond makes most crosslinked polymers thermosetting, with only a few exceptions to the rule: crosslinked

polymers that happen to break their crosslinks at relatively low temperatures. Example- Vulcanized rubber [6].

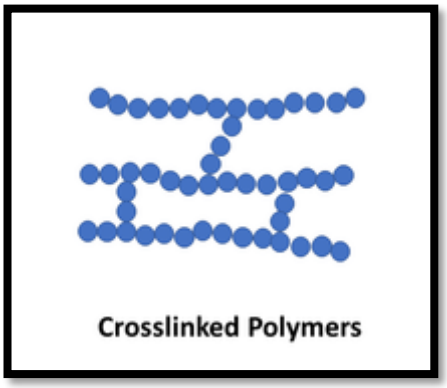

Fig 3- Crosslinked polymers

1.1.1.4. Network Polymers:

Network polymers are similar to crosslinked polymer but the individual polymer chains are more highly crosslinked, resulting in a more tightly connected network (fig-4). The structure can give rise to materials with unique properties such as elasticity, resilience and high strength. These polymers are nearly impossible to soften when heating without degrading the underlying polymer structure and are thus thermosetting polymers. Example- silicone rubber [7].

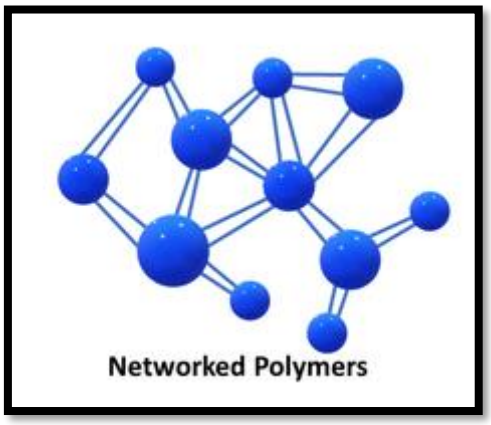

Fig 4- Networked polymers

1.1.2. <u>Classification of polymers by Composition</u>:

1.1.2.1. Homopolymers: Consist of a single type of monomer repeating along the chain (fig-5) [8].

1.1.2.2. Copolymers: Contain two or more different types of monomers in the polymer chain. There are 4 types of copolymers- Random, Alternating, Block, Graft (fig-6) [9].

- **Random Copolymers**: Monomers are randomly distributed along the chain.
- **Alternating polymer:** Monomers are distributer alternatively in a pattern.
- **Block Copolymers**: Monomers are grouped into blocks of repeating units.
- **Graft Copolymers**: Contain a main chain with side chains of different monomers.

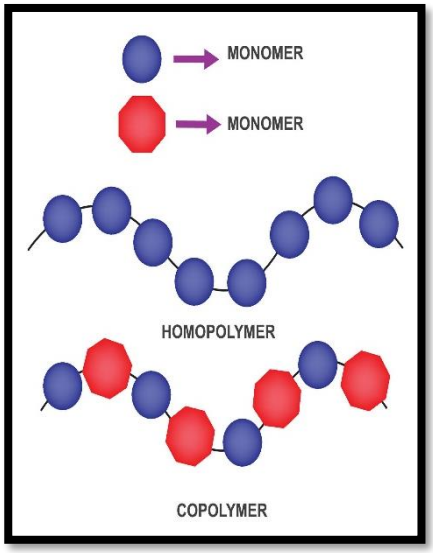

Fig 5- Homopolymer & Copolymer

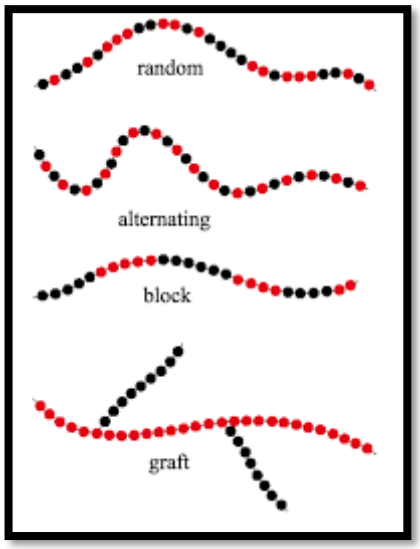

Fig 6- Classification of copolymers

1.1.3. Classification by Polymerization Mechanism:

1.1.3.1. Addition Polymers: An addition polymer is a polymer that forms when monomer units with carbon-carbon double bonds link together in a simple reaction, without creating other products. This process is also known as chain-growth polymerization (fig-7). Example- polyethylene [10].

1.1.3.2. Condensation Polymers: macromolecules that are formed when two or more monomers undergo a polymerization process that involves a condensation reaction. This process removes a molecule, usually water, but it can also be ammonia, hydrogen, or hydrogen cyanide. Condensation polymers are also known as step-growth polymers (fig-7). Example- nylon [11].

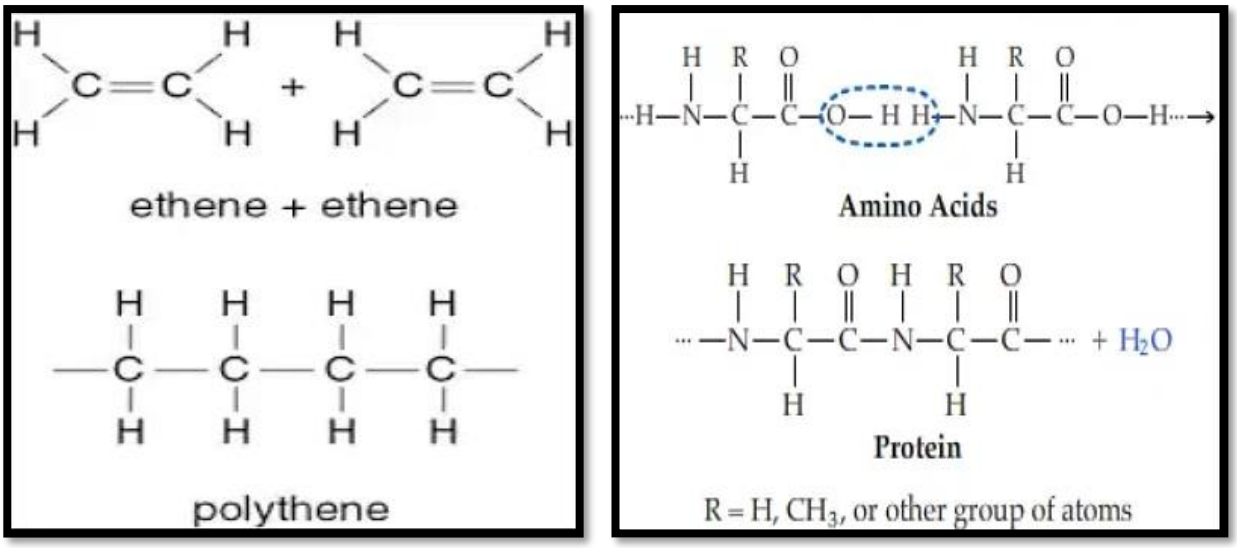

Fig 7- Addition polymer and Condensation polymer

1.1.4. Classification of polymers by Physical Properties:

1.1.4.1. Thermoplastics:

These are polymers that can be melted and reshaped multiple times without undergoing chemical degradation. The crosslinking bonds are reversible in this case (fig-8). Examples include polyethylene, polypropylene, and polystyrene. They're commonly used in packaging, bottles, and toys [12].

1.1.4.2. Thermosets:

These polymers undergo a chemical reaction during curing, irreversibly (crosslinked) hardening into a rigid structure. Once set, they cannot be melted and reshaped (fig-8). Examples include epoxy resins, phenolic resins, and silicone rubber. They're used in adhesives, coatings, and electrical insulation [12].

1.1.4.3. Elastomers:

Polymers that possess elastic properties, returning to their original shape after deformation, like rubber. Also known as rubber, elastomers are polymers with elastic properties. They can be stretched and return to their original shape when the force is removed (fig-8). Examples include natural rubber, synthetic rubber (like neoprene and silicone rubber), and elastomeric fibres like spandex [12], [13].

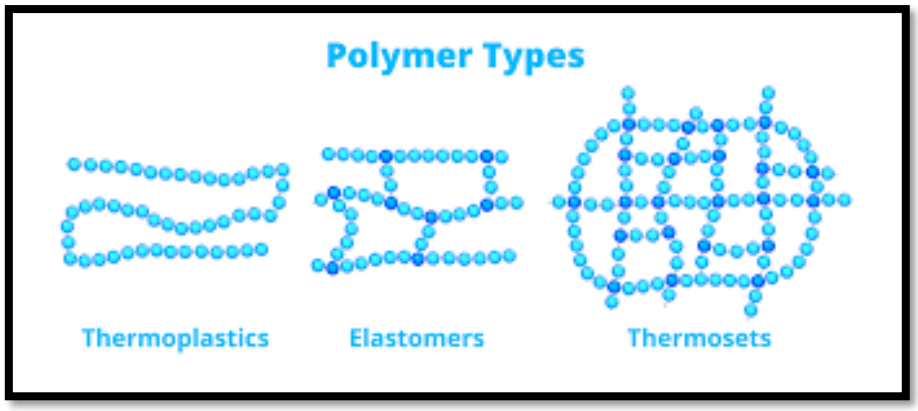

Fig 8- Classification of polymers by Physical Properties

1.1.5. Classification of polymers by Applications:

Each type of polymer has unique properties that make it suitable for various applications, from everyday consumer products to advanced industrial materials.

1.1.5.1. Thermoplastics: A thermoplastic, or thermos-softening plastic, is any plastic polymer material that becomes pliable or mouldable at a certain elevated temperature and solidifies upon cooling. Most thermoplastics have a high molecular weight [12].

1.1.5.2. Thermosetting Polymers: In materials science, a thermosetting polymer, often called a thermoset, is a polymer that is obtained by irreversibly hardening ("curing") a soft solid or viscous liquid prepolymer (resin). Curing is induced by heat or suitable radiation and may be promoted by high pressure or mixing with a catalyst [12].

1.1.5.3. Elastomers: these are rubbery material composed of long chainlike molecules, or polymers, that are capable of recovering their original shape after being stretched to great extents—hence the name *elastomer*, from "elastic polymer." Under normal conditions the long molecules making up an elastomeric material are irregularly coiled. With the application of force, however, the molecules straighten out in the direction in which they are being pulled. Upon release, the molecules spontaneously return to their normal compact, random arrangement [12], [13].

1.1.5.4. Biopolymers: These are polymers derived from renewable natural sources like plants and animals, or produced by microorganisms. Examples include cellulose, starch, proteins, and DNA. Biopolymers are gaining importance due to their biodegradability and sustainability [14].

1.1.5.5. Synthetic Polymers: These are man-made polymers produced through chemical synthesis. They include a wide range of materials such as polyethylene terephthalate (PET), polyvinyl chloride (PVC), nylon, and polycarbonate. Synthetic polymers are used extensively in everyday products due to their versatility and cost-effectiveness [15], [16].

1.1.5.6. Conductive Polymers: These polymers possess electrical conductivity. They have applications in electronics, such as organic light-emitting diodes (OLEDs), organic photovoltaic cells (OPVs), and sensors. Examples include polyaniline, poly-pyrrole, and polyacetylene [17].

1.1.5.7. Composite Polymers: These are polymers combined with other materials to enhance certain properties. For example, fiberglass consists of glass fibres embedded in a polymer matrix. Carbon fibre-reinforced polymers (CFRP) combine carbon fibres with a polymer resin, providing high strength and low weight [18].

1.1.6. Miscellaneous classification:

1.1.6.1. Natural Polymers: Occur in nature and include proteins (like silk and wool), cellulose, pectin, starch, chitin and rubber [19].

1.1.6.2. Synthetic Polymers: Man-made polymers like polyethylene, PVC, polyesters, polyamide and nylon.

1.1.6.3. Biodegradable Polymers: Designed to degrade through natural processes, reducing environmental impact.

1.2. Natural polymers:

These are large molecules composed of repeating structural units derived from natural sources. These polymers occur in living organisms and can be found in plants, animals, and microorganisms [19]. Some common examples of natural polymers include [20]:

1.2.1. Proteins: Proteins are one of the most abundant natural polymers found in living organisms. They are composed of amino acid monomers linked together by peptide bonds. Proteins serve various functions in organisms, such as enzymes, structural components, and hormones.

1.2.2. Polysaccharides: Polysaccharides are complex carbohydrates composed of monosaccharide units linked together by glycosidic bonds. Examples include cellulose, starch, glycogen, and chitin. These polymers serve as energy storage molecules (like starch and glycogen) and structural components (like cellulose and chitin) in plants and animals.

1.2.3. Nucleic Acids: Nucleic acids, including DNA (deoxyribonucleic acid) and RNA (ribonucleic acid), are natural polymers that store and transmit genetic information in living organisms. They are composed of nucleotide monomers linked together by phosphodiester bonds.

1.2.4. Rubber: Natural rubber is a polymer of isoprene units, which are derived from the latex sap of certain plants, such as the rubber tree (Hevea brasiliensis). It is known for its elasticity and is widely used in various applications, including tires, adhesives, and industrial components.

1.2.5. Silk: Silk is a natural protein fiber produced by certain insect larvae, such as silkworms. It is composed mainly of fibroin proteins, which form strong and

resilient threads. Silk has been used for centuries in textiles and is valued for its lustrous appearance and smooth texture.

Natural polymers have diverse properties and applications, making them essential components of various biological and industrial processes. Additionally, they often exhibit biocompatibility and biodegradability, making them attractive for use in biomedical and environmentally friendly materials. Natural polymers, derived from plants, animals, and microorganisms, have a wide range of applications due to their biocompatibility, biodegradability, and non-toxic nature [21], [22].

1.3. Types of Natural Polymers and Their Uses:

Some common and most utilized natural polymers and their uses are [20], [23]-

1.3.1. Cellulose- Source of cellulose are plants. Its main applications are-

- **Paper and Textiles**: Used in the production of paper, cardboard, and fabrics such as cotton and linen.
- **Food Industry**: Used as a thickener, stabilizer, and emulsifier in foods.
- **Pharmaceuticals:** Used as an excipient in tablet formulations and as a film-forming agent.
- **Bioplastics**: Used in the production of biodegradable plastics.

1.3.2. Starch- Corn, potato, wheat plants are excellent sources of starch. Starch is used in-

- **Food Industry**: Used as a thickening agent, stabilizer, and sweetener.
- **Biodegradable Plastics**: Used to produce compostable packaging materials.
- **Pharmaceuticals**: Used as a binder and disintegrant in tablets.
- **Textiles**: Used in fabric finishing and as a sizing agent.

1.3.3. Chitosan- Chitosan is obtained from shellfishes like- shrimp, crab and lobster. It is mainly used in-

- **Biomedicine**: Used for wound dressings, drug delivery systems, and tissue engineering.
- **Pharmaceuticals:** Used as a coating material, forms polyelectrolyte complexes etc.
- **Water Treatment**: Used for removing heavy metals and other contaminants from water.
- **Agriculture**: Used as a natural pesticide and plant growth enhancer.
- **Food Industry**: Used as a preservative and as a dietary supplement.

1.3.4. Alginate- Alginate is extracted from brown sea algae or seaweed such as *Laminaria hyperborea, Laminaria digitata,* and *Macrocystis pyrifera.* Alginate is used in-

- **Food Industry**: Used as a gelling agent, thickener, and stabilizer in products like ice cream, jelly, and sauces.
- **Biomedicine**: Used in wound dressings, drug delivery systems, and tissue engineering scaffolds.

- **Textiles**: Used in printing processes and as a dye thickener.
- **Pharmaceuticals**: Used as a tablet binder and disintegrant. Used in the preparation of hydrogels.

1.3.5. Gelatin- Gelatin is a flavourless, colourless, jelly-like substance made from the collagen of animal bones, cartilage, and skin. The primary sources of gelatin are pig and bovine skins, demineralized hooves, and bones. Gelatin is used as-

- **Food Industry**: Used as a gelling agent in products like jelly, marshmallows, and gummy candies.
- **Pharmaceuticals**: Used in capsule production, as a stabilizer for vaccines, and in tablet formulations.
- **Biomedicine**: Used for wound dressings, tissue engineering, and drug delivery systems.
- **Photography**: Used in photographic films and papers.

1.3.6. Collagen- collagen is sourced from animal connective tissues like skin, bone, tendons. It is gel like product. Its main uses are-

- **Biomedicine**: Used for wound dressings, tissue engineering, and as a biomaterial for implants.
- **Cosmetics**: Used in anti-aging creams, lotions, and other skin care products.
- **Food Industry**: Used in products like gelatin, sausages, and dietary supplements [24].

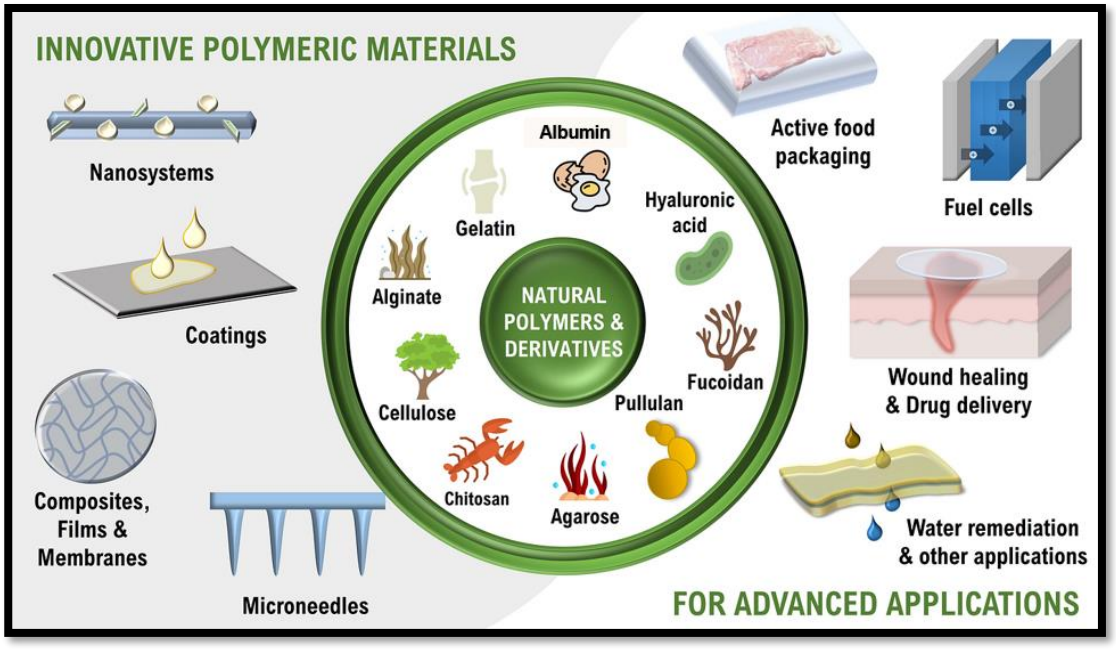

Fig 9- Applications of natural polymers

1.4. Polysaccharides:

Polysaccharides are large, complex carbohydrates composed of long chains of monosaccharide units linked together by glycosidic bonds. These molecules serve crucial roles in both energy storage and structural integrity across various organisms. For instance, starch and glycogen are storage polysaccharides in plants and animals, respectively, providing a reservoir of glucose that can be readily mobilized for energy. In contrast, structural polysaccharides like cellulose in plants and chitin in the exoskeletons of arthropods offer rigidity and protection. The diverse functions of polysaccharides highlight their importance in biological systems, where they contribute to processes ranging from metabolism to maintaining the physical integrity of cells and tissues. [25], [26], [27]. These are a few common examples of polysaccharides:

1.4.1. **Cellulose**: Cellulose is one of the most abundant organic compounds on Earth and is the main component of plant cell walls. It provides structural support to plant cells and is composed of repeating glucose units linked by β-1,4-glycosidic bonds.

1.4.2. **Starch**: Starch is the primary carbohydrate storage molecule in plants, found in seeds, tubers, and roots. It consists of two polysaccharide components: amylose and amylopectin. Amylose is a linear chain of glucose molecules linked by α-1,4-glycosidic bonds, while amylopectin is branched with occasional α-1,6-glycosidic bonds.

1.4.3. **Alginate**: Alginate is a naturally occurring anionic polymer typically obtained from brown seaweed, and has been extensively investigated and used for many biomedical applications, due to its biocompatibility, low toxicity, relatively low cost, and mild gelation by addition of divalent cations such as Ca^{2+}

1.4.4. **Glycogen**: Glycogen is the main carbohydrate storage molecule in animals, primarily stored in the liver and muscles. It is structurally similar to amylopectin but more highly branched, allowing for rapid mobilization of glucose when energy is needed.

1.4.5. **Chitin**: Chitin is a structural polysaccharide found in the exoskeletons of arthropods (such as insects and crustaceans) and the cell walls of fungi. It is composed of N-acetylglucosamine units linked by β-1,4-glycosidic bonds and provides rigidity and protection to these organisms.

1.4.6. **Hyaluronic Acid**: Hyaluronic acid is a polysaccharide found in connective tissues, such as skin and cartilage, as well as in the synovial fluid of joints. It consists of repeating units of glucuronic acid and N-acetylglucosamine linked by β-1,3 and β-1,4 glycosidic bonds and plays a role in lubrication and hydration.

1.4.7. **Pectin**: Pectin is a polysaccharide found in the cell walls of plants, particularly in fruits. It helps to regulate the firmness of plant tissues and is used as a gelling agent in food processing, especially in the production of jams and jellies.

1.5. Sodium alginate:

Sodium alginate is a natural polysaccharide extracted from brown seaweed, such as species of kelp and algae (Phacophycae). It is composed of long chains of alternating residues of guluronic acid and mannuronic acid, linked by 1-4 glycosidic bonds. Sodium alginate is commonly used in various industries due to its unique properties, including its ability to form gels in the presence of divalent cations like calcium [23]. Sodium Alginate is the sodium salt form of alginic acid and gum mainly extracted from the cell walls of brown algae, with chelating activity. Upon oral administration, sodium alginate binds to and blocks the intestinal absorption of various radioactive isotopes, such as radium Ra 226 (Ra-226) and strontium Sr 90 (Sr-90) [28].

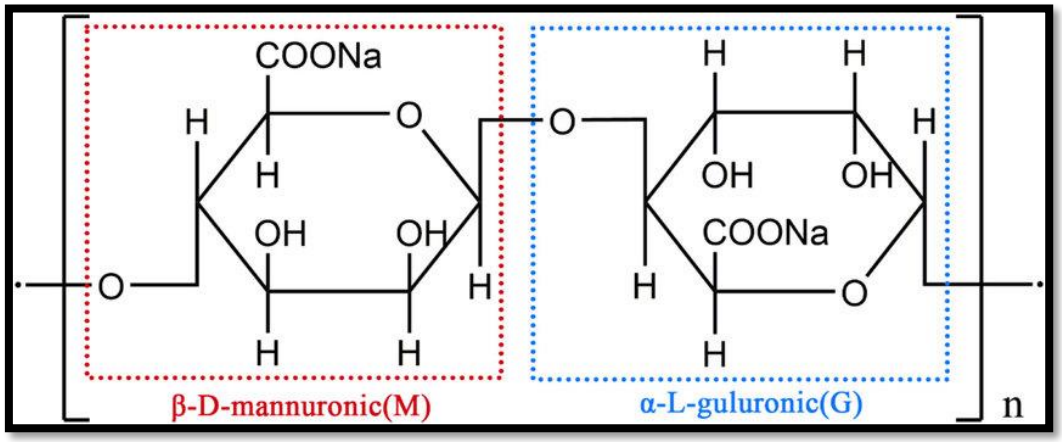

Fig 10- Chemical structure of sodium alginate

Some different key properties and uses of sodium alginate [29]-

1.5.1. Gelling Agent: One of the most notable properties of sodium alginate is its ability to form gels when it comes into contact with divalent cations, particularly calcium ions. This property makes it a valuable gelling agent in the food industry for applications such as making gel-like structures in foods, encapsulating flavours, and creating spherical gel beads (often referred to as "spherification" in molecular gastronomy).

1.5.2. Thickener and Stabilizer: Sodium alginate is also used as a thickening and stabilizing agent in a variety of food products, including sauces, dressings, ice cream, and yogurt. It helps improve the texture and viscosity of these products and prevents phase separation.

1.5.3. Biomedical Applications: Sodium alginate has several biomedical applications due to its biocompatibility and ability to form gels in physiological conditions. It is used in wound dressings, drug delivery systems, tissue engineering scaffolds, and dental impression materials.

1.5.4. Textile Industry: Sodium alginate is utilized in the textile industry as a thickener and binder for printing pastes. It helps to control the viscosity of the printing paste, improve colour penetration, and prevent spreading of the dye on the fabric.

1.5.5. Pharmaceuticals: In the pharmaceutical industry, sodium alginate is employed as a binder, disintegrant, and controlled-release agent in tablet formulations. It helps

to control the release of active pharmaceutical ingredients and improve the overall stability of the tablets.

1.6. Sodium alginate crosslinking with calcium chloride to produce hydrogel beads-

Sodium alginate dissolves in water to form a viscous, clear solution. When reacted with calcium chloride a double replacement reaction occurs where the calcium ions replace the sodium ions on the alginate, producing calcium alginate. The second product formed is sodium chloride which remains in solution. Mannuronic monomer of sodium alginate undergoes this rearrangement reaction with calcium chloride, and the final product after the crosslinking forms a structure similar to an "egg box" [30].

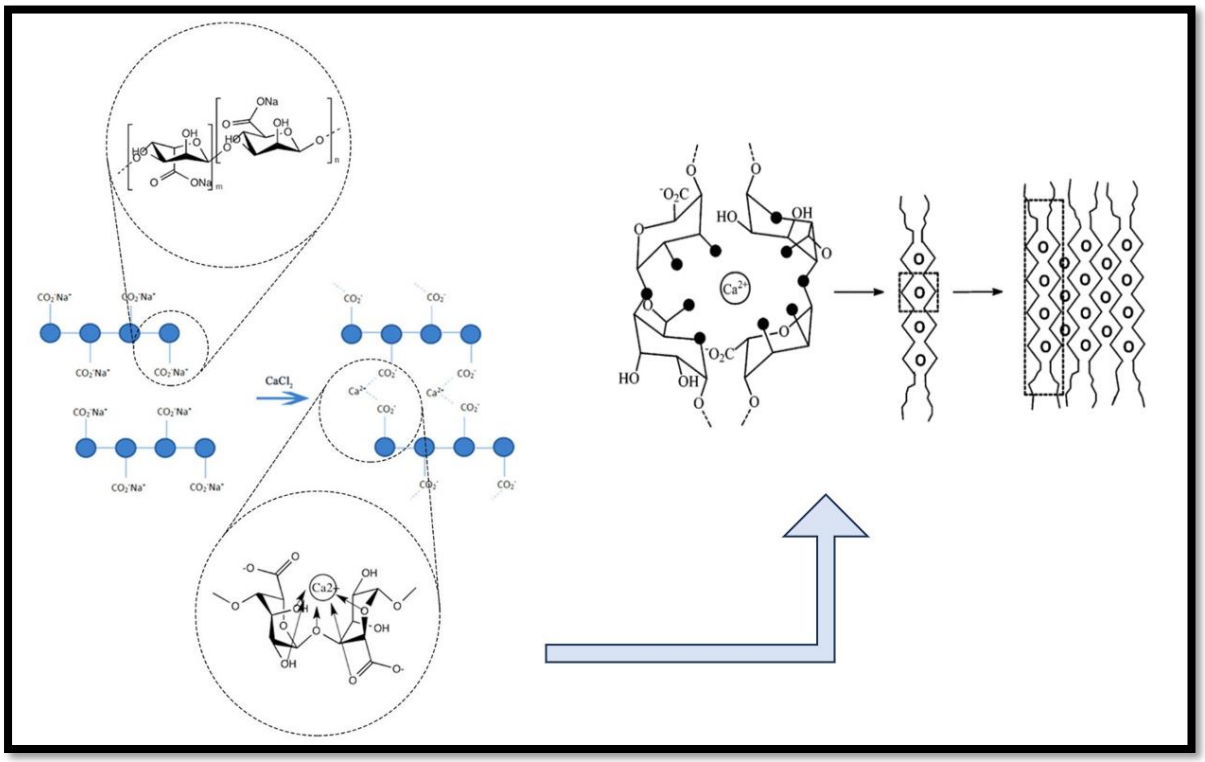

Fig 11– Reaction between sodium alginate and calcium chloride and formation of egg-box structured hydrogel

When sodium alginate and calcium chloride react, they undergo a double replacement reaction that produces calcium alginate and sodium chloride. The calcium ions in the calcium chloride replace the sodium ions in the sodium alginate, causing the polymer chains to bind together and form a gel. This process is known as ionic cross-linking. The characteristics of the gel can be controlled by the ratio, temperature, and concentration of the two components [31].

1.7. Hydrogels:

Hydrogels are three-dimensional networks of hydrophilic polymer chains that can absorb and retain large amounts of water or biological fluids. These materials have gained significant attention in various fields due to their unique properties, including high water content, biocompatibility, and adjustable mechanical properties. Hydrogels are highly versatile materials that have gained significant attention in various fields, particularly in biomedical applications. Composed of crosslinked polymer networks, these gels can absorb and retain large amounts of water while maintaining their structural integrity, mimicking the natural tissue environment. This unique property makes hydrogels ideal for use in drug delivery systems, wound healing, tissue engineering, and other medical applications. They can be engineered to respond to environmental stimuli such as pH, temperature, or the presence of specific biomolecules, allowing for controlled release of therapeutic agents. Additionally, hydrogels can be designed to be biocompatible and biodegradable, minimizing adverse reactions in the body. Their tunable mechanical properties and ability to incorporate bioactive molecules make them an invaluable tool in creating advanced medical treatments that are both effective and patient-friendly [32], [33], [34].

The networking of hydrogels refers to the intricate, three-dimensional polymer structure that gives these materials their unique properties. This network is formed by crosslinking polymer chains, creating a mesh-like structure capable of holding significant amounts of water or biological fluids. The degree of crosslinking in a hydrogel network determines its mechanical strength, porosity, and swelling behaviour, which can be finely tuned to suit specific applications. For instance, in drug delivery systems, the network can be designed to release therapeutic agents in a controlled manner, responding to changes in the environment such as pH or temperature. In tissue engineering, the network's architecture can be tailored to provide a scaffold that supports cell growth and tissue regeneration. Additionally, the network can incorporate functional groups that allow for the attachment of bioactive molecules, enhancing the hydrogel's interaction with biological tissues. The versatility of hydrogel networking makes it a powerful tool in developing advanced biomedical technologies [35], [36], [37].

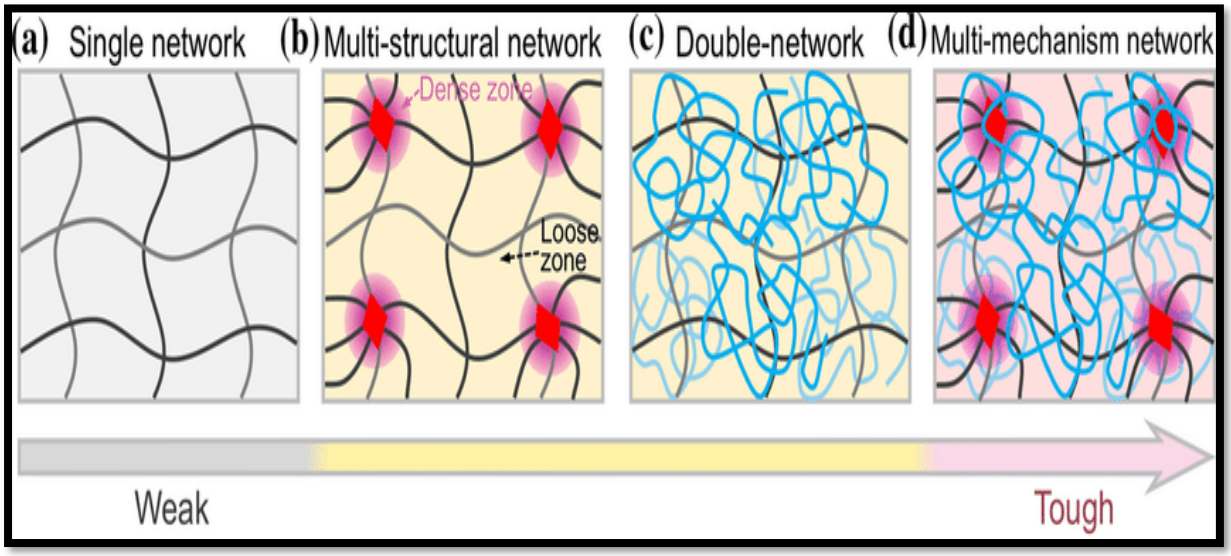

Fig 12- Network of hydrogel

1.8. Hydrogel beads:

Hydrogel beads are spherical structures composed of hydrogel material, typically containing a high percentage of water within a three-dimensional polymer network. These beads are formed through processes such as cross-linking polymerization, ionotropic gelation, or emulsification, resulting in a solid yet highly porous structure capable of absorbing and retaining large amounts of water or aqueous solutions [38], [39], [40].

1.8.1. Water Absorption and Swelling: Hydrogel beads have a high water-absorbing capacity due to their porous structure and hydrophilic nature. They can swell significantly when exposed to water or aqueous solutions, sometimes reaching several times their original size. This property makes them useful for applications requiring controlled release of water or solutes.

1.8.2. Drug Delivery: Hydrogel beads are employed as carriers for drugs, proteins, and other bioactive molecules. By incorporating these substances into the hydrogel matrix, controlled release of the active compounds can be achieved. The porous structure of the beads allows for diffusion of the loaded substances, providing sustained release over time. This feature is particularly advantageous for oral drug delivery, where prolonged drug release can enhance therapeutic efficacy and patient compliance.

1.8.3. Biomedical and Tissue Engineering: Hydrogel beads are utilized in various biomedical applications, including tissue engineering and regenerative medicine. They can serve as cell carriers or scaffolds for tissue regeneration, providing a supportive three-dimensional environment for cell growth, proliferation, and differentiation. By encapsulating cells within the hydrogel beads, their viability and functionality can be preserved during transplantation, facilitating tissue repair and regeneration.

1.8.4. Bio-separation and Biocatalysis: Hydrogel beads are employed in biotechnological processes for bio-separation and biocatalysis. Functionalized hydrogel beads containing specific ligands or enzymes can selectively bind target molecules or catalyse specific reactions, enabling purification of biomolecules, such as proteins and nucleic acids, or synthesis of desired products. These beads offer high specificity, reusability, and scalability, making them valuable tools in bioprocessing and biomanufacturing.

1.8.5. Environmental Applications: Hydrogel beads are utilized in environmental remediation and wastewater treatment. They can absorb and immobilize pollutants, such as heavy metals, organic contaminants, and nutrients, from aqueous solutions, thereby reducing environmental contamination and improving water quality. Functionalized hydrogel beads can selectively target specific pollutants, offering a sustainable approach to environmental cleanup.

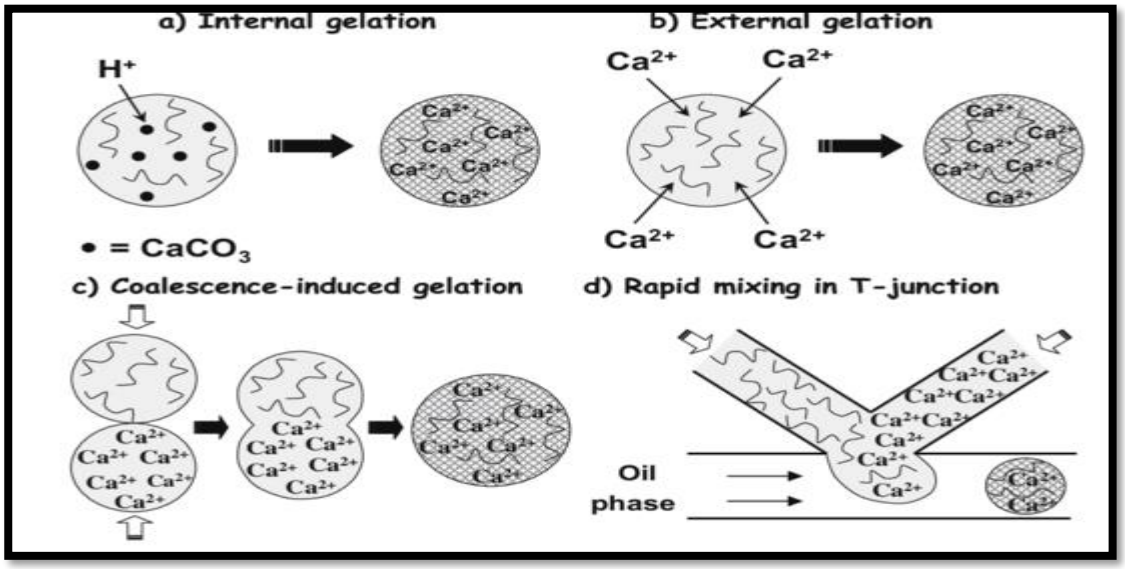

Fig 13- Types of gelation method

1.9. Types of hydrogel networking systems:

Hydrogel networks are based on their composition, structure, and the nature of crosslinking [41]. The classifications are [42]-

1.9.1. Chemical (Covalent) Hydrogels: These hydrogels are formed through covalent bonds between polymer chains, creating a stable and permanent network. This type of hydrogel is typically strong and durable, making it suitable for long-term applications such as tissue scaffolds and sustained drug release systems.

1.9.2. Physical (Non-covalent) Hydrogels:

1.9.2.1. Physically Crosslinked Hydrogels: In these hydrogels, the network is formed through non-covalent interactions, such as hydrogen bonding, ionic interactions, or hydrophobic interactions. These hydrogels are often reversible and can be sensitive to environmental changes, which is advantageous in applications like responsive drug delivery systems.

1.9.2.2. Ionic Hydrogels: These are a subset of physically crosslinked hydrogels where the network is formed by ionic interactions between oppositely charged groups. They are often used in drug delivery systems that require a response to pH or ionic strength changes [43].

1.9.3. Hybrid Hydrogels:

1.9.3.1. Interpenetrating Polymer Networks (IPNs): IPNs consist of two or more polymer networks that are physically or chemically interlaced but not covalently bonded to each other. This type of hydrogel combines the properties of different polymers, leading to enhanced mechanical strength and functionality.

1.9.3.2. Semi-Interpenetrating Polymer Networks (Semi-IPNs): Similar to IPNs, these hydrogels have one polymer network that is crosslinked while the other is not, providing a balance between flexibility and mechanical strength.

1.9.4. Biodegradable Hydrogels:

1.9.4.1. Enzymatically Degradable Hydrogels: These hydrogels are designed to degrade in the presence of specific enzymes. This property is particularly useful in biomedical applications where controlled degradation is required, such as in drug delivery systems or tissue engineering scaffolds.

1.9.4.2. pH-Sensitive Hydrogels: These hydrogels can degrade or swell in response to changes in pH, making them ideal for applications that require release in specific pH environments, such as in the gastrointestinal tract.

1.9.5. Smart or Responsive Hydrogels:

1.9.5.1. Thermo-responsive Hydrogels: These hydrogels respond to temperature changes, undergoing a phase transition that can trigger the release of drugs or other molecules. They are useful in applications where controlled release at body temperature is needed.

1.9.5.2. Dual or Multi-responsive Hydrogels: These hydrogels can respond to more than one stimulus, such as pH and temperature, providing a highly controlled and customizable platform for drug delivery and other biomedical applications.

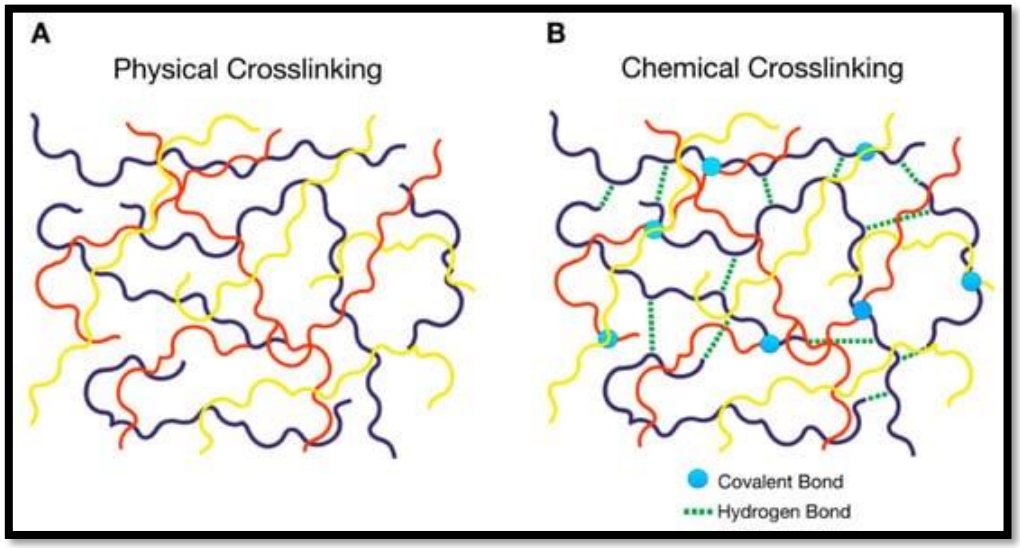

Fig 14- Physical and Chemical crosslinking of hydrogel

1.10. Overview on Conventional drug delivery system:

A conventional drug delivery system refers to methods and technologies used to deliver medications to the body in a manner that ensures optimal therapeutic effects [44]. These systems typically involve traditional routes of administration such as oral tablets, capsules,

injections (intravenous, intramuscular, subcutaneous), topical creams, ointments, and transdermal patches. Conventional drug delivery systems aim to optimize drug efficacy, minimize side effects, and improve patient compliance. However, they may have limitations such as variable absorption, degradation by enzymes, or patient discomfort with certain routes. Advances in pharmaceutical technology continue to refine these systems, aiming for improved drug stability, controlled release, and targeted delivery to specific tissues or cells within the body. In this method dosage forms are introduced in the system in specific time intervals which leads to fluctuation in drug concentration and toxicity [45].

1.11. Overview on sustained release drug delivery system:

A sustained release drug delivery system (SRDDS) is designed to achieve prolonged therapeutic effect by controlling the release rate of the drug over an extended period of time. This contrasts with conventional immediate-release formulations that deliver the entire dose of medication rapidly after administration. The key goals of sustained release systems include improving patient compliance, reducing dosing frequency, minimizing side effects, and optimizing therapeutic efficacy. However, designing sustained release systems can be complex, requiring consideration of drug properties, release kinetics, biocompatibility of materials, and regulatory requirements. Advances in polymer science, nanotechnology, and biotechnology continue to drive innovations in this field, expanding the range of drugs that can be effectively delivered using sustained release technologies [46], [47].

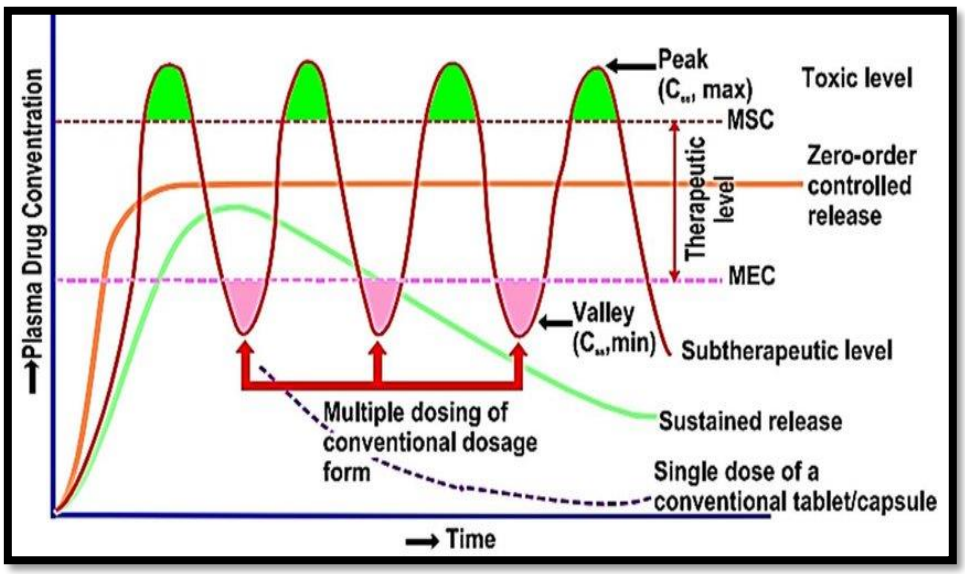

Fig 15- Release profile of Conventional, Sustained and Controlled drug delivery system

1.12. A sustained and controlled release drug delivery system using hydrogels:

This is a fascinating field of research in pharmaceuticals and biomaterials. Hydrogels are three-dimensional networks of hydrophilic polymer chains capable of absorbing and retaining large amounts of water. They can be designed to swell or shrink in response to changes in environmental conditions such as pH, temperature, or ionic strength [48], [49]. Steps of formulating a sustained release drug delivery system is discussed below [50]-

1.12.1. Hydrogel Selection: A suitable hydrogel based on its biocompatibility, swelling properties, and ability to encapsulate and release drugs is first chosen.

1.12.2. Incorporation of Drug: The drug of interest is typically encapsulated within the hydrogel matrix during its formulation. This can be achieved through methods such as physical entrapment, chemical conjugation, or electrostatic interactions.

1.12.3. Controlled Release Mechanism: Various factors can be utilized to control the release of the drug from the hydrogel matrix:

- **Diffusion**: The drug diffuses through the hydrogel matrix at a controlled rate determined by the polymer structure and drug properties.
- **Swelling/Deswelling**: Changes in environmental conditions trigger swelling or deswelling of the hydrogel, thereby modulating drug release.
- **Chemical Modification**: Incorporating chemical moieties sensitive to specific stimuli (e.g., pH, enzymes) can trigger drug release upon exposure to these stimuli.
- **External Stimuli**: External triggers such as temperature changes, light exposure, or magnetic fields can be employed to initiate drug release from hydrogels containing responsive components.

1.12.4. Characterization and Optimization: The release kinetics of the drug from the hydrogel system are carefully characterized and optimized through experimental studies and mathematical modelling. Parameters such as drug loading, hydrogel composition, and crosslinking density are adjusted to achieve the desired release profile.

1.12.5. Biocompatibility and Safety Assessment: Before translation to clinical applications, the hydrogel-based drug delivery system undergoes rigorous evaluation for biocompatibility, toxicity, and long-term safety to ensure it meets regulatory standards.

1.13. Applications of sustained and controlled release drug delivery systems:

Applications of sustained and controlled release drug delivery systems using hydrogels are diverse and include localized drug delivery to specific tissues or organs, prolonged systemic drug delivery, and targeted therapy for various diseases such as cancer, diabetes, and cardiovascular disorders. Sustained release drug delivery systems (SRDDS) are designed to release a drug at a predetermined rate, prolonging its therapeutic effect while maintaining

steady drug levels in the bloodstream. This system has several applications across various medical fields due to its ability to improve drug efficacy, reduce dosing frequency, and minimize side effects. Here are some of the key applications [51]:

- **Chronic Disease Management**- Cardiovascular diseases, Diabetes, Asthma and COPD.
- **Pain Management**- for chronic pain and post operative pain.
- **Central Nervous System Disorders**- Epilepsy, Depression and Anxiety, Parkinson's disease.
- **Infectious Diseases**- Antibiotics, Antiretroviral therapy (HIV/AIDS).
- **Hormonal Therapy**- Contraceptives, Hormone replacement therapy (HRT).
- **Oncology**- Chemotherapy, specific tumor targeting.
- **Gastrointestinal Disorders**- Ulcerative colitis and Crohn's disease, Gastroesophageal reflux disease (GERD).
- **Ophthalmology**- Glaucoma, Post operative care.
- **Transdermal Drug Delivery**- Nicotine patches, Hormonal patches.
- **Vaccination**- Controlled release vaccines.

1.14. Overview Infectious diseases:

Infectious diseases are caused by pathogenic microorganisms such as bacteria, viruses, fungi, and parasites. These diseases can be spread, directly or indirectly, from one person to another, through vectors, or through contact with contaminated surfaces, food, or water [52]. Here are some key points about infectious diseases:

1.14.1. Types of Infectious Agents-

- **Bacteria**: Single-celled organisms that can cause diseases such as tuberculosis, strep throat, urinary tract infections, and bacterial pneumonia.
- **Viruses**: Smaller than bacteria, viruses require a living host to multiply. They cause diseases such as influenza, HIV/AIDS, COVID-19, measles, and hepatitis.
- **Fungi**: Can be unicellular (yeasts) or multicellular (molds). They cause infections like athlete's foot, ringworm, and histoplasmosis.
- **Parasites**: Organisms that live on or in a host organism and cause harm. Examples include malaria (caused by Plasmodium parasites), giardiasis, and tapeworm infections.

1.14.2. Transmission Methods-

- **Direct Contact:** Person-to-person transmission through physical contact (e.g., touching, kissing, sexual contact) and Droplet transmission through coughing or sneezing.
- **Indirect Contact**: Contact with contaminated surfaces, objects, or vectors (e.g., mosquitoes, ticks).

- **Airborne Transmission**: Spread of infectious agents through the air over long distances (e.g., tuberculosis, measles).
- **Food and Waterborne Transmission**: Ingestion of contaminated food or water (e.g., cholera, salmonellosis).
- **Vector-Borne Transmission**: Transmission through vectors such as mosquitoes, ticks, or fleas (e.g., malaria, Lyme disease).

1.14.3. Common Infectious Diseases-

- **Respiratory Infections**: Influenza, common cold, COVID-19, tuberculosis, and pneumonia.
- **Gastrointestinal Infections**: Norovirus, rotavirus, cholera, and food poisoning.
- **Sexually Transmitted Infections (STIs)**: HIV/AIDS, syphilis, gonorrhoea, chlamydia, and human papillomavirus (HPV).
- **Vector-Borne Diseases**: Malaria, dengue fever, Zika virus, and Lyme disease.
- **Skin and Soft Tissue Infections**: Impetigo, cellulitis, fungal infections, and scabies.
- **Bloodborne Infections**: Hepatitis B, hepatitis C, and HIV.

1.14.4. Prevention and Control-

- Vaccination
- Hygiene Practices
- Sanitation and Clean Water
- Vector Control
- Antibiotics and Antivirals
- Public Health Measures [53]

1.14.5. Emerging Infectious Diseases-

- **COVID-19**: Caused by the novel coronavirus SARS-CoV-2, it emerged in late 2019 and led to a global pandemic [54].
- **Zika Virus:** Transmitted by mosquitoes, it caused a significant outbreak in the Americas in 2015-2016.
- **Ebola Virus**: Causes severe haemorrhagic fever with high mortality rates, with significant outbreaks in West Africa.
- **Antimicrobial Resistance (AMR)**: Increasing resistance of microorganisms to existing antibiotics, posing a significant threat to public health.

1.14.6. Research and Advances-

- **Genomic Sequencing**: Advanced techniques for identifying pathogens and understanding their genetic makeup.
- **Vaccine Development**: Rapid development and deployment of vaccines, as seen with COVID-19.
- **Novel Therapies**: Development of new antimicrobial agents, antiviral drugs, and biologics.
- **Global Health Initiatives**: Collaborative efforts to combat infectious diseases through organizations such as the WHO and CDC [55].

1.15. Overview on Stomach ulcer:

A stomach ulcer, also known as a gastric ulcer, is a sore that develops on the lining of the stomach. It's a type of peptic ulcer disease, which also includes ulcers that occur in the first part of the small intestine (duodenal ulcers) [56]. Peptic ulcer disease is characterized by discontinuation in the inner lining of the gastrointestinal (GI) tract because of gastric acid secretion or pepsin. It extends into the muscularis propria layer of the gastric epithelium. It usually occurs in the stomach and proximal duodenum. It may involve the lower oesophagus, distal duodenum, or jejunum [57].

1.15.1. Causes of stomach ulcer-

The primary causes of stomach ulcers include:

- **Helicobacter pylori (H. pylori) infection**: This bacterium can weaken the protective mucus lining of the stomach, making it more susceptible to damage from stomach acid.
- **Nonsteroidal Anti-Inflammatory Drugs (NSAIDs)**: Regular use of NSAIDs, such as aspirin, ibuprofen, and naproxen, can irritate or inflame the stomach lining, leading to ulcers.
- **Excessive acid production**: Conditions like Zollinger-Ellison syndrome, which causes the stomach to produce too much acid, can lead to ulcer formation.
- **Lifestyle factors**: Smoking, excessive alcohol consumption, and stress may exacerbate ulcers, although they are not direct causes [58].

1.15.2. Symptoms-

Common symptoms of a stomach ulcer include-

- Burning or gnawing pain in the upper abdomen, which may be worse when the stomach is empty and can be temporarily relieved by eating certain foods.
- Bloating or a feeling of fullness.
- Nausea or vomiting.

- Loss of appetite or weight loss.
- In severe cases, vomiting blood or having black, tarry stools, which indicates bleeding in the stomach.

1.15.3. Diagnosis-

To diagnose a stomach ulcer, doctors may perform:

- **Endoscopy**: A thin, flexible tube with a camera is inserted through the mouth to visually inspect the stomach lining.
- **Barium swallow**: A type of X-ray where the patient swallows a barium solution to highlight the stomach and small intestine.
- **H. pylori tests**: These can include breath, blood, or stool tests to detect the presence of H. pylori bacteria.

1.15.4. Treatment for stomach ulcer-

The treatment of stomach ulcer includes,

1.15.4.1. Medications:

- **Proton pump inhibitors (PPIs):** Reduce stomach acid production, allowing the ulcer to heal.
- **H2-receptor antagonists**: Also reduce stomach acid production.
- **Antibiotics**: If H. pylori is present, a combination of antibiotics is prescribed to eradicate the infection.
- **Antacids**: Provide temporary relief by neutralizing stomach acid.

1.15.4.2. Lifestyle changes:

- Avoiding NSAIDs or taking them with caution.
- Reducing alcohol intake and quitting smoking.
- Managing stress through relaxation techniques.

1.15.4.3. Surgery:

- In rare, severe cases where ulcers do not heal with medication or cause complications like bleeding or perforation, surgery may be necessary.

1.15.5. Complications in stomach ulcer-

If left untreated, stomach ulcers can lead to serious complications, such as [57]:

- **Internal bleeding**: Which can cause anaemia or be life-threatening.
- **Perforation**: A hole in the stomach wall, which can lead to peritonitis, a serious abdominal infection.
- **Gastric outlet obstruction**: When the ulcer blocks the passage of food through the digestive tract.

1.15.6. Prevention of stomach ulcer-

The prevention of stomach ulcer can be done by-

- Limit the use of NSAIDs and use alternatives if possible.
- Treat H. pylori infections promptly.
- Avoid excessive alcohol and smoking.
- Maintain a healthy diet and manage stress.

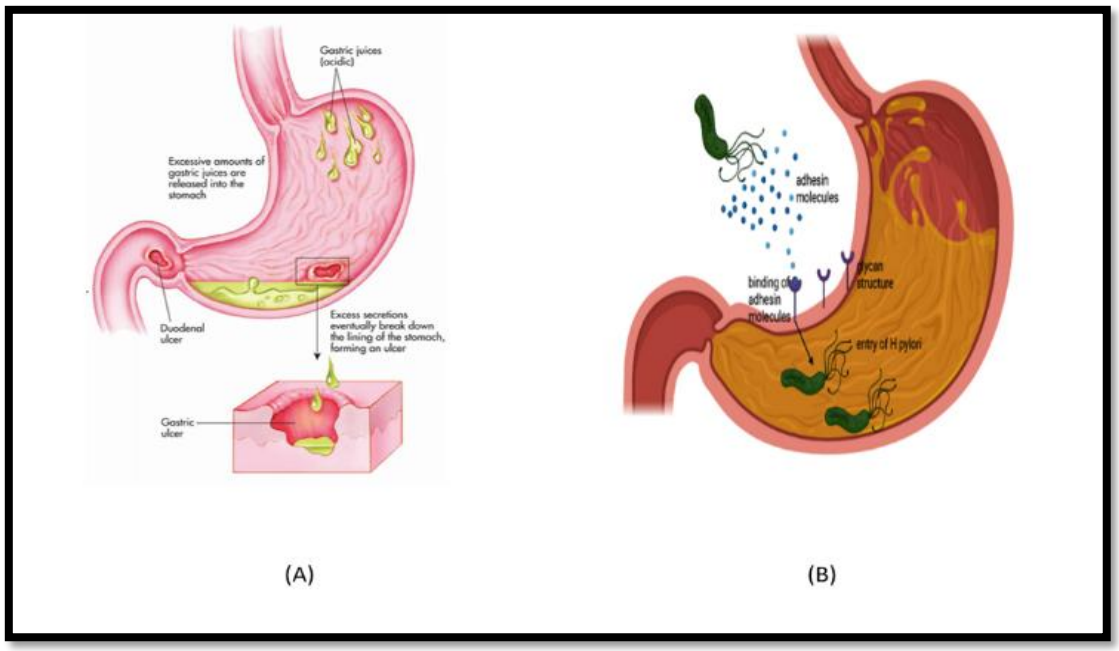

Fig 16- Pathophysiology of stomach ulcer induced by (A) excessive stomach acid secretion, (B) H. pylori infection

CHAPTER 2

LITERATURE REVIEW

2. LITERATURE REVIEWS-

2.1. The study aims to formulate an oral in-situ gel for sustained paracetamol delivery, targeting pediatric and geriatric patients. A blend of sodium alginate, chitosan, and Gelucires was used to create the gel. Characterization techniques, such as rheology and in vivo bioavailability tests on rat models, were employed. The in-situ gel transitioned into a gel-matrix system in 0.1N HCl, effectively controlling the release of paracetamol at different pH levels (1.2, 5.4, and 6.8). Gels made solely of sodium alginate or sodium alginate-chitosan exhibited rapid drug release at pH 6.8. The formulation containing paracetamol in a Gelucire (G33/01):3-3% sodium alginate - chitosan ratio of 1:1:4 w/w showed an extended drug release time of over 8 hours. Bioavailability in rats revealed a higher time to maximum concentration (Tmax) and lower peak concentration (Cmax) but comparable mean residence time (MRT) and area under the curve (AUC0-∞) to commercial formulations. The gel's synergistic blend of chitosan, sodium alginate, and Gelucire G33/01 ensures a sustained release of paracetamol, making it a promising drug delivery system for vulnerable populations like children and the elderly [59].

2.2. In this study, an inorganic–organic composite system was developed through biomineralization of calcium carbonate in the quince-seed mucilage-based hydrogel. Drug-polymer interactions were studied by FTIR, DSC, XRD and SEM analysis. The water absorption capacity was calculated by swelling index. Drug release was determined at various pH. Several in vitro kinetic models were applied to observe drug release behaviour. Studies of drug-polymer interactions and particle flow characteristics of the developed composite material have shown that there is good compatibility between drug and the excipients. The XRD and SEM results confirmed calcite polymorphs in the developed composite material. Thermograms showed that the developed composite material was heat stable. A restricted drug release was observed in an acidic medium (pH 1.2). A controlled drug release was depicted from the developed system at pH 6.8. The drug release mechanism of Super Case II was suggested. The developed system was considered to be an effective drug carrier for colon targeted oral delivery of non-steroidal anti-inflammatory drugs (NSAIDs) to avoid gastric irritation and risk of ulceration [60].

2.3. New gastroretentive floatable polymeric beads were developed for efficient encapsulation and prolonged release of amoxicillin trihydrate (AMT). Herein, sunflower oil (SFO) was entrapped into alginate (Alg)/iota carrageenan (*i*-CG) doubly networked polymeric beads, and followed by surface-coating with aminated chitosan (AmCs) layer. Diverse analysis tools were employed to investigate the chemical structure, thermal and morphological properties of the formulated AmCs@ (SFO/Alg/*i*-CG) polymeric beads. The formulated polymeric beads exhibited exceptional floating ability exceeded 24 h without floating lag time. Additionally, approximately 93.29% of AMT-drug was successfully encapsulated into the floatable coated polymeric beads. The AMT-drug burst release at pH.1.2 was meaningfully

dwindled with increasing AmCs concentration up to 4%., while a prolonged release manner took place up to 25 h. Kinetically, the release mechanism obeyed Peppas-Sahlin model, while the Fickian diffusion was the dominant. The *in vitro* bio-evaluation assessments revealed that coated polymeric beads possessed excellent mucoadhesion percent reached 93.333%, potent antimicrobial activity and respectable biodegradability under the physiological enzymatic conditions. The cytotoxicity assessment confirmed the safety of the formulated floatable polymeric beads with cell viability reached 96%, suggesting their potential applicability as effectual mucoadhesive carriers for the oral delivery of antibiotics [61].

2.4. This study was aimed at developing and validating a UV spectrophotometric method for the estimation of paracetamol in chitosan coated alginate beads throughout their pharmaceutical development. Paracetamol content was assessed at 234 nm in various buffers to cover the physiological range of gastrointestinal fluid from pH 1.2 to pH 6.8. The linearity range was found to be 0.5–10 μg/mL. The proposed UV method was validated in accordance with main ICH guidelines. The findings showed that this UV spectrophotometric method is accurate, precise, and reproducible while also being uncomplicated, cost-effective, and not requiring a lot of time. It can be used to estimate paracetamol in routine quality control and drug dissolution studies [62].

2.5. The aim of this overview is the removal of amoxicillin via different methods, emphasizing removal by biopolymers and its derivatives. Although pharmaceutical compounds such as antibiotics have been of great help to animals and humans, the excessive use of them have become a global problem due to the resistance of pathogens to these drugs, for this reason a series of methods have been reported that we will see below that allow to remove efficiently, economically, and environmentally friendly compounds such as antibiotics. A wide variety of organic compounds that we currently know are used in different areas of the work where pharmaceutical products are one of the most used compounds worldwide and their effects have been studied extensively, so that different authors have established that these species are not biodegradable and it is estimated that more than 76% of the species that enter the different environmental matrices without presenting major Changes. These compounds have physiological impacts on different organisms. Specifically, antibiotics are the pharmaceutical compounds with the greatest impact on different organisms, as well as on the environment. These are detected with high frequency in the aqueous medium due to their great use, both in the veterinary, human and aquaculture areas, where the elimination is of low or no efficiency in wastewater treatment plants, finding concentrations ranging from nanograms to milligrams per liter, in surface fresh waters they can reach up to 50 g L^{-1} in the African continent, 10 g L^{-1} in Europe, 15 g L^{-1} in America and up to 450 g L^{-1}, in Asian countries. Although these concentrations do not have a major direct impact on humans, they do have an indirect impact, since microorganisms are seriously affected by antibiotics at concentrations below 10 μg L^{-1}. When antibiotics reach the environment, they can cause toxicity in some organisms, added to this, is one of the biggest problems caused by antibiotics that is

related to the development of resistant bacteria where every year about 33,000 people die. The presence of these compounds and their metabolites in water bodies are causing different types of human health problems due to these bacteria resistant and multidrug-resistant to different antibiotics, causing genotoxicity, mutagenicity, endocrine disruption, different types of cancer and even miscarriages. It has been recorded that the consumption of antibiotics ranges between 100,000 and 200,000 tons per year, however, consumption in humans registered an increase of 36% between 2000 and 2010. There are 3 main pathways in which antibiotics can enter freshwater bodies: 1) Effluents from wastewater treatment plants, 2) chemical manufacturing plants, and 3) animal husbandry and aquaculture. With the information given, this article will review general aspects regarding antibiotics, resistance to them, effects and different methods of removal [63].

2.6. The occurrence of acetaminophen in surface water has been reported worldwide, indicating the need of alternative wastewater treatments. Activated hydrochar (AHC) is efficient for pharmaceuticals removal. Powdered AHC presents challenges that hamper its expansion. However, these issues can be overcome by adding polymers, such as alginate, in composite beads. Therefore, the present study aimed to develop and characterize alginate/brewer's spent grain AHC beads, applying them to acetaminophen adsorption in batch and fixed-bed experiments. The adsorbent presented a high surface area (533.42 $m^2\ g^{-1}$) and Fourier-transform infrared spectroscopy (FTIR) showed that alginate assigned new functional groups to the composite. Batch studies revealed an endothermic behavior and maximum adsorption capacity of 165.94 mg g^{-1}, with an equilibrium time of 240 min. The fixed-bed maximum adsorption capacity was 127.01 mg g^{-1}, with a mass transfer zone of 5.89 cm. The importance of alginate for the adsorbent development has been successfully proven [64].

2.7. Water pollution via pharmaceutical drugs such as paracetamol has been a highly concerning issue, and effective measures must be taken to treat these aquatic contaminants. Hence, the present study explored the use of cellulose nanocrystals (CNC) isolated from oil palm fronds (OPF), combined with commercial activated carbon (AC) to produce OPF CNC-AC hydrogel beads for paracetamol removal from aqueous media. The BET analysis showed that the OPF CNC-AC hydrogel beads possess a high BET surface area of 85.19 $m^2\ g^{-1}$. FTIR analysis showed several peaks had higher intensities and were slightly shifted than those before adsorption, and the SEM analysis confirmed these findings. Adsorption studies were conducted to infer how solution pH, contact time, and initial paracetamol concentration affect the adsorption behaviour. It was revealed that the adsorption studies of paracetamol could be achieved at 0.6 g of adsorbent dosage, at a pH 3 with a contact time of 170 min under room temperature. Meanwhile, the pseudo-second order kinetic model and Langmuir isotherm model revealed the best correlation for the adsorption of paracetamol with a q_{max} value of 21.34 mg g^{-1} and Gibbs free energy of adsorption (ΔG) of −10.27 kJ mol^{-1}. Thus, monolayer adsorption was thought to occur at the

surface of OPF CNC-AC hydrogel beads. This study suggests that OPF CNC-AC hydrogel beads could be a viable adsorbent for paracetamol removal from water used for consumption, which showed an efficiency of up to 79.98% in eliminating paracetamol dissolved in enriched aqueous solutions [65].

2.8. In this study development of Chitosan-coated paracetamol alginate beads using electrospray to obtain spherical beads with size below 1.5 mm. The encapsulation efficiency (EE) of the uncoated beads decreased with increased gelation time to reach 5±1.32% at 60 min. Chitosan coating enhanced EE to 50-76% depending on chitosan type and concentration. EE significantly improved to 99.0±1.1% by saturating the gelation bath with paracetamol. In vitro taste masking test and in vivo palatability evaluation using 12 human volunteers demonstrated that dry chitosan-coated paracetamol alginate beads were superior to the wet ones for taste masking, which was similar to the 30 marketed paracetamol suspension and even better in aftertaste evaluation. This indicates that the microencapsulation in alginate with further chitosan coating can compensate for the usage of sweetening and flavouring agents. This helps to formulate paediatric dosage forms with minimal undesired excipients [66].

2.9. Paracetamol is a common antipyretic and analgesic medicine used in childhood illness by parents and physicians worldwide. Paracetamol has a bitter taste that is considered as a significant barrier for drug administration. This study aimed to develop an oral dosage form that is palatable and easy to swallow by paediatric patients as well as to overcome the shortcomings of liquid formulations. The paracetamol was encapsulated in beads, which were prepared mainly from alginate and chitosan through electrospray technique. The paracetamol beads were sprinkled on the instant jelly prepared from glycine, ι-carrageenan and calcium lactate gluconate. The paracetamol instant jelly characteristics, in terms of physical appearance, texture, rheology, *in vitro* drug release and palatability were assessed on a human volunteer. The paracetamol instant jelly was easily reconstituted in 20 mL of water within 2 min to form jelly with acceptable consistency and texture. The jelly must be ingested within 30 min after reconstitution to avoid the bitter taste. The palatability assessment carried out on 12 human subjects established the similar palatability and texture of the paracetamol instant jelly dosage comparable to the commercial paracetamol suspension and was found to be even better in overcoming the aftertaste of paracetamol. Such findings indicate that paracetamol instant jelly will compensate for the use of sweetening and flavouring agents as well as develop paediatric dosage forms with limited undesired excipients [67].

2.10. Evaluation of the potential for oral sustained drug delivery of formulations with *in-situ* gelling properties is the main objective of the present investigation. Oral administration of aqueous dispersion of sodium alginate (1.5% w/v) containing calcium ions in complex form resulted in the formation of gel matrix as a consequence of the release of the calcium ions in the acidic environment of stomach fluid. Addition of methylcellulose, sodium chloride and polyethylene glycol improved the drug

retention efficacy of the gel. In this investigation, the study on the influence of added excipients on the rheological and drug release properties of the formulations has been focused. *In-vitro* studies demonstrated diffusion-controlled release of paracetamol from the gels. The bioavailability of orally administered paracetamol from the *in-situ* gel F4 (composed of 1.5% sodium alginate, 1.5% methyl cellulose, 3% $CaCO_3$, 2% NaCl 0.05% polyethylene glycol) administered in the stomach of rabbit, was more sustained as compared to the commercially available suspension Calpol® containing an identical dose of paracetamol [68].

2.11. To improve the durability and bioavailability of alginate, a one-step extrusion method was successfully applied to prepare alginate/gelatin core–shell beads. Gelatin cross-linked with glutaraldehyde was used as the core, while sodium alginate was used as the shell. To evaluate the effect of the sodium alginate shell on the in vitro drug release properties of the beads for biomedical applications, two drug models were used: water-soluble metformin hydrochloride and water-insoluble indomethacin. The structure and properties of different core–shell beads were characterized by Fourier transform infrared spectroscopy, scanning electron microscopy and swelling tests. The results showed that the beads consist of obvious inner core and outer skin layer which coats the surface stably. In addition, the core–shell structure improved the thermal stability of the beads and the entrapment efficiency reached 90% with a sodium alginate shell. As demonstrated, there is a gradual decrease in the swelling degree as the GTA or alginate concentration increases. For indomethacin, the cumulative release was 8.7% after 360 min in HCl buffer. The anomalous transport mechanism was the predominant factor affecting the release behavior of the metformin hydrochloride-loaded beads and indomethacin loaded beads were controlled by case-II transport. This work suggests that the core–shell structure could improve the swelling properties and drug release behaviour of the beads [69].

2.12. The report presents the formulation of hydrogel based on biopolymers chitosan and guar gum after cross-linking for sustained release of a commonly used orally prescribed analgesic Paracetamol. The oral ingestion of Paracetamol is associated with complications of the gastric tract and liver metabolism that can be effectually avoided by using transdermal drug delivery systems. The formulated transdermal patch was characterized for physicochemical properties including swelling, bonding pattern (using FTIR Fourier Transform Infra-Red and Scanning Electron Microscopy SEM) and antimicrobial activity. Biocompatibility and cytotoxicity were examined in vitro using cell culture in HeLa cell lines. After characterizing the novel formulated hydrogel were employed for the preparation of drug encapsulated in alginate beads as a transdermal patch. After formulation of the transdermal patch, the drug release was studied using an avian skin model. The results followed zero order kinetics and Non-Fickian law for diffusion. Paracetamol due to its small molecular mass (151.163 g/mol) released in a sustained manner. The released drug successfully retained its biological effects including anti-inflammatory and anti-protease activity, indicating no interaction between the drug

and the formulated hydrogel. It was shown that the formulated hydrogels could be safely used as a dermal patch for the sustained drug release of Paracetamol [70].

2.13. The objective of this work was that alginate beads are not soluble in the acid leading to small portion released in the stomach. This may not be favourable for drugs administered for fast action like paracetamol. So, this study was aimed to increase the immediate release of paracetamol from alginate beads, i.e. the release in the acidic pH. The beads were prepared by dropwise paracetamol/alginate suspension in divalent cation solution. Two attempts were used to increase the dissolution of paracetamol in the acidic pH. First attempt was by only changing preparation variables: needle size, alginate viscosity and drug loading using 23 full factorial design. The second approach was by adding excipients like carbopol, tween and polyethylene glycol. The beads were characterized for their size, encapsulation efficiency and release profile. Results: First approach, changing preparation variables without excipient adding, helped to increase the drug release in the acid but to a maximum of 26% using a smaller needle, lower drug loading and higher alginate viscosity. However, optimising the formulation with suitable excipients increased the drug release in the acid to 77.3%. The optimised formulation included carbopol 940 (pH sensitive polymer) and tween 80 (facilitates water entry) in the beads, with using barium chloride instead of calcium chloride together with PEG 400 in the complexing solution. To achieve immediate release of paracetamol from alginate beads in the acidic pH, excipients need to be added. Rational selection of excipients is critical to achieve the desired drug release [71].

2.14. The aim of this study is to investigate *in vitro* drug release profiles of pH-sensitive hydrogels composed of hydroxyethylacryl chitosan (HC) and sodium alginate (SA). The hydrogels were crosslinked by dipping method using different ionic crosslinkers (*e.g.*, Ca^{2+}, Zn^{2+} and Cu^{2+}). The crosslinking reaction was confirmed by FT-IR. Swelling behavior and stability of the hydrogels in simulated digestive media were investigated. The result indicated that the combination between HC and SA could delay the degradation time of the hydrogels. Calcium crosslinking system showed higher stability than that of zinc or copper crosslinking system. *In vitro* drug release profiles were studied using paracetamol as a soluble model drug. The amount of paracetamol release in simulated gastric fluid (SGF) was relatively low (<20%). In simulated intestinal fluid (SIF), the burst release of paracetamol was depressed with increasing HC content and/or applying crosslinker. The HC75SA25 formulation demonstrated the linearity of drug release profile. Additionally, the amount of drug release from the 0.5 M calcium HC50SA50 hydrogel in SIF was lower than 20%. The comprehensive results of this study suggested their potential in the application of site-specific oral drug delivery in intestine and colon [72].

2.15. The present work is to formulate the mucoadhesive microspheres loaded Paracetamol using two different natural gums with an aim to increase the GI retention time, enhance bioavailability over prolonged period of time in the stomach and upper GIT and decreased GI side effect. Paracetamol mucoadhesive microspheres were formulated using sodium alginate, different concentration of Xanthan gum and Guar gum by ionic gelation technique. Six formulations were prepared and evaluated for relevant parameters. Percentage yield is found between 52.34 ± 0.58% to 84.21 ± 0.21% in all formulations. The surface morphology of microspheres was characterized by SEM; it was discrete, spherical in shape and showed free flowing properties. The mean particle size of microspheres significantly increases and it was the range between 37.05 ± 0.05 µm to 45.29 ± 0.06 µm. Among all the formulations, XG-III showed a high entrapment efficiency is 94.80 ± 0.54% and highest percentage sorption in distilled water is observed. The in-vitro drug release studies revealed that XG-III is controlled and found to be 77.04 ± 0.22% at the end of the dissolution studies. The mechanism of drug release was evaluated using the linear regression coefficient. Stability studies of selected mucoadhesive microspheres showed good results. It could be also concluding that the all the formulations were shown satisfactory results and suitable for potential therapeutic uses [73].

2.16. The aim of this study is to develop three simple, specific and accurate spectrophotometric methods manipulating ratio spectra for the determination of paracetamol in binary mixture with drotaverine hydrochloride in tablet dosage form. In these methods, the absorption spectra of paracetamol were divided by 8 µg/ml of drotaverine hydrochloride to get the ratio spectra. In the first method (ratio difference), the difference in peak amplitudes of the ratio spectra were measured at 262 and 272 nm. The second method is a ratio subtraction which is based on determination of paracetamol at 248 nm after subtraction of interference exerted by drotaverine hydrochloride. In the third method (mean centering), the mean centered values of the ratio spectra were measured at 262 nm. The proposed methods were accurate, precise and selective for determination of paracetamol in presence of drotaverine hydrochloride in pure form and in pharmaceutical dosage forms. Beer's law was obeyed in the concentration range of 1–10 µg/ml in all methods. The developed methods were used to determine the studied drug in bulk powder, laboratory prepared mixtures and pharmaceutical dosage form with good accuracy and precision. All methods were validated according to ICH guidelines and the results obtained were statistically compared to those obtained from a reported method and were found to be in good agreement [74].

2.17. Stability indicating UV spectrophotometric methods for simultaneous estimation of amoxicillin trihydrate and metronidazole in bulk and in-house tablet has been developed by two methods. First method is simultaneous equation based on measurement of absorbance at 230 nm and 310 nm as two wavelengths selected for quantification of amoxicillin trihydrate and metronidazole. The second method is absorbance ratio based on the measurement of absorbance at iso-absorptive point at 237.3 nm and 310 nm as second wavelength selected as for quantification. Both methods obeyed Beer-Lambert's law in the concentration range of 15-90 µg/ml for amoxicillin trihydrate and 5-30 µg/ml for

metronidazole with correlation coefficient (r^2) values 0.999 for amoxicillin trihydrate and 0.998 for metronidazole in method-I, whereas 0.998 for amoxicillin trihydrate and 0.998 for metronidazole in method-II. Both methods showed good accuracy and precision with % RSD less than 2. LOD and LOQ values were 0.349 µg/ml and 1.06 µg/ml for amoxicillin trihydrate and 0.215 µg/ml and 0.652 µg/ml for metronidazole in method-I, whereas 0.558 µg/ml and 1.689 µg/ml for amoxicillin trihydrate and 0.215 µg/ml and 0.652 µg/ml for metronidazole in method-II respectively. The % assay was found to be 99.85% and 99.86% in method-I, whereas 99.63% and 99.86% in method-II for amoxicillin trihydrate and metronidazole respectively. Stress degradation was studied in different acidic, basic, neutral, oxidative, photolytic and thermal condition [75].

2.18. This study investigates the design of sunflower oil entrapped floating and mucoadhesive beads of amoxicillin trihydrate using sodium alginate and hydroxypropyl methylcellulose as matrix polymers and chitosan as coating polymer to localize the antibiotic at the stomach site against *Helicobacter pylori.* Beads prepared by ionotropic gelation technique were evaluated for different physicochemical, *in-vitro* and *in-vivo* properties. Beads of all batches were floated for >24 h with a maximum lag time of 46.3 ± 3.2 s. Scanning electron microscopy revealed that the beads were spherical in shape with few oil filled channels distributed throughout the surfaces and small pocket structures inside the matrix confirming oil entrapment. Prepared beads showed good mucoadhesive-ness of 75.7 ± 3.0% to 85.0 ± 5.5%. The drug release profile was best fitted to Higuchi model with non-fickian driven mechanism. The optimized batch showed 100% *Helicobacter pylori* growth inhibition in 15 h in *in-vitro* culture. Furthermore, X-ray study in rabbit stomach confirmed the gastric retention of optimized formulation. The results exhibited that formulated beads may be preferred to localize the antibiotic in the gastric region to allow more availability of antibiotic at gastric mucus layer acting on *Helicobacter pylori*, thereby improving the therapeutic efficacy [76].

2.19. The purpose of this work was to develop a multiparticulate system exploiting the pH-sensitive property and biodegradability of calcium alginate beads for intestinal delivery of ceftriaxone sodium (CS). CS was entrapped in beads made of sodium alginate and sodium carboxymethylcellulose (CMC), acacia, HPMC K4M and HPMC K15M as drug release modifiers. Beads were prepared using calcium chloride as a cross-linking agent, followed by enteric coating with cellulose acetate phthalate (CAP). The beads were then evaluated for entrapment efficiency using HPLC, in vitro drug release examined in simulated gastric fluid (pH 1.2) and simulated intestinal fluid (pH 6.8), swellability, particle size and surface characterization using optical microscopy, scanning electron microscopy (SEM), and atomic force microscopy (AFM). Thermal gravimetric analysis (TGA) was utilized to check the polymer matrix strength and thermal stability. The drug entrapment efficiency of the optimized formulation was determined to be 75 ± 5 %. Swelling properties of drug-loaded beads were found to be in a range of 0.9–3.4. Alginate beads coated with CAP and containing CMC as a second polymer exhibited sustained release. The drug release followed first-order kinetics via non-Fickian diffusion and erosion mechanism. The particle size of the beads was between 1.04 ± 0.20 and

2.15 ± 0.36 mm. TGA, AFM, and SEM data showed composition and polymer-dependent variations in cross-linking, thermal stability, surface structure, morphology, and roughness. The physico-chemical properties of the developed formulation indicate suitability of the formulation to deliver CS orally [77].

2.20. This article is based on preparation and characterization of Guar gum succinate-sodium alginate (GGS-SA) beads, which was cross-linked with barium ions, administered as a pH sensitive carrier for colon-specific drug delivery. The structure of GGS-SA beads was confirmed by FT-IR spectroscopy. Scanning Electron Microscope (SEM) studies revealed that the drug loaded GGS-SA beads prepared using 2:2 (w/v) weight percent of GGS and SA had a diameter about 1.4 mm and roughly spherical in shape. X-ray diffraction (XRD) studies showed that the peaks corresponding to GGS and SA at 13.5°, 17.5°, 20.2° and 13.5°, 22°, 24.1°, respectively were destroyed in GGS-SA beads which show that these beads are more amorphous in nature. Swelling studies demonstrated the pH-dependent swelling behavior of GGS-SA beads. The beads showed higher swelling degrees in pH 7.4 than that in pH 1.2 due to the existence of anionic groups in the polymer chains. The drug release study showed that the amount of model drug, ibuprofen, released from the GGS-SA beads was higher in pH 7.4 than that in pH 1.2 due to the pH-dependent swelling behavior of the beads. MTT assay revealed that GGS-SA beads at a concentration range of 0–30 μg/ml had no cytotoxic effect on the cultured mouse mesenchymal stem cells (C3H10T1/2). These results suggest that GGS-SA beads can be used as effective colon-specific drug delivery system with pH-dependent drug release ability [78].

2.21. This literature on in situ formation of cross-linked poly (sodium acrylate) (SA) network within the calcium alginate (CA) hydrogel beads to investigate the release of model drug methylene blue. The beads were found to be stable for more than 48h, in the physiological fluid (pH 7.4), while plain alginate beads dis integrated in couple of hours. The water uptake capacity of the beads was increased multiple times due to the use of poly (SA). The water uptake of beads was investigated under various composition parameters such as the amount of alginate, concentration of ionic cross-linker Ca^{++} ions, monomer sodium acrylate (SA) contents, and degree of cross-linking. The beads also exhibited fair stability in the media of varying pH. The characterisation of the beads was performed by FITR, TGA, SEM, XRD. The drug release study showed that plain CA and CA/poly (SA) composite beads exhibited different release mechanisms. Plain CA beads sample A1 demonstrates an almost 100% release in a duration of 2 h. On the other hand, the sample B1 i.e. CA/poly(SA) beads exhibits a relatively slower release extended over a time span of 20h [79].

2.22. Alginate microspheres are versatile tools for the delivery of a wide range of therapeutic biomacromolecules. This naturally occurring biopolymer has many unique properties making it an ideal candidate for tailoring with different composites of polymers leading to the formation of strong complexes for a broad range of applications. This article overviews

various types of composite alginate microspheres, methods of preparation, new technologies available, physico-chemical characteristics, controlled release profiles, applications and the future directions of composite alginate microsphere delivery system for biomacromolecules. Composite alginate microsphere systems are the ideal carriers for controlled delivery applications because of their ability to encapsulate a myriad of therapeutic drugs, proteins, enzymes, DNA, antisense oligonucleotides, vaccines, growth factors and chemokines as well as the ease of processing, mechanical properties, biocompatibility, high bioavailability, controlled release rates, stability, suitability for different administration modes, targeted/localized delivery of different agents and large-scale production with cost-effectiveness. This article presents updated information of applying microalginate-based technologies and tools in the biomedical field which will benefit research scientists and clinical physicians or biopharmaceutical industries keen in the development of application-based new therapeutic and diagnostic strategies for various diseases. Furthermore, this technology will play more important roles in biosensors, vaccination, tissue engineering, cancer chemotherapeutics and stem cell research [80].

2.23. The objective of this study was to develop a sustained release dosage form of Trimetazidine dihydrochloride (TMZ) using a natural polymeric carrier prepared in a completely aqueous environment. TMZ was entrapped in calcium alginate beads prepared with sodium alginate by the ionotropic gelation method using calcium chloride as a crosslinking agent. The drug was incorporated either into preformed calcium alginate gel beads (sequential method) or incorporated simultaneously during the gelation stage (simultaneous method). The beads were evaluated for particle size and surface morphology using optical microscopy and SEM, respectively. Beads produced by the sequential method had higher drug entrapment. Drug entrapment in the sequential method was higher with increased CaCl2 and polymer concentration but lower with increased drug concentration. In the simultaneous method, drug entrapment was higher when polymer and drug concentration were increased and also rose to a certain extent with increase in CaCl2 concentration, where further increase resulted in lower drug loading. FTIR studies revealed that there is no interaction between drug and CaCl2. XRD studies showed that the crystalline drug changed to an amorphous state after formulation. Release characteristics of the TMZ loaded calcium alginate beads were studied in enzyme-free simulated gastric and intestinal fluid [81].

2.24. Metronidazole (MZ), a common antibacterial drug used in treatment of *H. pylori*, was prepared in chitosan-treated alginate beads by the ionotropic gelation method. A ($3 \times 2 \times 2$) factorially designed experiment was used in which 3 viscosity-imparting polymers namely, methyl cellulose, carbopol 934P and κ-carrageenan, 2 concentrations (0.2 and 0.4% w/v) of chitosan as encapsulating polymer and 2 concentrations (2.5 and 5% w/w) of the low-density magnesium stearate as a floating aid were tested. The drug entrapment efficiency (%), the percent of floating beads and the time for 80% of the drug to be released ($T_{80\%}$) were the responses evaluated. The bead formula containing 0.5% κ-carrageenan, 0.4% chitosan and 5% magnesium stearate showed immediate buoyancy, optimum drug entrapment efficiency and extended drug release. The histopathological

examination of mice stomachs and *in vivo H. pylori* clearance tests were carried out by orally administering MZ floating alginate beads or MZ suspension, to *H. pylori* infected mice under fed conditions as a single daily dose for 3 successive days in different doses 5, 10, 15 and 20 mg/kg. The histopathological examination showed that groups receiving MZ in the form of floating alginate beads at doses 10, 15 and 20 mg/kg were better than the corresponding suspension form, regarding eradication of *H. pylori* infection. The *in vivo H. pylori* clearance tests showed that MZ floating beads with a dose of 15 mg/kg provided 100% clearance rate whereas the MZ suspension with a dose of 20 mg/kg gave only 33.33% [82].

CHAPTER 3

OBJECTIVE OF WORK

3. OBJECTIVE OF WORK-

Objective of the work is to formulate hydrogel beads containing Amoxicillin trihydrate and Acetaminophen (paracetamol) to administer for various infectious diseases and prolonging the release of drugs for better patient compliance.

3.1. The plan of experiment comprises of these following steps-

(a) Preparation of standard curve of amoxicillin trihydrate and Acetaminophen individually in different pH media- pH 1.2, 6.8, 7.4 and neutral 7 (double distilled water).
(b) Preparation of standard curve of amoxicillin trihydrate and paracetamol (5:3) combined in different pH media- pH 1.2, 7.4 and neutral 7 (double distilled water).
(c) Preparation of hydrogel beads in different polymer and crosslinking agent ratios.
(d) Fabricating different methods for sustained effect like- coating, copolymer etc.
(e) Determination of particle size
(f) Determination of drug entrapment efficiency and drug loading of the prepared beads.
(g) Determination of swelling index.
(h) The release of drug from the beads.
(i) Antimicrobial study.
(j) Thermogravimetric differential thermal analysis (TG/DTA)
(k) X-Ray Diffraction pattern analysis.
(l) Surface morphological study of the beads.
(m) FTIR
(n) Release kinetics

3.2. Relevance of current research work

a. Spectrophotometric method development of the drugs individually
b. Simultaneous method development
c. Amoxicillin trihydrate stability in different pH solvents
d. HPLC method used to detect degradation of amoxicillin trihydrate in acidic media
e. Combined beads formation

- **Spectrophotometric method development of Amoxicillin Trihydrate and Acetaminophen individually-**

Firstly, different pH solutions [83] were prepared such as– pH 1.2, 6.8, 7.4, neutral 7 (DDW). In those solutions required amount of pure API of amoxicillin trihydrate and acetaminophen were dissolved individually. These solutions were diluted in a concentration range of 2 to 10 µg/ml and checked for their absorbance maxima in UV-spectrophotometer. Amoxicillin trihydrate showed its lambda max at 228nm [84] whereas for acetaminophen it was at 243nm [85]. The absorbances of amoxicillin trihydrate and acetaminophen were determined at 228nm and 243nm for all the concentrations in all of the pH solvents. These absorbances were plotted against concentration to obtain the standard curve of amoxicillin and acetaminophen in different pH medias, and the effect of different pH on them was observed. The main difference between different pH media observed by the UV-spectrophotometer was an additional peak

near 200-205nm in case of pH 1.2, 6.8 and 7.2, no such peaks was observed in case of neutral pH, which may be due to the noise of the instrument due to the presence of buffer [86]. These studies were repeated more than 3 times, in 3 different instruments in different environmental conditions throughout the year to validate the method.

- **Simultaneous method development of the drug combination-**

Secondly, in those four solvents- pH 1.2, 6.8, 7.4 [83], neutral 7 (DDW), amoxicillin trihydrate and acetaminophen was added together in a 5:3 ratio and dissolved completely by manual shaking. This ratio was selected because of two reasons-

a. The dose of amoxicillin trihydrate is 25mg/kg every 4hours, and dose of acetaminophen is 15mg/kg every 4 hours [87].
b. The area under curve of 10 µg/ml amoxicillin trihydrate was similar to that of area under curve of 6 µg/ml of paracetamol.

These drugs were dissolved and diluted in a concentration range of 2 to 10 µg/ml and checked for its maximum absorbances. As both the drugs have absorbance maxima near each other, their combination shows a maximum absorbance at 232nm, which is a middle point of lambda max both the drugs. The rest of the studies were continued based on this lambda max only. Analysis of these two drugs were determined by simultaneous equation method from this combination. And this method was validated as per the guidelines of International Council for Harmonisation of Technical Requirements for Pharmaceuticals for Human Use- Q2R2 [88].

- **Amoxicillin trihydrate stability in different pH solvent**

Amoxicillin trihydrate is a semisynthetic antibiotic belongs to the Penicillin class of antibiotics. Amoxicillin trihydrate has a beta-lactam ring in its structure which acts as bactericidal agent. The beta lactam ring of amoxicillin trihydrate hydrolyses easily when exposed to acidic environment (below pH 2). This may decrease some of its antimicrobial activity. The stability of amoxicillin trihydrate depends on the integrity of penam cycle- They are bicyclic ring systems containing a β-lactam moiety fused with a five-member thiazolidine ring. **Penams** are the primary skeleton structures that define the penicillin subclass of the broader β-lactam family of antibiotics and related compounds. They are bicyclic ring systems containing a β-lactam moiety fused with a five-member thiazolidine ring. Due to ring strain and limitations on amide resonance, the structure is unstable and highly susceptible to catalytic cleavage at the amide bond. Benzylpenicillin (penicillin G) is the natural product parent that contains the penam structure. So, hydrolysis of the beta-lactam causes instability of the compound. Amoxicillin has amphoteric properties [89], a property conferred by its three main functional groups, COOH (pKa_1= 2.7), NH_2 (pKa_2 = 7.4) and OH (pKa = 9.6) as shown in (fig-17) [90], [91], [92]. In this way, the molecular structure is affected by the pH changes to which it may be subjected. In this way, at pH 10 amoxicillin degradation is recorded in time of 24 h at pH 5 there is no further degradation and at pH 1 degradation is recorded transforming amoxicillin into amoxicilloic acid (fig- 18) [93], [94], [95]. Thus, at pH values close to neutral, amoxicillin is more stable and has less degradation than at acidic or basic pH. However, it

should be considered that at high temperatures (55°C) approximately amoxicillin, even if it is in a solution at neutral pH, it decomposes [96].

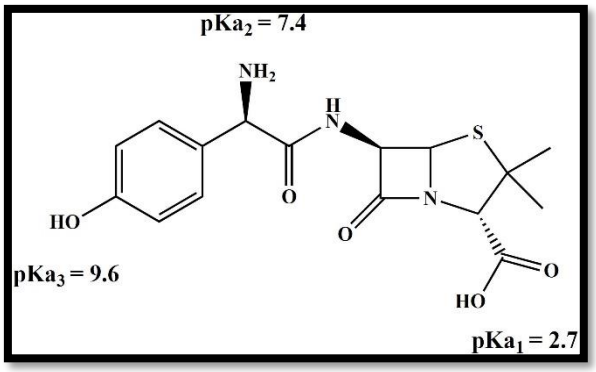

Fig 17- Amphoteric properties of Amoxicillin trihydrate

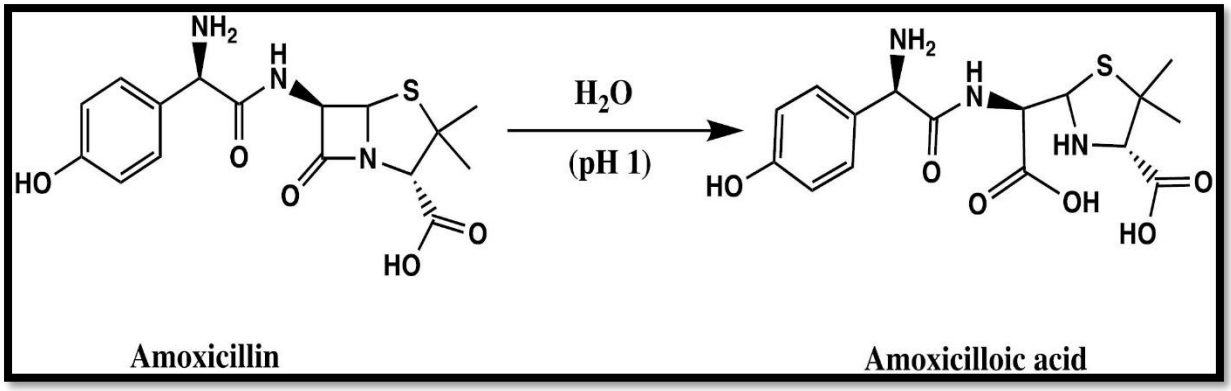

Fig 18- transformation of Amoxicillin trihydrate in acidic pH

- **HPLC method for detection of degradation of Amoxicillin trihydrate in acidic pH-**

After repeating analysis of Amoxicillin trihydrate many times by UV-spectrophotometer, there was no significant changes observed in the absorbance maxima or wavelength in different pH media, so another more sensitive method- HPLC was applied. In the HPLC method slight change of area of peak of observed in case of Amoxicillin trihydrate in acidic media compared to neutral media. But it cannot be confirmed if it occurred due to production of amoxicilloic acid. Further studies are needed to confirm this.

- **Formulation of sustained release hydrogel beads with a combination of Amoxicillin trihydrate and Acetaminophen-**

The main application of this calcium alginate hydrogel beads containing amoxicillin trihydrate and paracetamol, are in severe infectious conditions with hyperthermia. Mankind has been directly and indirectly depended on antipyretics and antibiotics since the last few decades for various infectious diseases. Antipyretics like Acetaminophen (paracetamol) and Ibuprofen

were used to alleviate fever and mild to moderate pain associated with the viral and bacterial infection [88]. Antibiotics were used to minimize the effect of bacteria and viruses directly [97]. Though most available antibiotics were inactive against the coronavirus itself but they had a great role in treating bacterial coinfections like severe inflammations in respiratory tracts or other organs. Amoxicillin was one of several semisynthetic derivatives of 6-aminopenicillanic acid (6-APA); In 2021, it was the 38th most commonly prescribed medication in the United States, with more than 16 million prescriptions [98].

Body temperature increases due to the pyrogenic activity of prostaglandins. This begins with the formation of arachidonic acid from phospholipids, and arachidonic acid is then converted to prostaglandin by cyclooxygenase pathway. Prostaglandin acts via certain receptor to affect specific neurons within the hypothalamus that aid in thermoregulation. The action of prostaglandin begins when exogenous pyrogens (e.g., bacteria, viruses) stimulate endogenous pyrogens to alter the hypothalamic set point via the organum vasculosum of the lamina terminalis (OVLT) and raise the core body temperature. Endogenous pyrogens also act to trigger an immune and inflammatory response. The immune response includes leukocytosis, T cell activation, B cell proliferation, NK cell killing, and increased white blood cell adhesion. The inflammatory response includes increased acute phase reactants, increased muscle protein breakdown, and increased synthesis of collagen [99], [100].

So, if we combine an antibiotic along with an antipyretic drug to administer in the initial stages of severe infections with fever, it will reduce the intake of two or more medications and improve patient compliance. This combination therapy can be helpful to produce better therapeutic actions in the initial stages of an infection to reduce the fever and fight against the microorganisms at the same time with no time loss.

3.3. The characteristics of a drug that make it suitable for sustained release formulations include:

a) High Dosage Frequency: Drugs that require frequent dosing throughout the day can benefit from sustained release formulations to reduce dosing frequency and improve patient compliance.
b) Short Half-Life: Drugs with a short half-life in the body may benefit from sustained release formulations to maintain therapeutic levels over an extended period, thus avoiding the need for frequent administration.
c) Narrow Therapeutic Index: Drugs with a narrow therapeutic index, where small changes in plasma concentration can lead to significant clinical effects or toxicity, can benefit from sustained release formulations to maintain steady and predictable drug levels.
d) Gastrointestinal Irritation: Drugs that cause gastrointestinal irritation or side effects may benefit from sustained release formulations that release the drug gradually, potentially reducing irritation and improving tolerability.
e) Targeted Delivery: Drugs that need to be delivered to specific sites in the body over a prolonged period may benefit from sustained release formulations designed for localized or targeted delivery.

f) Chronic Conditions: Drugs used to treat chronic conditions where long-term therapy is required can benefit from sustained release formulations to provide continuous therapeutic effect and improve patient adherence to treatment regimens.
g) Compliance Enhancement: Drugs for which poor patient compliance is a concern due to frequent dosing requirements can benefit from sustained release formulations that reduce the number of daily doses needed.
h) Improvement of Therapeutic Effect: Drugs that exhibit improved therapeutic efficacy when maintained at constant levels in the body, rather than fluctuating concentrations, may benefit from sustained release formulations.
i) Pharmacokinetic Profile: Drugs with pharmacokinetic profiles (such as erratic absorption or rapid metabolism) that can be improved by controlled release mechanisms may be suitable candidates for sustained release formulations [45], [101].

Considering the previously stated facts acetaminophen and amoxicillin trihydrate are eligible for making sustained release dosage forms. Acetaminophen has systemic half-life of 2 to 3 hours [102] and amoxicillin trihydrate has systemic half-life of around 61 minutes [103]. So, they have relatively low half-life which can be made sustained for the better bioavailability.

Paracetamol if used frequently causes hepatotoxicity, so repeated doses may cause irritation in the liver. That is why sustaining the dosage form can help with reducing the dose administration of the drug which leads to the lesser toxicity to the liver and more patient compliance.

Dose of Amoxicillin trihydrate has to be adjusted in case of patients with renal impairment otherwise it may cause accumulation of drug and renal toxicity. Although amoxicillin trihydrate is well-absorbed orally, widely distributed in tissues, primarily eliminated unchanged via renal excretion, but it has a relatively short elimination half-life, which is why sustaining its dose can help with the therapeutic effect for a longer period of time and increases patient compliance.

CHAPTER 4

MATERIALS AND METHODS

4. MATERIALS AND METHODS

4.1. Material-

a. Amoxicillin trihydrate API (SRL Pvt, Ltd),
b. Acetaminophen API (Loba Chemie Pvt. Ltd.),
c. Sodium alginate (Loba Chemie Pvt. Ltd.),
d. Calcium chloride (Loba Chemie Pvt. Ltd.),
e. Sodium chloride (SRL Pvt, Ltd),
f. Potassium chloride (SRL Pvt, Ltd),
g. Disodium hydrogen phosphate (Merck Life science Pvt. Ltd.),
h. Potassium dihydrogen phosphate (Merck Life science Pvt. Ltd.),
i. Hydrochloric acid (Merck Life science Pvt. Ltd.),
j. Glacial acetic acid (Merck Life science Pvt. Ltd.),
k. Chitosan (SRL Pvt. Ltd.),
l. Aloe vera gel (aloe vera plant),
m. Corn starch (Merck Life science Pvt. Ltd.),
n. Trisodium orthophosphate dodecahydrate (Merck Life Sciences Pvt. Ltd.),
o. Double distilled water.

4.1.1. AMOXICILLIN TRIHYDRATE-

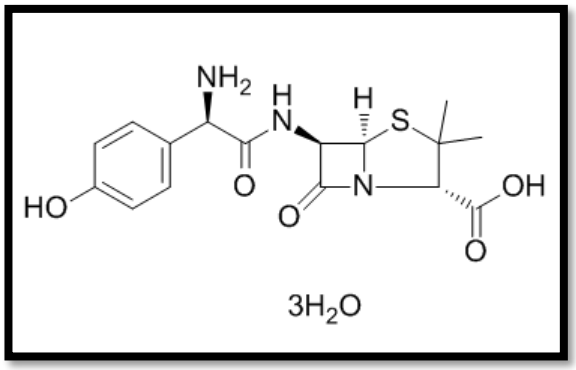

Fig 19- structure of Amoxicillin

Amoxicillin Trihydrate (fig-19) (AMOX) or α-amino-*p*-hydroxybenzyl penicillin; trihydrate, a trihydrate form of amoxicillin, a widely used moderate to broad-spectrum, semisynthetic aminopenicillin antibiotic with bactericidal activity, used in various bacterial infections like skin and soft tissue infection, ulcer, bladder infection, urinary tract infection, throat infection etc. its molecular weight is 419.5 g/mol. Amoxicillin is a beta-lactam antibiotic and it binds to the cell wall of target bacteria at the penicillin binding protein (PBP) site to inhibit crosslinking of peptidoglycan chains which are necessary for the major strength of cell walls of bacteria. This results in the disruption of cell wall synthesis of bacteria and causes in cell lysis [104]. Amoxicillin trihydrate is mostly stable in pH range of 2 to 8 [105]. In extreme acidic pH (below pH 2) the beta-lactam ring of amoxicillin hydrolyses and forms Amoxicilloic acid (figure 23) [105] which is a thiazolidine monocarboxylic acid. It is a conjugate acid of amoxicilloate.

Formation of amoxicilloic acid minimizes the effect of amoxicillin as an antimicrobial agent [106]. But no significant change in absorbance maxima or peak amplitudes, of amoxicillin trihydrate in acidic media cannot be detected in UV-spectrophotometric analysis, which indicates that the formation of amoxicilloic acid does not show any shift in its wavelength. However, its efficacy can be compromised by bacterial resistance mechanisms, such as the production of beta-lactamase enzymes that hydrolyse the beta-lactam ring of amoxicillin, rendering it inactive. To overcome this, amoxicillin is sometimes combined with beta-lactamase inhibitors like clavulanic acid, which protect amoxicillin from degradation by beta-lactamase-producing bacteria.

4.1.1.1. Mechanism of action of Amoxicillin trihydrate-

It is a β-lactam antibiotic that belongs to the group of penicillin [107], [108]. The basic structure of penicillin, 6-aminopenicillanic acid (fig-20) consists of a ring of thiazolidine fused with a ring of β-lactam with a side chain. Amoxicillin (molecular weight: 365.4 g mol^{-1}) presents in the side chain an amino group that improves stability towards acids, however, it can be part of consecutive reactions in neutral or alkaline conditions.

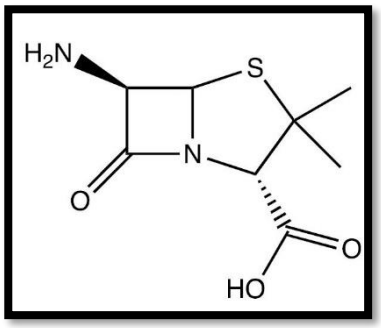

Fig 20- Molecular structure of 6-aminopenicillanic acid.

In human medicine, penicillin are the most commonly consumed antibiotics in the European Union, where amoxicillin is consumed in 22 of 30 countries. Also in other countries such as India [109] or Brazil [110]. Amoxicillin is very active against both Gram positive (Gram+) and Gram-negative (Gram-) organisms, including several enteric pathogenic organisms. Amoxicillin is widely used in veterinary practice for the treatment of systemic gastrointestinal infections. Amoxicillin is a known penicillin that is added to medicated foods at a level of 250 to 500 mg kg^{-1}, due to its resistance to gastric juice. In the case of humans, after oral intake of amoxicillin, 43 – 75% is excreted and not metabolized [108], [111], [112]. Considering that there is a high rate of excretion and that its half-life is 9 days, this antibiotic has been found in wastewater [113], [114] and effluents from wastewater treatment plants and even in surface water [115].

This antibiotic is commonly used due to the broad spectrums in terms of its mechanism of action (Fig. 21) as it stops the proliferation of different bacteria. In general, penicillin [116], [117] inhibit a bacterial enzyme called the transpeptidase enzyme that is involved in the synthesis of the bacterial cell wall [118]. The β-lactam rings are involved in the inhibition mechanism. Penicillin covalently binds to the active site of the enzyme, leading to irreversible

inhibition. In addition to the above, it is important to mention that amoxicillin has amphoteric properties [89], a property conferred by its three main functional groups, COOH (pKa_1= 2.7), NH_2 (pKa_2 = 7.4) and OH (pKa = 9.6) as shown in Figure 22 [92], [91], [90].

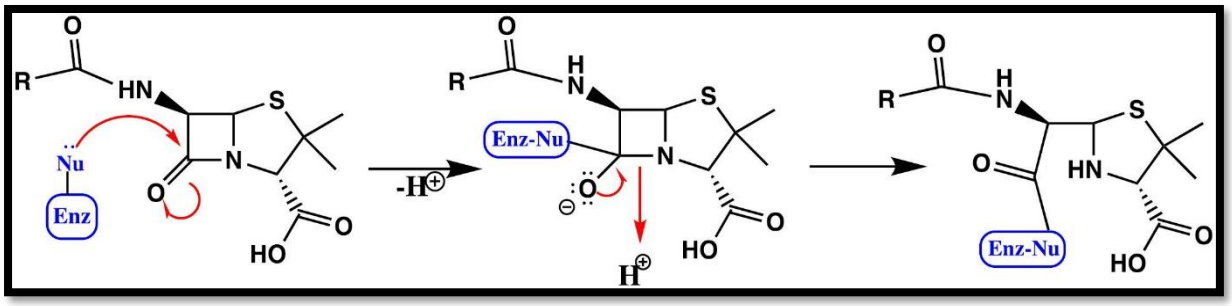

Fig 21- Mechanism of action of amoxicillin

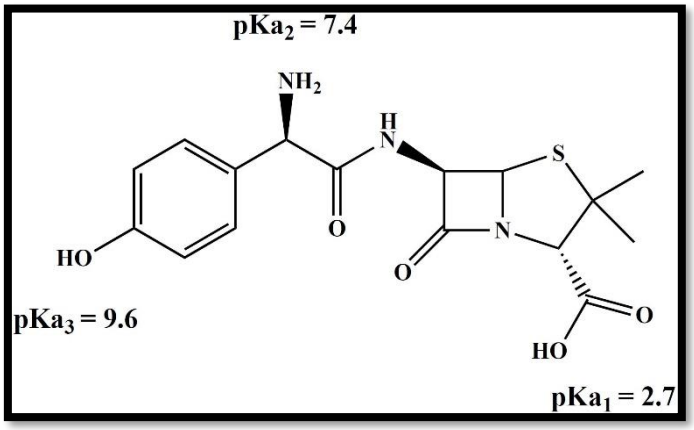

Fig 22- pKa values of the main groups of amoxicillin.

In this way, the molecular structure is affected by the pH changes to which it may be subjected. In this way, at pH 10 amoxicillin degradation is recorded in time of 24 h at pH 5 there is no further degradation and at pH 1 degradation is recorded transforming amoxicillin into amoxicilloic acid (fig-) [93], [94], [95].

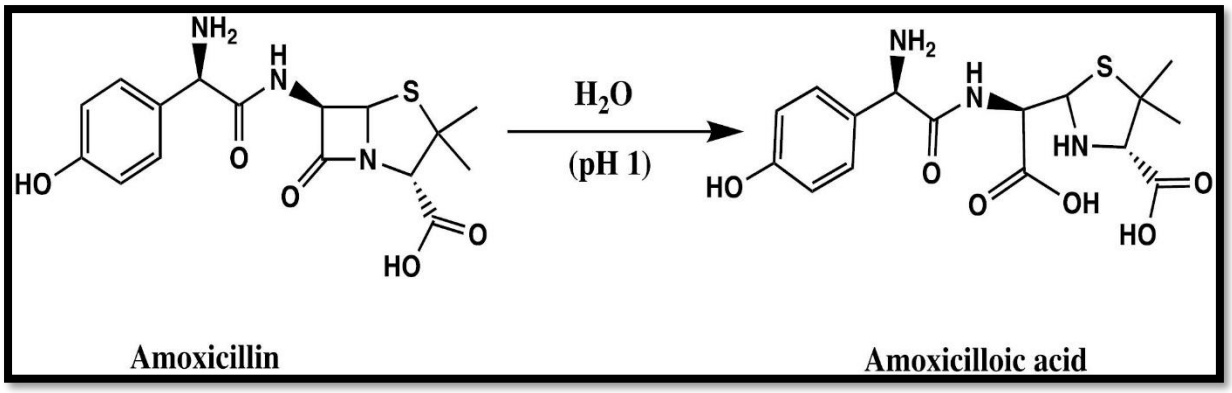

Fig 23- Passage from amoxicillin to amoxicilloic acid at acidic pH

Thus, at pH values close to neutral, amoxicillin is more stable and has less degradation than at acidic or basic pH. However, it should be considered that at high temperatures (55°C) approximately amoxicillin, even if it is in a solution at neutral pH, it decomposes [96].

In short primary mechanism of action involves the inhibition of bacterial cell wall synthesis, which is crucial for bacterial growth and survival.

a. Penetration and Binding:

Amoxicillin is absorbed and distributed throughout the body, reaching various tissues and fluids. Once it reaches the site of infection, it penetrates the bacterial cell wall and binds to specific penicillin-binding proteins (PBPs).

b. Inhibition of Cell Wall Synthesis:

PBPs are enzymes involved in the final stages of the synthesis of peptidoglycan, critical component of the bacterial cell wall. Amoxicillin binds to these PBPs, particularly PBP-1A, PBP-1B, and PBP-2. By binding to PBPs, amoxicillin inhibits their activity, preventing the cross-linking of peptidoglycan chains. This cross-linking is essential for the structural integrity and rigidity of the bacterial cell wall.

c. Weakening of the Cell Wall:

The inhibition of PBPs leads to the accumulation of peptidoglycan precursors and a weakened cell wall. This weakened cell wall cannot withstand the osmotic pressure within the bacterial cell.

d. Cell Lysis and Death:

The compromised cell wall ultimately leads to cell lysis (bursting) and the death of the bacterium. The bacterium is unable to maintain its shape and integrity, resulting in its destruction [103].

4.1.1.2. Pharmacokinetic properties of Amoxicillin trihydrate-

- **Absorption-**

Bioavailability: Amoxicillin trihydrate is well absorbed from the gastrointestinal tract, with an oral bioavailability of approximately 70-90%.

Peak Plasma Concentration (Cmax): Peak plasma concentrations are typically reached within 1-2 hours after oral administration.

Effect of Food: The presence of food does not significantly affect the absorption of amoxicillin.

- **Distribution-**

Volume of Distribution (Vd): The volume of distribution is approximately 0.3-0.4 L/kg, indicating that amoxicillin is widely distributed throughout the body fluids and tissues.

Protein Binding: Amoxicillin is approximately 17-20% bound to plasma proteins.

Tissue Penetration: Amoxicillin penetrates well into various tissues and body fluids, including the middle ear effusions, sinuses, bile, peritoneal fluid, and pleural fluid. However, it penetrates poorly into the cerebrospinal fluid unless the meninges are inflamed.

- **Metabolism-**

Amoxicillin is not significantly metabolized in the body. Most of the drug is excreted unchanged in the urine.

- **Elimination-**

Half-Life (t1/2): The elimination half-life of amoxicillin is approximately 1-1.5 hours in individuals with normal renal function.

Renal Clearance: Amoxicillin is primarily eliminated by the kidneys. Approximately 60-70% of the administered dose is excreted unchanged in the urine within the first 6 hours.

Biliary Excretion: A small amount of amoxicillin is excreted in the bile.

- **Other Pharmacokinetic Parameters-**

Clearance (Cl): The total body clearance of amoxicillin is about 15-25 mL/min/kg.

Steady-State Concentration (Css): Achieved within 24-48 hours with repeated dosing.

- **Special parameters-**

Renal Impairment: In patients with renal impairment, the elimination half-life of amoxicillin is prolonged, and dosage adjustments may be necessary.

Hepatic Impairment: Hepatic impairment has minimal impact on the pharmacokinetics of amoxicillin, as it is primarily eliminated by the kidneys.

Paediatrics: In children, the pharmacokinetics of amoxicillin are generally similar to those in adults, although the dosage may need to be adjusted based on body weight and renal function.

Geriatrics: In elderly patients, renal function may be reduced, necessitating dosage adjustments to avoid accumulation and toxicity.

- **Drug Interactions**

Probenecid: Co-administration with probenecid can decrease the renal tubular secretion of amoxicillin, leading to increased plasma concentrations and prolonged half-life.

Allopurinol: Concurrent use may increase the risk of rash.

- **Clinical Implications**

Dosing Frequency: Given its relatively short half-life, amoxicillin is typically administered multiple times a day to maintain effective plasma concentrations. Its normal dose is 500mg every 8hours or 25mg/kg every 4 hours.

Therapeutic Uses: Effective against a wide range of bacterial infections, including respiratory tract infections, urinary tract infections, skin infections, and Helicobacter pylori eradication in combination with other agents [103].

4.1.2. ACETAMINOPHEN-

Acetaminophen (Paracetamol/PCM) (fig-24), scientifically known as N-acetyl-para-aminophenol, commercially popular as Tylenol and Panadol, is a COX-1,2 and 3 inhibitors, a non-narcotic and non-opioid analgesic, an antipyretic, a NSAID, used to treat fever and mild to moderate pain also headaches, muscle aches, arthritis, backaches, and toothaches. It is a widely used OTC drug or over the counter medication [119]. It is an odourless white powder with bitter taste. Its molar mass is 151.163 g/mol. It helps to reduce the fever and pain when given in required dose. The absorption of drug is unaffected by food. But alcohol intake may increase the risk of hepatotoxicity of the drug.

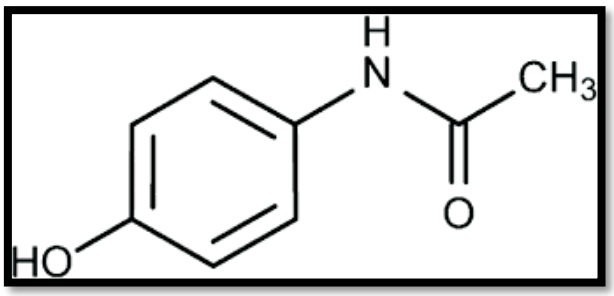

Fig 24- Structure of Acetaminophen

4.1.2.1. Mechanism of action of Acetaminophen-

The exact mechanism of action of acetaminophen (acetaminophen) isn't fully understood, but it is believed to work through several mechanisms:

- **Inhibition of Prostaglandin Synthesis:**

Acetaminophen is thought to reduce pain and fever primarily by inhibiting the synthesis of prostaglandins. Prostaglandins are chemicals in the body that promote inflammation, pain, and fever. Unlike nonsteroidal anti-inflammatory drugs (NSAIDs) like ibuprofen, which inhibit prostaglandin synthesis throughout the body, acetaminophen is believed to selectively inhibit a specific form of the enzyme cyclooxygenase (COX), particularly COX-2 in the brain, which is involved in prostaglandin production related to pain and fever.

- **Action in the Central Nervous System:**

Acetaminophen has a more significant effect in the central nervous system (CNS) compared to the periphery. It is thought to act on the central nervous system to reduce the perception of pain and to regulate the body's temperature control mechanisms. It may influence the serotonergic system in the brain, which is involved in modulating pain.

- **Interaction with Endocannabinoid System:**

Some research suggests that acetaminophen may interact with the endocannabinoid system, which plays a role in regulating pain and inflammation. Specifically, acetaminophen might increase the availability of endocannabinoids, which can contribute to its analgesic effects.

- **Effects on Nitric Oxide Pathways:**

Acetaminophen may also affect nitric oxide pathways, which are involved in pain and inflammatory responses [100].

4.1.2.2. Pharmacokinetic Properties of Acetaminophen-

Acetaminophen (Paracetamol) has well-defined pharmacokinetic properties, which describe how the drug is absorbed, distributed, metabolized, and excreted in the body. Here's an overview:

- **Absorption:**

Route: Acetaminophen is usually administered orally, but it can also be given rectally, intravenously, or as a suppository.

Onset: After oral administration, it is rapidly absorbed from the gastrointestinal tract. Peak plasma concentrations are typically reached within 30 to 60 minutes.

Bioavailability: The oral bioavailability of acetaminophen is approximately 70-90%, meaning most of the drug reaches systemic circulation after oral ingestion.

- **Distribution:**

Volume of Distribution: The volume of distribution is relatively large, about 0.9-1.0 L/kg. This suggests that acetaminophen is widely distributed throughout body tissues.

Protein Binding: Acetaminophen is only mildly bound to plasma proteins, with binding generally reported around 10-25%. This means a significant portion of the drug remains unbound and active.

- **Metabolism:**

Acetaminophen is primarily metabolized in the liver. It undergoes three main metabolic pathways:

Glucuronidation: The majority of acetaminophen is conjugated with glucuronic acid to form glucuronides.

Sulfation: Another significant portion is conjugated with sulfate to form sulfate conjugates.

Oxidation: A small amount is metabolized by the cytochrome P450 enzyme system to form a reactive metabolite, N-acetyl-p-benzoquinone imine (NAPQI), which is normally detoxified by conjugation with glutathione.

Toxic Metabolite: In cases of overdose, the capacity of the liver to detoxify NAPQI may be overwhelmed, leading to liver damage.

- **Excretion:**

Route: Acetaminophen and its metabolites are primarily excreted via the kidneys.

Half-Life: The elimination half-life of acetaminophen is approximately 1-3 hours in healthy individuals, though it can be longer in individuals with liver impairment or in overdose situations.

Urine: About 90-95% of the administered dose is excreted in the urine within 24 hours, mostly as conjugates (glucuronides and sulphates) [120], [121].

3.2. Methods-

3.2.1. Preparation of pH 1.2 hydrochloric acid buffer-

At first, 0.2M potassium chloride (KCl) solution was prepared. To prepare that we have to take 14.91gm KCl in a 1000ml volumetric flask and add sufficient amount of double distilled water to dissolve it completely. After dissolving the KCl rest amount of double distilled water was added to the flask to make the volume up to 1000ml. By this method 0.2M KCl was prepared. [Molecular weight of KCl is 74.55g/mol (39.090g/mol of potassium +35.5g/mol of chloride) so to prepare 0.2M KCl we will need 14.91g KCl.]

Secondly, we need to prepare 0.2M Hydrochloric acid solution. For that we need to take 7.2ml of concentrated Hydrochloric acid and pour it dropwise in a 1000ml volumetric flask containing some double distilled water. When the two liquids are mixed completely rest amount of double distilled water was added to flask to make the volume up to 1000ml. With this procedure we have prepared 0.2M HCl. [Molecular weight of HCl is 36.5g/mol (1g/mol of hydrogen +35.5g/mol of chloride, so to prepare 0.2M HCl we will need 7.2g hydrochloric acid. The specific gravity (density relative to the density of water) of hydrochloric acid solution is 1.18 g/ml. So, 7.2 ml of hydrochloric acid solution is taken, then 7.2 ml/(1.18 g/ml)= 6.101ml HCl is taken.]

Finally, 50ml of the prepare 0.2M KCl solution and 85ml of the prepared 0.2M HCl solution was taken in a 200ml volumetric flask and rest of the volume was made up using double distilled water to prepare pH 1.2 hydrochloric acid buffer according to Indian Pharmacopoeia (2018, vol-1, page- 885) [83].

3.2.2. Preparation of pH 6.8 phosphate buffer-

Firstly, some amount of double distilled water was taken in a 1000ml volumetric flask. After that 11.45g potassium dihydrogen phosphate, 28.80g disodium hydrogen phosphate was accurately weighed by Precisa Electronic balance model XB 600M/C, Switzerland. Then these reagents were added to the volumetric flask containing double distilled water, one by one. The flask was shaken vigorously to dissolve all the solids in the water. After the solids are dissolved completely the volume of the solution was made up to 1000ml using double distilled water. With this method pH 6.8 phosphate buffer was prepared according to Indian Pharmacopoeia (2018, vol-1, page- 889-889) [83].

3.2.3. Preparation of pH 7.4 phosphate buffer-

To start with some amount of double distilled water was taken in a 1000ml volumetric flask. Thereafter Precisa Electronic balance model XB 600M/C, Switzerland was used to accurately weigh 2.38 g of disodium hydrogen phosphate, 0.19 g of potassium dihydrogen phosphate and 8.0 g of sodium chloride. Then these compounds are added to the double distilled water in the volumetric flask one by one. The flask was vigorously shaken for a few minutes to completely dissolve the substances. Finally, when the components are dissolved completely double distilled water is added to the volumetric flask up to the mark of 1000ml. Lastly the preparation of pH 7.4 phosphate buffer saline was prepared according to Indian Pharmacopoeia (2018, vol-1, page- 889) [83].

3.2.4. Calibration curve of Amoxicillin trihydrate in pH 1.2, 6.8, 7.4 and neutral 7 (double distilled water)-

Accurately weighed (Precisa Electronic balance model XB 600M/C, Switzerland) amount of 10 mg Amoxicillin trihydrate was dissolved in 100ml of four different types of media which are pH 1.2, 6.8, 7.4 buffers and double distilled water. Then the solution was diluted 10times with each specific media to get stock solution which have concentration of 10µg/ml. Aliquots of this solution was further diluted to 10ml to get the standard working solutions having concentration of 2 to 10µg/ml, with 2µg/ml incrementation. All the concentrations were scanned in the Shimadzu double beam UV-2450, UV-Vis spectrophotometer from 200nm to 400nm against each specific media as blank and readings were taken at the lambda max 228nm [122]. The standard working solution was prepared 3 times a from the 10µg/ml stock solutions and their mean was taken. This process was also repeated 3times, for 3 constructive days, in 3 different seasons, in 3 different instruments to check its repeatability.

3.2.5. Calibration curve of Acetaminophen in pH 1.2, 6.8, 7.4 and neutral 7 (double distilled water)-

Accurately weighed (Precisa Electronic balance model XB 600M/C, Switzerland) amount of 10 mg Acetaminophen was dissolved in 100ml of four different types of media which are pH 1.2, 6.8, 7.4 buffers and double distilled water. Then the solution was diluted 10times with each specific media to get stock solution which have concentration of 10µg/ml. Aliquots of this solution was further diluted to 10ml to get the standard working solutions having concentration of 2 to 10µg/ml, with 2µg/ml incrementation. All the concentrations were scanned in the Shimadzu double beam UV-2450, UV-Vis spectrophotometer from 200nm to 400nm against each specific media as blank and readings were taken at the lambda max 243nm [123]. The standard working solution was prepared 3 times a from the 10µg/ml stock solutions are scanned. This process was also repeated 3times, for 3 constructive days, in 3 different seasons, in 3 different instruments checking for its repeatability.

3.2.6. Calibration curve of the combination of Amoxicillin trihydrate and Acetaminophen in pH 1.2, 7.4 and neutral 7 (double distilled water)-

Accurately weighed (Precisa Electronic balance model XB 600M/C, Switzerland) amount of Amoxicillin trihydrate and Acetaminophen (ratio-5:3) was dissolved in 100ml of pH 1.2, 7.4 and neutral 7 (double distilled water). Then the solution was diluted 10times with each specific media to get stock solution which have concentration of 10µg/ml. Aliquots of this solution was further diluted to 10ml to get the standard working solutions having concentration of 2 to 10µg/ml, with 2µg/ml incrementation. All the concentrations were scanned in the Shimadzu double beam UV-2450, UV-Vis spectrophotometer from 200nm to 400nm against each specific media as blank and readings were taken at the lambda max 228nm, 243nm and 232nm. The standard working solution was prepared 3 times a from the 10µg/ml stock solutions and their mean was taken. This process was also repeated 3times, for 3 constructive days, in 3 different seasons.

3.2.7. Assessment by HPLC method-

Required amount of amoxicillin trihydrate and acetaminophen was weighed and dissolved in DD water (neutral pH7) and 1.2 pH media to attain 100µg/ml solutions. Also, another two solutions were made using these two drugs in the mentioned neutral and 1.2 acidic buffer solutions. Lasty one acidic (pH 1.2) and one neutral solution was made of amoxicillin trihydrate and acetaminophen in 5:3 ratio. After that 1ml of the acidic solutions were taken and diluted with 1ml of HPLC grade acetonitrile (as highly acidic pH can cause damage to the column). Then these solutions were passed through a syringe filter for removal of particulate impurities before loading the samples to the HPLC instrument. And then the graph was observed and interpreted for any changes.

Chromatographic conditions-

i. The separation technique was performed on a 4.60×250mm, 5-micron Phenomenex Luna 5µm C18 (2) 100A column, installed in Shimadzu, LC-AD20. The solvent system of mobile phase for each sample was set at different ratio of Acetonitrile (pump A) and DD water (pump B).
ii. For acetaminophen the mobile phase ratio was 50:50 (for A: B) (fig 9).
iii. For amoxicillin trihydrate the ratio was, 97.5:2.5 (for A: B) (fig 10).
iv. And for the combination, the ratio was set at, 70:30 (for A: B) (fig 11).
v. Flow rate- 1ml/min.
vi. Dejection wavelength- 243nm for acetaminophen, 228nm for amoxicillin trihydrate, and both for the combination.
vii. Injected volume- 20µl [124], [125].

3.2.8. Preparation of sodium alginate hydrogel beads-

Sodium alginate powder was accurately weighed and added in required amount of double distilled water. Then it was kept on a magnetic stirrer at 500rpm for 1 hour or until the powder is completely dispersed in the system homogeneously. The addition of acetaminophen and amoxicillin trihydrate was done in this step. Another calcium chloride solution was prepared in distilled water for crosslinking of the beads. The alginate solution was poured in a syringe with 22G needle and it was dropwise added to the calcium chloride solution with constant stirring of 500rpm (fig-25). The beads were formed instantly. They were cured for 5mins in the calcium chloride solution, then strained and rinsed to wash of excess crosslinking agent. And dried in a petri dish for overnight or sometimes occasionally used a hot air oven [81].

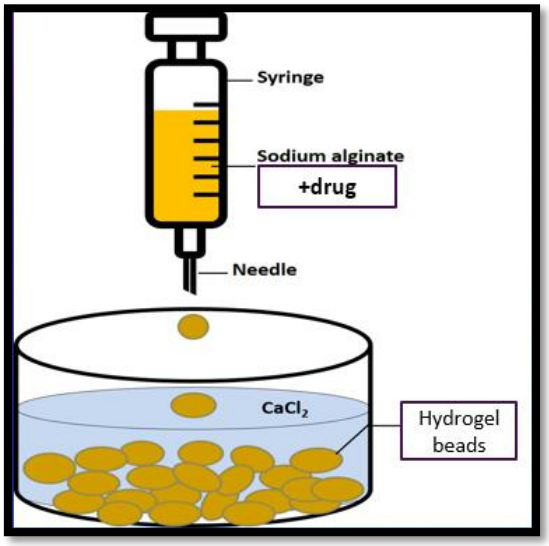

Fig 25- Preparation of sodium alginate beads by dropping gel method

3.2.9. Modifications of calcium alginate hydrogel beads for better sustained release effects-

3.2.9.1. Coating of beads-

The prepared calcium alginate beads were coated to prolong the drug release. Coating of beads was done by two methods-

- **Aloe-Corn starch coating**- Drug loaded calcium alginate beads were freshly prepared and dipped in aloe vera gel and corn starch paste (20:1) mixture and then dried over night or in a hot air oven if needed [126].
- **Homopolymer coating**- A highly viscous sodium alginate polymeric solution was prepared (10%w/v). In that solution freshly prepared beads were dipped and then they were dried over-night [127], [128].

3.2.10. Evaluation of drug loaded sodium alginate beads-

3.2.10.1. Determination of particle size-

The size of the dried acetaminophen and amoxicillin trihydrate loaded calcium alginate beads were determined by an optical microscope (Eurolab, 10x eye piece, 10x objective). The optical micrometer was calibrated using a standard stage micrometer having an accuracy of 0.01mm. 10 optical division is equal to 15 division of stage micrometer. So, 1 division of optical micrometer measures at 0.015mm. The mean diameter was determined for randomly selected 50 beads from each formulation by multiplying with the calibration factor. In case of non-spherical beads an average of its long diameter and short diameter was considered [129]. . Average size of randomly selected 50 beads were calculated using the following formula-

$$X = \frac{\sum \mathrm{Xi}}{N}$$

Where, X = the mean bead diameter, X_i = is the individual bead diameter, and N= is the number of beads selected for particle size measurement.

3.2.10.2. Drug entrapment efficiency-

At first some quantities of beads were accurately weighed and placed in a conical flask where 100ml of pH 7.4 phosphate buffer was added. The beads were allowed to swell for a few hours to overnight on a mechanical shaker. As sodium alginate is easily swellable in basic media it took less time to swell and eventually the beads broke down in the buffer. After that we filtered the solution and the filtrate was taken, diluted 10 times using the same buffer solution and its absorbances were recorded. The observed absorbance was divided by the slope of the respective drug and the practical yield was calculated. It was then divided by the theoretical yield to get %DEE. It is calculated using the following equation [130] :

$$\%Drug\ entrapment\ efficiency = \frac{practical\ amount\ of drug}{theoritical\ amount\ of\ drug} \times 100$$

3.2.10.3. Swelling study-

Swelling studies of drug loaded calcium alginate beads have been carried out at different pH viz.; 1.2, and 7.4. The dried, pre-weighed beads were loaded in a pre-weighed tea bag and the total system was immersed in the chosen medium, at room temperature. The tea bags were then removed from the buffered medium after a definite time interval. The liquid drops that adhering on the tea bag surfaces were wiped by using blotting papers and weight increase has been monitored by means of an electronic balance of accuracy ±0.1 mg (Precisa Electronic balance model XB 600M/C, Switzerland). The process has been repeated until the beads attained an equilibrium swelling.

The degree of swelling (%S) has been determined by using the equation [131], [132]:

$$\%swelling\ index = \frac{weight\ of\ swollen\ beads - initial\ weight\ of\ beads}{initial\ weight\ of\ beads}$$

3.2.10.4. Drug release study-

Drug release from the beads were checked by using the USP dissolution type 2 (paddle) apparatus. The baskets were filled with 750ml pH 1.2 hydrochloric acid buffer. The dissolution apparatus was plugged in and the heater was started. When the temperature of the vessels turned 37±0.5ºC, accurately weighed amount of 100mg beads were added to the baskets and the rotation of the paddles were turned on. After 2 hours 250ml of trisodium orthophosphate dodecahydrate solution was added to each basket for changing the pH of the solution to 7.4 by continuous dissolution method mentioned in the Indian Pharmacopoeia (2018, vol-1, page-306) [83]. Samples of 10ml were withdrawn every 5, 10, 15, 30, 45, 60, 90, 120, 180mins for upto 8 hours and 10ml of fresh appropriate buffers were added to maintain the sink condition. The samples were then tested for their absorbances to check the cumulative percentage release of drug from the beads [133], [134].

3.2.10.5. Antimicrobial study-

Antimicrobial study is performed to check for the antimicrobial activity of the drug. The agar well diffusion assay is extensively applied to assess the antimicrobial activity of natural products [135], [136]. This assay is based on the measurement of the size of a growth inhibition zone around the sample, which may be placed onto a paper disc or into a well cut into the agar. Briefly, in this assay the agar plate surface is inoculated by spreading a volume of the microbial inoculum over the entire agar surface. Then a circular hole (6–8 mm) is made aseptically into the agar using a sterile cork borer, and a suitable volume (200 µL) of the sample solution at the chosen concentration is applied into the well. The agar plate is then incubated under proper conditions to allow the antibacterial agent to diffuse into the agar medium and inhibit the growth of the microbial strain tested. This results in a measurable growth inhibition zone [137].

3.2.10.6. Thermogravimetry Differential Thermal Analysis -

Thermogravimetry Differential Thermal Analysis also known as TG/DTA is a technique mainly used to check purity of a compound by exposing the material to heat. DTA or differential thermal analysis is used to measure the temperature change between a specimen and a reference when both are subjected to the same amount of heat. DTA can be used to determine the temperatures of endo and exothermic events, and to show phase transitions. Whereas TGA or thermogravimetric analysis measures weight gain or loss as a material is heated to understand vaporization, absorption, decomposition, and more. TGA can also be used to determine the organic and inorganic content of materials, and to study the kinetics and thermodynamics of decomposition reactions. Effectively a combination of a DSC and a TGA, this instrument

allows easy correlation of data for samples up to over 1500° C as both tests are be run concurrently. Collecting both the DTA curve showing delta temperature and the weight loss allows a greater understanding of what happens in the material.

Experimental conditions were-

The thermal characteristics of the beads were determined by Thermogravimetry Differential Thermal Analysis (TG/DTA) (Pyris Diamond TG/DTA, Perkin Elmer, Singapore), and compared with those obtained using both blank beads and drug as raw material. 3-10mg sample was taken and kept in an open top T-zero aluminium pan. The temperature was kept at 25-250 ^{o} C with an increase rate of 10 ^{o} C/min. A constant air flow of dry N_2 gas was administered throughout the experimentation. The data was detected by the detector and the graph was plotted against Temperature (^{o}C) vs %weight. Amoxicillin trihydrate and Acetaminophen in their pure form and a formulation containing both the drugs were evaluated to check for their in determining purity and composition of materials, drying and ignition temperatures of materials and knowing the stability temperatures of compounds. The data obtained in DTA is used to determine temperatures of transitions, reactions and melting points of substances. With the change of temperature and time if any changes of the mass of the compound is observed or not can be determined with this method [138], [139].

3.2.10.7. X-ray diffraction analysis-

It is a non-destructive technique that provides detailed information about the crystallographic structure, chemical composition, and physical properties of a material. It is based on the constructive interference of monochromatic X-rays and a crystalline sample. An X-ray instrument contains three main items: an X-ray source, a sample holder and an XRD detector. The X-rays are produced by the source illuminate the sample. It was then diffracted by the sample phase and entered the detector. By moving the tube or sample and detector to change the diffraction angle (2θ, the angle between the incident and diffracted beams), the intensity was measured, and diffraction data were recorded. Depending on the geometry of the diffractometer and the type of sample, the angle between the incident beam and the sample can be either fixed or variable and is usually paired with the diffracted beam angle [140], [141].

The experimental parameters were-

Drug loaded beads were measured for their X-Ray diffraction pattern by using X-Ray diffractometer (D8, Bruker, Germany). With Transmission mode- 2θ scale of 5-42^{o}, with an exit slit of 0.6mm. The step size taken was 0.02^{o}, with a counting time of 0.3sec/step, and voltage 45Kv, current 30 mA. The values were detected and recorded. Finally, the graph was plotted against 2θ degrees vs Intensity. Amoxicillin trihydrate and Acetaminophen in their pure form and a formulation containing both the drugs were evaluated to check their structure and if any impurities are present in the substances [138].

3.2.10.8. Scanning Electron Microscopy-

Scanning electron microscopy or SEM is a type of electron microscope that produces images of a sample by scanning the surface with a focused beam of electrons. The electrons interact with atoms in the sample, producing various signals that contain information about the surface topography and composition of the sample. The instrumentation is configured with mainly 4 parts- A electron source, lenses, scanning coil, detector. Firstly, a layer of carbon tape is stick on top of two SEM stubs. Two batches of beads were selected for evaluation in Scanning electron microscopy, one batch with blank beads of the polymer and one batch with both the drugs with the polymer. Then a few sphere-shaped beads were selected from both the batches and mounted on the carbon paper tape on top of the SEM stubs. Then the beads were coated with gold in HITACHI MC1000 Ion Sputter Coater. Gold coating thickness was 6nm. Coating parameters were 40mA for 8 seconds. After the coating the SEM stubs containing the beads were installed in the SEM machine, for which we used- HITACHI SU3800 Scanning Electron Microscope with EDS (Energy Dispersive Spectroscopy) facility. Suitable images of the beads were selected [142], [143].

3.2.10.9. Fourier Transform Infrared Spectroscopy -

Fourier Transform Infrared Spectroscopy, also known as FTIR Analysis or FTIR Spectroscopy, is an analytical technique used to identify organic, polymeric, and, in some cases, inorganic materials. The FTIR analysis method uses infrared light to scan test samples and observe chemical properties. FTIR spectra of Amoxicillin trihydrate, Acetaminophen and drug loaded beads were recorded in IR spectra were recorded on a Bruker, FT-IR spectrophotometer using KBr optics. Each sample was mixed with KBr and converted into disc at 100 kg pressure using a hydraulic press. The spectra were recorded within 4000-400 cm-1 wave numbers [144], [145].

3.2.11. Data treatment of Release kinetics-

It was observed that the drug release from alginate beads depends on the test method as well as the media used in the experiment [146]. Differences between the release profiles obtained using various dissolution tests were observed. These results suggest the necessity of knowledge about the underlying in vivo processes and the need to translate this research to the in vitro test systems [147]. The obtained release profiles were analysed with zero-order, first-order kinetics as well as Higuchi [148], [149] and Korsmeyer-Peppas [150], [151] (fig-26).

- **Zero-order model**

Drug dissolution from dosage forms that do not disaggregate and release the drug slowly can be represented by the equation:

$$Q_0 - Q_t = K_0 t$$

Rearrangement of the equation yields:

$$Q_t = Q_0 + K_0 t$$

Where Q_t is the amount of drug dissolved in time t, Q_0 is the initial amount of drug in the solution (most times, $Q_0 = 0$) and K_0 is the zero order release constant expressed in units of concentration/time. To study the release kinetics, data obtained from in vitro drug release studies were plotted as cumulative amount of drug released versus time [152], [153].

Application: This relationship can be used to describe the drug dissolution of several types of modified release pharmaceutical dosage forms, as in the case of some transdermal systems, as well as matrix tablets with low soluble drugs in coated forms, osmotic systems, etc. [154].

- **First order model**

This model has also been used to describe absorption and/or elimination of some drugs, although it is difficult to conceptualize this mechanism on a theoretical basis. The release of the drug which followed first order kinetics can be expressed by the equation:

$$\frac{dC}{dt} = -Kc$$

Where K is first order rate constant expressed in units of time^{-1}.

This equation is also expressed as:

$$logC = logC_0 - \frac{Kt}{2.303}$$

Where C_0 is the initial concentration of drug, k is the first order rate constant, and t is the time [153], [155]. The data obtained are plotted as log cumulative percentage of drug remaining vs. time which would yield a straight line with a slope of (-K/2.303).

Application: This relationship can be used to describe the drug dissolution in pharmaceutical dosage forms such as those containing water-soluble drugs in porous matrices [156], .

- **Higuchi model**

The first example of a mathematical model aimed to describe drug release from a matrix system was proposed by Higuchi in 1961 [149]. Initially conceived for planar systems, it was then extended to different geometrics and porous systems [157]. This model is based on the hypotheses that-

(i) Initial drug concentration in the matrix is much higher than drug solubility;
(ii) Drug diffusion takes place only in one dimension (edge effect must be negligible);
(iii) Drug particles are much smaller than system thickness;
(iv) Matrix swelling and dissolution are negligible;
(v) Drug diffusivity is constant; and
(vi) Perfect sink conditions are always attained in the release environment.

Accordingly, Higuchi model expression is given by the equation:

$$f_t = Q = A\sqrt{D(2C - C_s)C_s t}$$

Where Q is the amount of drug released in time t per unit area A, C is the drug initial concentration, Cs is the drug solubility in the matrix media and D is the diffusivity of the drug molecules (diffusion coefficient) in the matrix substance.

This relation is valid during all the time, except when the total depletion of the drug in the therapeutic system is achieved. To study the dissolution from a planar heterogeneous matrix system, where the drug concentration in the matrix is lower than its solubility and the release occurs through pores in the matrix, the expression is given by the following equation:

$$f_t = Q = \sqrt{\frac{D\delta}{\tau}(2C - \delta C_s)C_s t}$$

Where D is the diffusion coefficient of the drug molecule in the solvent, δ is the porosity of the matrix, τ is the tortuosity of the matrix and Q, A, Cs and t have the meaning assigned above. Tortuosity is defined as the dimensions of radius and branching of the pores and canals in the matrix. In a general way it is possible to simplify the Higuchi model [149] as (generally known as the simplified Higuchi model):

$$f_t = Q = K_H \times t^{\frac{1}{2}}$$

Where, K_H is the Higuchi dissolution constant. The data obtained were plotted as cumulative percentage drug release versus square root of time [156].

Application: This relationship can be used to describe the drug dissolution from several types of modified release pharmaceutical dosage forms, as in the case of some transdermal systems and matrix tablets with water soluble drugs [149], [158] .

- **Korsmeyer-Peppas model**

Korsmeyer et al. (1983) derived a simple relationship which described drug release from a polymeric system equation. To find out the mechanism of drug release, first 60% drug release data were fitted in Korsmeyer Peppas model [151].

$$\frac{M_t}{M_\infty} = Kt^n$$

Where Mt / M∞ is a fraction of drug released at time t, k is the release rate constant and n is the release exponent. The n value is used to characterize different release for cylindrical shaped matrices.

In this model, the value of n characterizes the release mechanism of drug as described in Table 1. For the case of cylindrical tablets, $0.45 \leq n$ corresponds to a Fickian diffusion mechanism, $0.45 < n < 0.89$ to non-Fickian transport, $n = 0.89$ to Case II (relaxational) transport, and $n > 0.89$ to super case II transport [159]. To find out the exponent of n the portion of the release curve, where Mt / M∞ < 0.6 should only be used. To study the release kinetics, data obtained

from in vitro drug release studies were plotted as log cumulative percentage drug release versus log time.

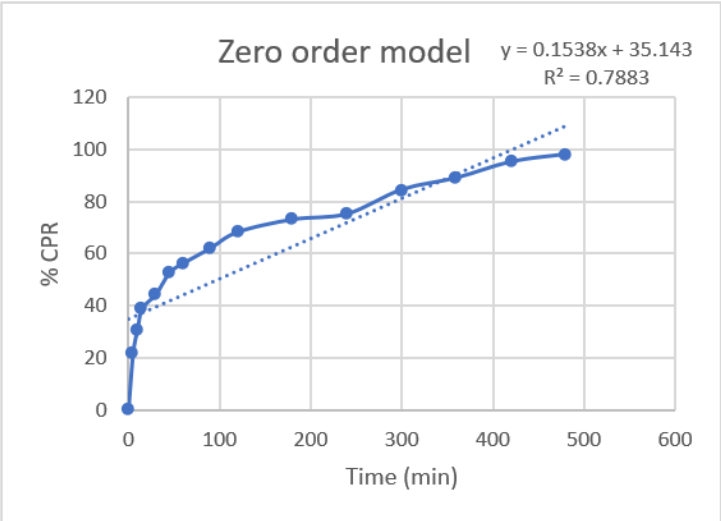

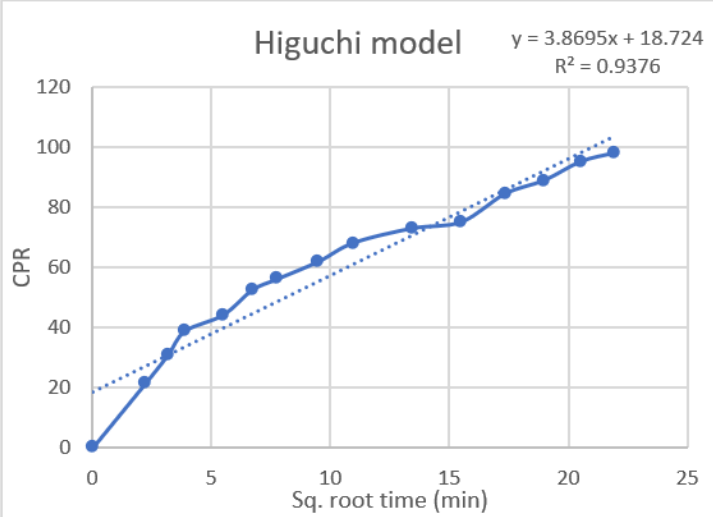

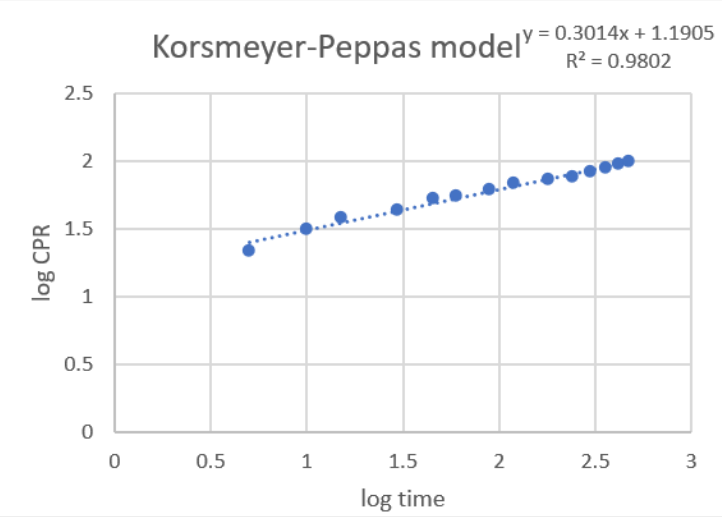

Fig 26- Drug release kinetics models

CHAPTER 5

RESULT AND DISCUSSION

5. RESULT AND DISCUSSION

5.1. Materials

No further modifications were done of the chemical compounds. Experimentations were conducted by using the bought laboratory grade chemicals only.

5.2. Method development and Validation-

5.2.1. Development of Amoxicillin Trihydrate Calibration curve in different pH media-

The experiment was conducted by preparing four solutions of amoxicillin trihydrate in four different pH media- pH 1.2 hydrochloric acid buffer, 6.8 phosphate buffer, 7.4 phosphate buffer [83] and neutral pH 7 (DD water) and checking it absorbance at 228nm for all the concentrations (2-10 µg/ml). All the concentrations were scanned from 200nm to 400nm in the Shimadzu double beam UV-2450, UV-Vis spectrophotometer against each specific media as blank (fig. 27,28) and readings were taken at the lambda max 228nm [122] (table:1). Similar to acetaminophen another sharp peak is observed in cases of buffer media at around 200-205nm, which does not form when neutral DD water is used. This peak maybe the result from interference of buffer solutions [160][161].

The regression coefficient (R^2) values of amoxicillin trihydrate it was found to be 0.9916±0.002 in 1.2 pH, 0.9933±0.00185 in 6.8 pH, 0.992±0.000585 in 7.4 pH, 0.99463±0.002063 in neutral pH, at 228nm lambda max.

Table-1: Absorbance spectrum of Amoxicillin trihydrate:

CONCENTRATION (µg/ml)	**ABSORBANCE (228nm) (mean±sd)**			
	In 1.2 pH buffer	In 6.8 pH buffer	In 7.4 pH buffer	In neutral pH 7 (DDW)
0	0	0	0	0
2	0.041±0.003	0.05±0.005	0.038±0.002	0.057±0.0024
4	0.079±0.002	0.092±0.002	0.078±0.003	0.098±0.005
6	0.119±0.001	0.131±0.003	0.105±0.001	0.137±0.002
8	0.159±0.002	0.186±0.001	0.135±0.002	0.177±0.001
10	0.221±0.004	0.244±0.001	0.177±0.002	0.246±0.003
R^2 Value	**0.9916±0.002**	**0.9933±0.00185**	**0.992±0.000585**	**0.99463±0.00206**

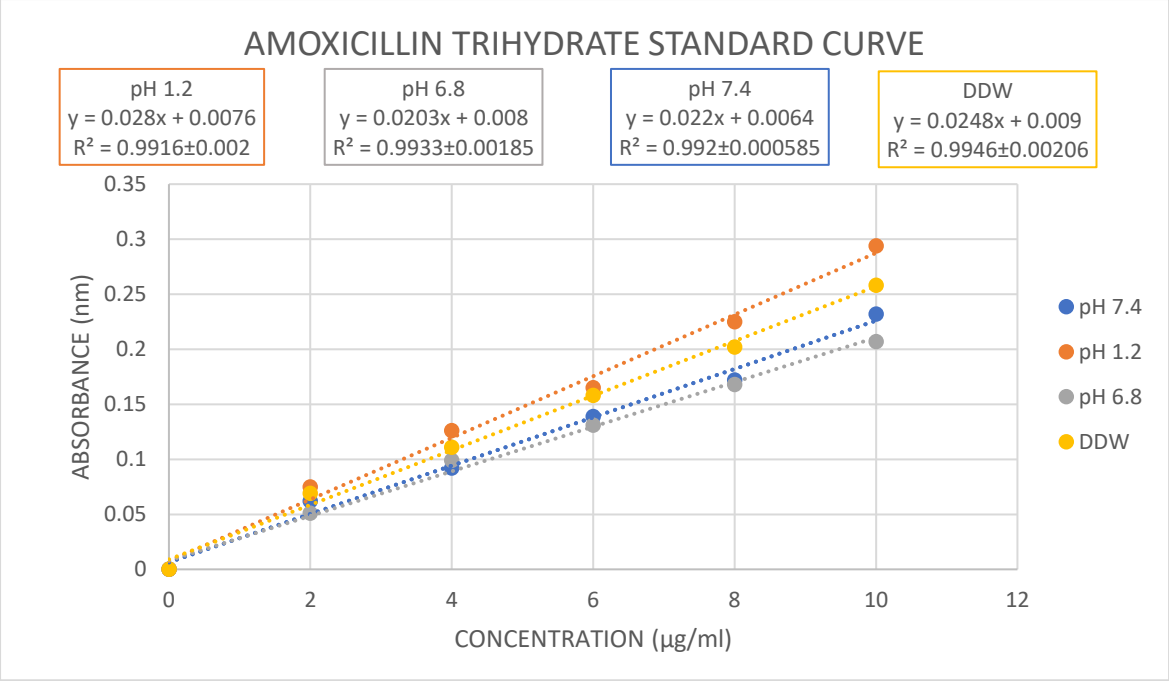

Fig 27: Standard curve of Amoxicillin Trihydrate (lambda max 228nm)

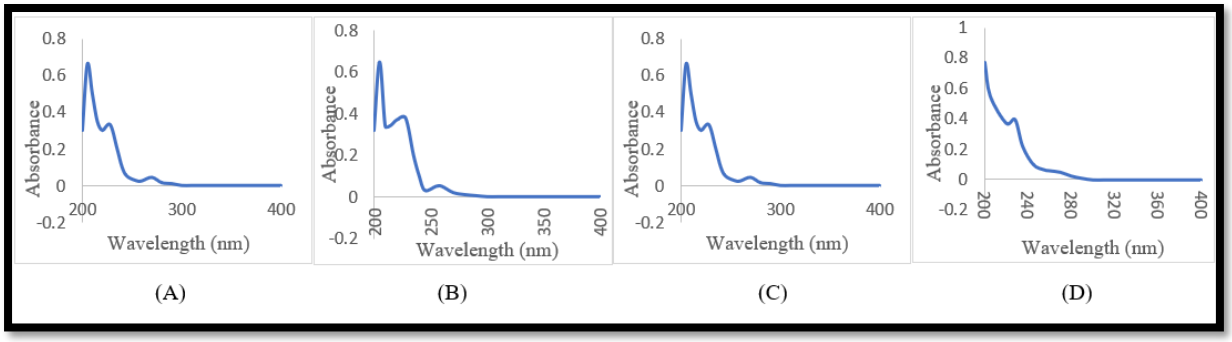

Fig 28: Spectrophotometric scan of Amoxicillin trihydrate (lambda max 228nm) in pH (A) 1.2, (B) 6.8, (C) 7.4, (D) neutral.

5.2.2. Development of Acetaminophen Calibration curve in different pH media-

After conducting the experiment of acetaminophen in 4 different pH media- pH 1.2 hydrochloric acid buffer, 6.8phosphate buffer, 7.4 phosphate buffer [83] and neutral pH 7 (DD water) in different concentration (2-10 µg/ml), and the absorbances are recorded at 243nm to construct the standard curve (table-2). The UV- spectrum of acetaminophen in various pH media shows its absorbance maxima at 243nm [123] (fig- 29,30). Although we found that there is a formation of an extra peak at around 200-205nm [2][3] when buffers are used as a solvent media. But this peak is not observed when we are using neutral double distilled water. That is why we can say the extra peak may appear due to the presence of solvent buffers.

The regression coefficient (R^2) values of acetaminophen in neutral pH- 0.99917±0.00035, in pH 7.4 is- 0.9989±0.00025, in pH 6.8 is- 0.9932±0.0006, in pH 1.2 is- 0.9959±0.00044. All the R^2 values are greater than 0.99, which indicates better linearity of the method.

Table-2: Absorbance spectrum of Acetaminophen in different solvent:

CONCENTRATION (µg/ml)	**ABSORBANCE (243nm) (mean±sd)**			
	In Double Distilled Water	In 7.4 pH buffer	In 6.8 pH buffer	In 1.2 pH buffer
0	0	0	0	0
2	0.141±0.003	0.167±0.002	0.192±0.002	0.144±0.004
4	0.299±0.003	0.288±0.003	0.395±0.004	0.254±0.001
6	0.474±0.003	0.438±0.004	0.585±0.003	0.384±0.002
8	0.633±0.002	0.588±0.002	0.787±0.008	0.529±0.002
10	0.800±0.003	0.730±0.005	0.891±0.002	0.612±0.003
R^2 Value	**0.99917±0.00035**	**0.9989±0.00025**	**0.9932±0.0006**	**0.9959±0.00044**

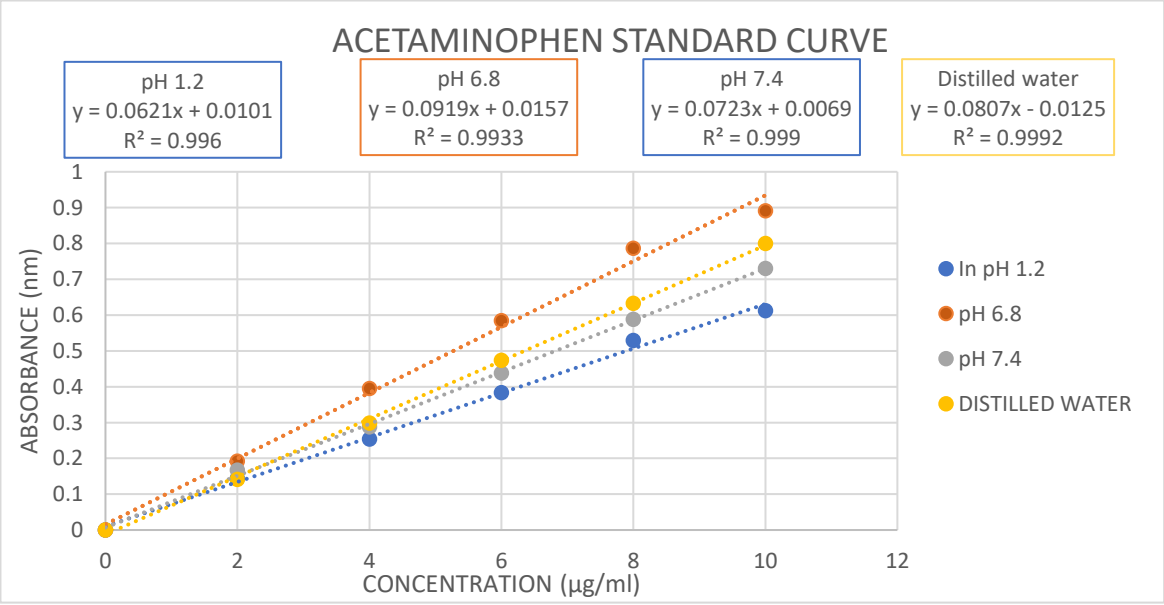

Fig 29: Standard Curve of Acetaminophen (lambda max 243nm)

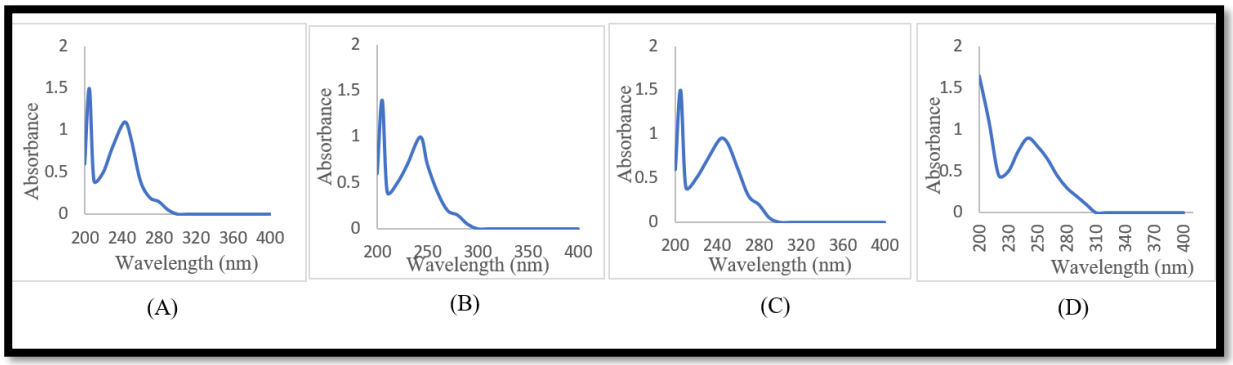

Fig 30: Spectrophotometric scan of Acetaminophen (lambda max 243nm) in pH (A) 1.2, (B) 6.8, (C) 7.4, (D) neutral.

5.2.3. Development of Calibration curve of paracetamol and amoxicillin trihydrate combination in different pH media-

The above-mentioned experiment was conducted by preparing a solution combining amoxicillin trihydrate and paracetamol (5:3 ratio) in pH 1.2 hydrochloric acid buffer, 7.4 phosphate buffer [83], and neutral 7 (double distilled water). The overlay of these two drugs has isoabsorptive point at 232nm (fig-33). And the combination shows its absorbance maxima at 232nm as well (fig-32). So, we took the absorbances of the various concentrations of the combination in 232nm, 243nm, and 228nm and constructed the standard curve accordingly (fig-31) (table-3).

Table-3: absorbance of Acetaminophen and Amoxicillin trihydrate in combination in neutral pH 7-

CONCENTRATION (µg/ml)	ABSORBANCE Amoxicillin trihydrate (228 NM)	ABSORBANCE Acetaminophen (243 NM)	ABSORBANCE combination (232 NM)
0	0	0	0
2	0.173±0.003	0.167±0.002	0.173±0.003
4	0.305±0.001	0.295±0.004	0.305±0.004
6	0.406±0.002	0.412±0.002	0.426±0.001
8	0.525±0.003	0.533±0.004	0.551±0.004
10	0.690±0.003	0.700±0.001	0.726±0.003
R^2 Values	**0.9934±0.000153**	**0.9961±0.0001**	**0.9958±0.000252**

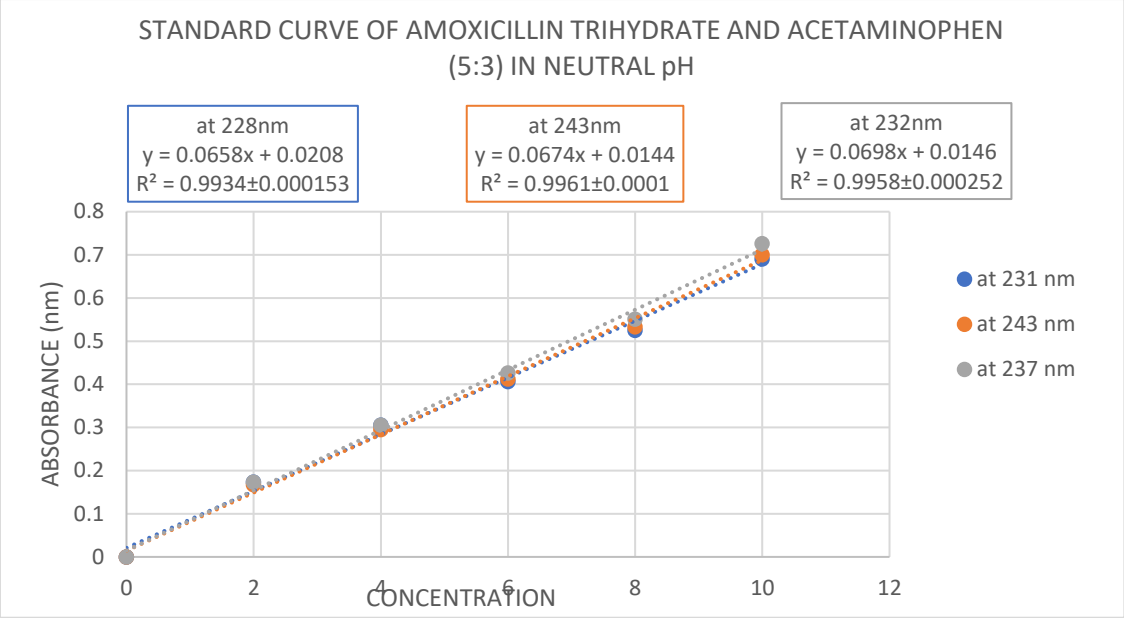

Fig 31: Standard Curve of Acetaminophen + Amoxicillin trihydrate combined (lambda max 243nm, 228nm, 232nm)

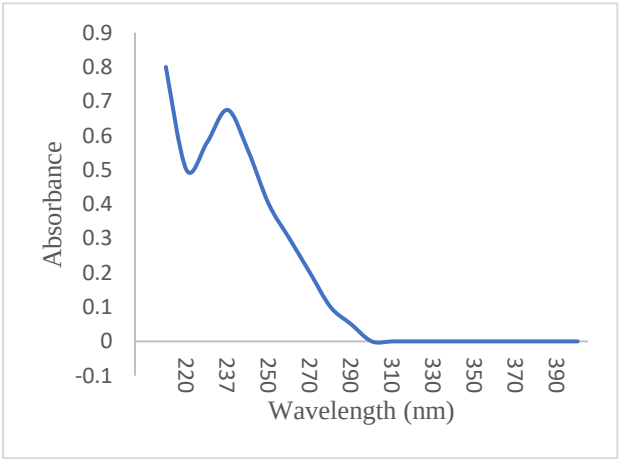

Fig 32: Scan of Acetaminophen and Amoxicillin trihydrate (10µg/ml each) in a combination and the lambda max was found at 232nm. (the additional peak around 210nm occurred due to the presence of buffer media)

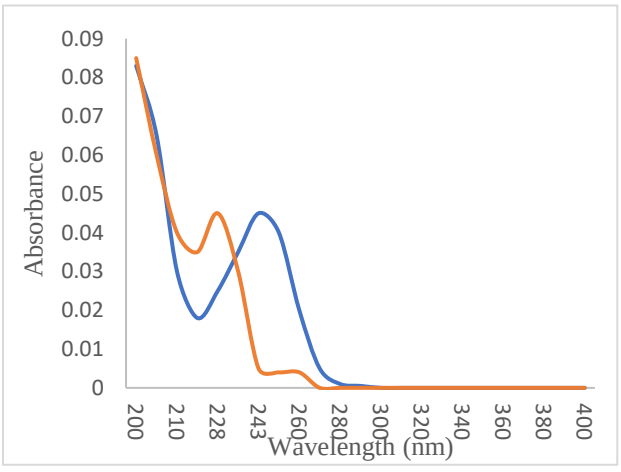

Fig 33: Scan of Acetaminophen (243nm)[blue] and Amoxicillin trihydrate (228nm) [orange] (3:5 ratio) separately (overlay) with isoabsorptive point at 232nm

5.2.4. HPLC analysis of Amoxicillin trihydrate and Acetaminophen-

The percentage area detected by the HPLC technique indicates the purity of the substance [107][162]. HPLC analytical curves of amoxicillin, Acetaminophen and its 5:3 combination is shown in fig-34,35,36. It was found that for amoxicillin trihydrate at 228nm wavelength in neutral media shows 97% area at 2.8 min retention time, but in acidic media it is detecting 80% area at 2.8 min retention time. Which specifies slight decrease in the AUC of drug, in another word may be due to the degradation of pure Amoxicillin. In the combination at 228nm and 243nm, the same phenomena where neutral media shows 90% area but acidic media shows 72% area indicating possibilities of degradation in the acidic media. With these results we can conclude this might be the result of formation of amoxicilloic acid from amoxicillin trihydrate in acidic media, but no extra peak detected when checked in UV spectrophotometer. Further confirmatory tests yet to be conducted.

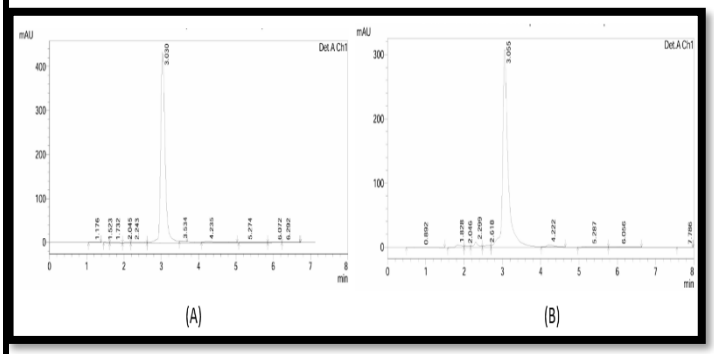

Fig 34- HPLC graph of Amoxicillin trihydrate in (A) neutral and (B) acidic1.2 pH

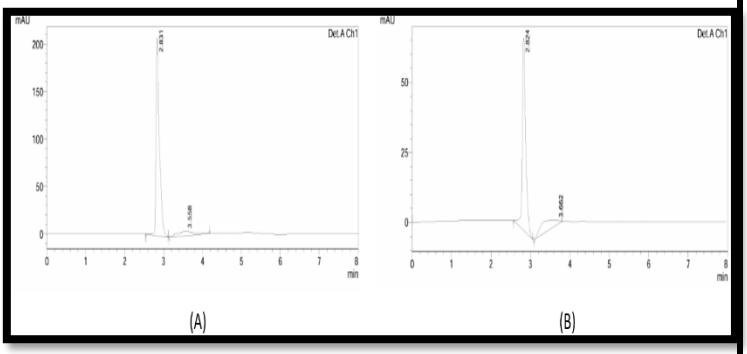

Fig 35- HPLC graph of Acetaminophen in (A) neutral and (B) acidic1.2 pH

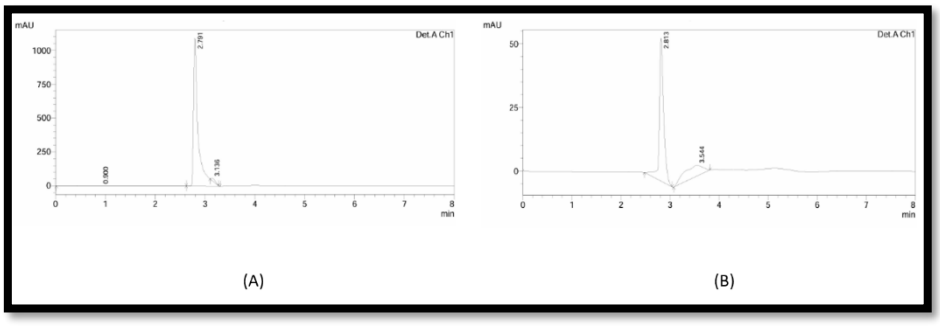

Fig 36- HPLC graph of Amoxicillin trihydrate and Acetaminophen (5:3) in (A) neutral and (B) acidic 1.2 pH

5.2.5. Simultaneous equation Method-

When a sample contains two or more drugs which shows absorbances in the UV-Spectrophotometer, and each of which absorbs at λ_{max} of others, it is possible to determine the drugs simultaneously using multi-component analysis by UV-Spectrophotometric Simultaneous Equation method. Two equations are are formed using the absorptivity coefficient values to check the concentrations of each drugs. The equations to determine the concentrations are-

$Cx = A_2ay_1 - A_1ay_2/(ax_1ay_2 - ax_2ay_1)$

$Cy = A_1ax_1 - A_2ax_1/(ax_1ay_2 - ax_2ay_1)$

Here,

A_1= absorbance of the mixture at 243nm.

$A_{2=}$ absorbance of the mixture at 228nm.

ax_1 and ax_2 are absorptivity of Acetaminophen at two wavelenths (243 & 228nm) respectively.

Ay_1 and ay_2 are absorptivity of Amoxicillin trihydrate at two wavelenths (243 & 228nm) respectively.

Cx= concentration ofAcetaminophen

Cy=concentration ofAmoxicillin trihydrate [163] [164].

5.2.6. Marketed solution preparation:

20 tablets of acetaminophen and 20 capsules of amoxicillin trihydrate were purchased from the market. The capsules were emptied and the tablets were finely crushed using a mortar and pestle. The quantity of powder equivalent to 10mg of acetaminophen and amoxicillin trihydrate were transferred into a 100ml volumatric flask and dissolved in distilled water, then filtered to get 100ug/ml solutions of each drug formulations. Required working concentrations were made as per necessary dilutions with water [164].

5.2.7. Validation parameters for simultaneous method:

The current methods and techniques were validated according to the parameters and guidelines given by *International Council for Harmonisation* or (ICH) (Q2R2) [88] like accuracy, linearity, intraday and interday precision, limit of detection, limit of quantification, ruggedness [165].

5.2.7.1. Linearity and Range:

Linearity stands for an event or series of events where one event follows another one directly and they show similar results. A linear analytical procedure has an ability to produce results proportional to the analyte concentrations.

Range of an analytical procedure refers to the intervals in between the upper and lower limits of analyte concentrations in the sample. Selection of a constant range is important as accuracy, precision and linearity all are examined in the range of analyte amount (concentration). In this experiment 5 concentrations of three standard working solutions of acetaminophen and

amoxicillin trihydrate, and their combination were prepared in a constant range of 2 to 10 µg/ml with 2µg/ml incrementations to examine their linearity. And this was evaluated as per slope and regression values.

5.2.7.2. Precision:

Precision is described as the closeness of the results obtained by measuring the same sample under same conditions as given. Interday and Intraday precision are checked. Precision can have 3 levels: repeatability, reproducibility and intermediate precision. For a precision study a homogeneous and authentic sample must be taken.

5.2.7.3. Intraday Precision:

The stock solutions of acetaminophen and amoxicillin trihydrate and their combination was diluted in the range of 2 to 10µg/ml and each concentration were checked for their absorbances at specific lambda max for 3 times a day and the %RSD was calculated.

5.2.7.4. Interday Precision:

From the same stock solutions, different concentrations of working standard solutions were diluted in the range of 2 to 10µg/ml and all the concentrations were checked for their absorbance variation at specific lambda max for 3 consecutive days and the %RSD was calculated.

5.2.7.5. Accuracy:

The accuracy or trueness of any analytical process is defined as the difference between measured value and the true value. Accuracy can be determined by recovery studies, where the previously analysed solutions were spiked by different concentrations of standard drug solutions.

5.2.7.6. Limit of Detection (LOD):

The detection limit of any analytical procedure is defined as the smallest amount of sample that can be detected but not always measured as a precise value. A simple equation is provided by ICH to calculate the LOD value-

$LOD = 3.3 \times (\sigma/S)$

Where σ= standard error of regression line and S= slope of calibration curve.

5.2.7.7. Limit of Quantification (LOQ):

The LOQ or limit of quantification of any analyte is the lowest amount of sample which is measured quantitatively with respect to accuracy and precision. This method is used to detect very small amounts components present in a sample like impurities or degradation. LOQ can be calculated by-

$LOQ = 10 \times (\sigma/S)$

Where, σ= standard error of regression line, S= slope of calibration curve.

5.2.7.8. Robustness:

Robustness of an analytical procedure is known as its capacity to produce similar results even after making small and deliberate changes in different parameters in the method, example- using different instrument or analyst.

5.2.8. Results of validation methods:

All the standard curves and validation tests were performed more than nine times throughout the year (summer, winter, monsoon) in UV spectrophotometer, but no significant changes of amoxicillin trihydrate in acidic media in the presence of acetaminophen, was observed. A sharp peak was observed near 205-210 lamda max, in acidic as well as phosphate buffer solutions, but not in neutral pH (doubled distilled water). So, this type of peak obtained in buffer solution only, due to interference of buffer [34,35]. After performing the experiments multiple times in three different UV spectrophotometer apparatus (1. Shimadzu double beam UV-2450, 2. LabIndia UV-2300 double beam, 3. SpectraMax M5), in various pH solutions we could not identify the changes in absorbance maxima or amplitudes of the peak due to the reported hydrolysis of beta-lactam ring of amoxicillin trihydrate to form amoxicilloic acid which occurs in acidic pH (<2) [105]. So, we performed HPLC for both the drugs and their combinations in acidic and neutral pH, but we could not find any distinguishable difference between them as well. Amoxicillin trihydrate does not produce any shift in its wavelength in acidic media. The ratio taken for amoxicillin trihydrate and acetaminophen in the combination is 5:3 according to their adult dose per kg body weight. Amoxicillin trihydrate has 25mg/kg every 4 hours [87] and acetaminophen has adult dose of 15mg/kg every 4 hours [166]. So, considering their dose the ratio of 5:3 is taken which shows similar effect and absorbance of these two drugs when checked in UV spectroscopy.

5.2.8.1. Linearity and Range:

The linearity of acetaminophen and amoxicillin trihydrate individually and in combination was examined in the range of 2 to 10 µg/ml in various pH media and the regression value was found accordingly. In pH 1.2, 6.8, 7.4 and neutral media (DD water) the regression values ± SD of acetaminophen were found to be- 0.9959±0.00044, 0.9932±0.0006, 0.9989±0.00025, 0.99917±0.00035 respectively at 243nm lambda max (table:1); and for amoxicillin trihydrate it was found to be- 0.9916±0.002, 0.9933±0.00185, 0.992±0.000585, 0.99463±0.002063 respectively at 228nm lambda max (table:2); there was an extra peak observed at around 200-205nm which occurred due to the presence of the aqueous buffer solvents [160], [161]. The combined solution was prepared, diluted and scanned against pH 1.2, 7.4 and neutral DD water and the regression values were found at 3 different lambda max that is 228nm (for amoxicillin), 243nm (for acetaminophen), 232nm (isoabsorptive point) which are- 0.9936±0.002, 0.9942±0.0031, 0.9936±0.0015 in pH 1.2, 0.9976±0.0011, 0.9969±0.0013, 0.9983±0.0021 in pH 7.4 and lastly 0.9934±0.000153, 0.9961±0.0001, 0.9958±0.000252 in Neutral pH (table:3).

5.2.8.2. Precision:

5.2.8.2.1. Intraday Precision:

The intraday precision in terms of % RSD of Acetaminophen was found to be 1.2816% at 243nm and the intraday precision of Amoxicillin trihydrate was found to be 1.467% at 228nm.

5.2.8.2.2. Interday Precision:

The interday precision in terms of % RSD of Acetaminophen was found to be 1.2057% at 243nm and the intraday precision of Amoxicillin trihydrate was found to be 1.7144% at 228nm.

5.2.8.3. LOD and LOQ:

The LOD values of acetaminophen in pH 1.2, 6.8, 7.4 and neutral DD water are found to be- 0.4208 µg/ml, 0.5715 µg/ml, 0.2028 µg/ml, 0.0819 µg/ml respectively. And similarly, the LOQ values are- 1.2752 µg/ml, 1.7318 µg/ml, 0.6145 µg/ml, 0.2484 µg/ml respectively.

The LOD values of amoxicillin trihydrate in different solvent medias such as pH 1.2, 6.8, 7.4, and neutral DD water are- 0.5315 µg/ml, 0.3047 µg/ml, 0.5939 µg/ml, 0.2596 µg/ml respectively. And the LOQ values were found to be- 1.6107 µg/ml, 0.9233 µg/ml, 1.7999 µg/ml, 0.7867 µg/ml respectively.

5.2.8.4. Accuracy:

Accuracy is checked by conducting recovery studies which show the ability of a method to reproduce similar results even after spiking the sample solutions with 50%, 100% and 150% of standard drug solutions. The recovery of amoxicillin trihydrate and acetaminophen was found in the range of 96 to 101% and 99 to 104%. The data is shown in table 4 and 5.

Table 4- Data for recovery studies of acetaminophen in Calpol (650 mg)-

Level of recovery (%)	Amount of formulation	Amount of pure drug	Total amount of drug	Absorbances (nm)	%RSD	Mean recover (%)
				0.154		
50	2	1	3	0.153	0.992	100.26
				0.156		
				0.181		
100	2	2	4	0.181	0.321	96.7
				0.180		
				0.238		
150	2	3	5	0.238	0.243	101.1
				0.232		

Table 5- Data for recovery studies of Amoxicillin Trihydrate in MOX capsule (500 mg)-

Level of recovery (%)	Amount of formulation	Amount of pure drug	Total amount of drug	Absorbances (nm)	%RSD	Mean recover (%)
				0.068		
50	2	1	3	0.075	5.753	99.16
				0.068		
				0.091		
100	2	2	4	0.088	1.701	101.1
				0.090		
				0.103		
150	2	3	5	0.097	4.232	104.3
				0.095		

4.8.1.5. Robustness:

Robustness studies were carried out by changing the instrument (LABINDIA UV-2300 double beam spectrophotometer) for both the drugs by scanning each concentration 3 times

(T1, T2, T3) for 3 days at both the wavelengths and later the %RSD was calculated. Ruggedness studies data is shown in table no. 6 and 7.

Table 6: Robustness studies of Acetaminophen at 243 nm

By changing instrument (LabIndia UV-2300 double beam) -

Drug	Wavelength	Conc. (µg/ml)	T1	T2	T3	Mean±SD	%RSD
Acetaminophen	243nm	0	0	0	0	0	0
		2	0.169	0.183	0.175	0.176±0.00989	5.62471
		4	0.323	0.346	0.337	0.3345±0.01626	4.86202
		6	0.504	0.53	0.569	0.517±0.01838	3.55605
		8	0.702	0.733	0.718	0.7175±0.02192	3.05509
		10	0.933	0.966	0.951	0.9495±0.02333	2.45755

Table 7: Robustness studies of Amoxicillin trihydrate at 228 nm

By changing instrument (Lab India UV-2300 double beam**)-**

Drug	Wavelength	Conc. (µg/ml)	T1	T2	T3	Mean±SD	%RSD
Amoxicillin trihydrate	228nm	0	0	0	0	0	0
		2	0.042	0.038	0.04	0.040±0.00282	7.07106
		4	0.078	0.077	0.076	0.077±0.00070	0.91239
		6	0.144	0.139	0.137	0.14±0.00565	4.04061
		8	0.183	0.174	0.177	0.178±0.00636	3.56524
		10	0.224	0.229	0.228	0.228±0.0056	2.48107

Table 8: Simultaneous Estimation Analysis Data and Summary of Validation Parameter

Parameter	Acetaminophen	Amoxicillin Trihydrate
Wavelength (nm)	243	228
Beer's Law Limit (µg/ml)	2-10	2-10
Regression Equation [in pH 1.2, 6.8, 7.4 and Neutral DD water]	y = 0.0621x + 0.0101 y = 0.0919x + 0.0157 y = 0.0723x + 0.0069 y = 0.0807x - 0.0125	y = 0.028x + 0.0076 y = 0.0203x + 0.008 y = 0.022x + 0.0064 y = 0.0248x + 0.009
Slope (m) [in pH 1.2, 6.8, 7.4 and Neutral DD water]	0.0621 0.0919 0.0723 0.0807	0.028 0.0203 0.022 0.0248
Intercept (c)	0	0
Regression Factor (R^2) [in pH 1.2, 6.8, 7.4 and Neutral DD water]	0.9959±0.0004 0.9932±0.0006 0.9989±0.00025 0.99917±0.00035	0.9916±0.002 0.9933±0.00185 0.992±0.000585 0.99463±0.002063

Intraday (n=3) (%RSD)	1.281%	1.467%
Interday (n=3) (%RSD)	1.205%	1.714%
LOD (µg/ml) [in pH 1.2, 6.8, 7.4 and Neutral DD water]	0.4208 0.5715 0.2028 0.0819	0.5315 0.3047 0.5939 0.2596
LOQ (µg/ml) [in pH 1.2, 6.8, 7.4 and Neutral DD water]	1.2752 1.7318 0.6145 0.2484	1.6107 0.9233 1.7999 0.7867

5.2.9. Explanation of validation tests-

The maximum absorbances of acetaminophen and amoxicillin trihydrate were found at 243 nm (fig. 4) and 228 nm respectively (fig. 6). As the values are relatively close to each other, their combination only shows one sharp peak the middle of these two points, i.e. at 232nm (fig, 8). The combination of these two drugs showed higher absorbances than their individual forms. Especially the absorbances of amoxicillin trihydrate increased rapidly when combined with acetaminophen (fig. 7,8).

There is an extra peak which appears near around 200-205nm, seen only in the case when we used buffers. But there were no such peaks when neutral DD water is used. So, it may be said that the extra peak was seen in the case of using buffers are caused by the interference of buffer solutions detected in the UV machine [160] [161].

Different solvent, we used 4 types of different solvent medias- pH 1.2, 6.8, 7.4 buffer and neutral DD water, which mimics the natural physiological pH of Gastrointestinal tracts in human beings. The stomach has pH around 1.2-2 to 2-4 which is highly acidic to moderately acidic, for the first 1-2 hours [167]. After the stomach the pH increases drastically from 6-7 in intestine. Then it increases even more in the colon around 7-7.4.

Amoxicillin trihydrate is mostly stable in a large pH range (2-8) [104] but it is unstable in strong acidic pH (lower than 2). The beta-lactam ring of Amoxicillin trihydrate hydrolyses in acidic pH and forms amoxicilloic acid [105] which is reported to slightly decrease the antimicrobial activity of amoxicillin itself [106]. But we found out that it does not alter any spectroscopic effect of amoxicillin.

After repeating the experiment numerous times in UV spectrophotometer, for further confirmation by using a highly sensitive instrument- HPLC was used to verify if the formation of amoxicilloic acid in acidic media actually shows no effect in the structural configuration of amoxicillin trihydrate. We prepared solutions of each drug and their combination in neutral and acidic pH, and injected the solutions in the HPLC column in respective lambda max of the drugs and their combinations. The desired peaks appeared indicating that there are no chromatographic change of amoxicillin trihydrate in acidic media.

In the HPLC technique the percentage area indicates the purity of the substance. It was found that for amoxicillin trihydrate at 228nm wavelength in neutral media shows 97% area at 2.8 min retention time, but in acidic media it is detecting 80% area at 2.8 min retention time. Which specifies slight decrease in the AUC of drug, in another word may be due to the degradation of pure Amoxicillin. In the combination at 228nm and 243nm, the same phenomena where neutral media shows 90% area but acidic media shows 72% area indicating possibilities of degradation

in the acidic media. With these results we can conclude this might be the result of formation of amoxicilloic acid from amoxicillin trihydrate in acidic media, but no extra peak detected when checked in UV spectrophotometer. Further confirmatory tests yet to be conducted.

Linearity of a method is justified by the regression value which should be near to 1 (from 0.9 to 1) for acceptance. Here for both the methods all the solutions of acetaminophen (table 1) and amoxicillin trihydrate (table 2) and their combinations (table 3) in different pH media has regression values of 0.9 and above, so all the batches show proper linearity.

The intraday and interday precision was determined by %RSD. The results obtained were 1.281%, 1.467% and 1.205%, 1.714% for PCM and AMOX respectively (table 8). As per ICH guidelines less than 2% RSD is acceptable. The results obtained are <2% which indicates greater precision of the above method.

The LOD values of acetaminophen in pH 1.2, 6.8, 7.4 and neutral DD water are found to be- 0.4208 µg/ml, 0.5715 µg/ml, 0.2028 µg/ml, 0.0819 µg/ml respectively. And similarly, the LOQ values are- 1.2752 µg/ml, 1.7318 µg/ml, 0.6145 µg/ml, 0.2484 µg/ml respectively. The LOD values of amoxicillin trihydrate in different solvent medias such as pH 1.2, 6.8, 7.4, and neutral DD water are- 0.5315 µg/ml, 0.3047 µg/ml, 0.5939 µg/ml, 0.2596 µg/ml respectively. And the LOQ values were found to be- 1.6107 µg/ml, 0.9233 µg/ml, 1.7999 µg/ml, 0.7867 µg/ml respectively. As per ICH guidelines minimum amount was detected by neutral DD water than other buffer media (table 8).

The accuracy was determined by spiking the marketed formulations with pure drug solutions and examined for their % recovery. The % recovery of acetaminophen (Calpol) was found to be 99-104% (table 5) and amoxicillin trihydrate (MOX) to be 96-101% (table 6), which falls in the acceptable range of 70-120% given by ICH guidelines.

5.2.10. Conclusions of the validation methods-

In conclusion, this study has investigated a simple, quick, cost effective and easy technique for the estimation of Acetaminophen and amoxicillin trihydrate in combination by simultaneous equation method. The method was validated by ICH guidelines Q2R2. The findings suggest that the following method is linear (R^2 values are >0.99), precise (%RSD values are lesser than 2%), accurate (%recovery falls under the range of 70-120%). These results have important implications for method validation and provide valuable insights into the simultaneous estimation of both the drugs separately as well as in a combination (at lambda max 232 nm). Moving forward, further research is warranted to explore the synergistic properties of the two drugs, acetaminophen and amoxicillin trihydrate combined in a single dosage form, can be administered in bacterial infections accompanying fever like- urinary tract infection, stomach ulcer, skin infections, lower respiratory tract infection, which is not yet available in the market. Overall, this study contributes to the understanding of simultaneous estimation of amoxicillin in presence of acetaminophen in pure drug form, combination and marketed dosage form.

5.3. FORMULATION DEVELOPMENT-

5.3.1. Formation of hydrogel beads-

Sodium alginate beads were prepared by crosslinking with calcium chloride. Few formulation variables (table 9) were considered which are-

a. **Concentration of Sodium Alginate**- 2%, 2.5%, 3% w/v
b. **Drug amount-**
    - Amoxicillin trihydrate- 60, 100, 140 mg.
    - Acetaminophen- 60, 100, 140 mg.
    - Combination- amoxicillin trihydrate: paracetamol – 100:60, 100:100.
c. **Concentration of crosslinking agent**- 1%, 2% w/v
d. **Gelation time**- 5, 10, 30 min

The ratio taken for amoxicillin trihydrate and acetaminophen in the combination is 5:3 according to their adult dose per kg body weight. Amoxicillin trihydrate has 25mg/kg every 4 hours [87] and acetaminophen has adult dose of 15mg/kg every 4 hours [166]. So, considering their dose the ratio of 5:3 is taken which shows similar effect and absorbance of these two drugs when checked in UV spectroscopy.

Table 9- Drug loaded calcium alginate beads with variations.

Batch	Sodium Alginate (%)	Calcium chloride (%)	Amoxicillin trihydrate (mg)	Acetaminophen (mg)	% Yield
I1	2%	1%	100	60	95%
I2	2.5%	1%	100	60	97%
I3	3%	1%	100	60	90.71%
I4	2.5%	1%	100	100	98.48%
I5	2.5%	1.5%	100	60	99.23%
I6	2.5%	2%	100	60	102.3%
A1	2%	1%	100	0	96%
A2	2.5%	1%	100	0	98.852%
A3	3%	1%	100	0	99%
A4	2.5%	1%	60	0	89.231%
A5	2.5%	1%	140	0	79.875%
A6	2.5%	2%	100	0	103.454%
E1	2%	1%	0	100	96%
E2	2.5%	1%	0	100	98.33%
E3	3%	1%	0	100	93.652%
E4	2.5%	1%	0	60	84.745%
E5	2.5%	1%	0	140	77.659%
E6	2.5%	2%	0	100	99.998%

Fig 37- Drug loaded calcium alginate beads

e. <u>Coating of the beads-</u>

- **Aloe-Corn starch coating**
- **Homopolymer coating**

Theoretically coating of beads should enhance drug entrapment as well as decrease the drug release rate from the beads. But as both of the drugs- amoxicillin trihydrate and acetaminophen belong to BCS class 1, i.e., high solubility and high permeability, leaching of the drug occurs in the coating solution leading to drug loss. This is why the coating method did not bring fruitful results.

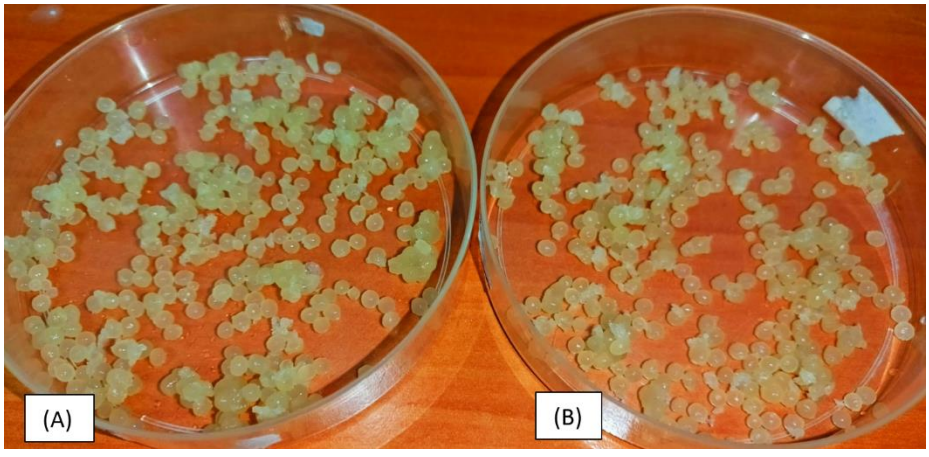

Fig 38- (A) Aloe vera and corn starch coated beads, (B) Homopolymer coated beads

5.4. EVALUATION STUDIES-

5.4.1. Particle size analysis:

The particle size of the dried Amoxicillin trihydrate and Acetaminophen loaded calcium alginate beads was measured using an Optical microscope (fig-39). Most beads appeared to be spherical in size, but the ones with unsymmetrical shape, the mean of major diameter and minor diameter were taken as equivalent diameter of the bead [168]. Average size of randomly selected 50 beads were calculated using the following formula (table-10)-

$$X = \frac{\sum \mathrm{Xi}}{N}$$

where X is the mean bead diameter, X_i is the individual bead diameter, and N is the number of beads selected for particle size measurement.

Table 10: Mean diameter of prepared hydrogel beads

Batch code	Diameter A	Diameter B	Diameter C	Mean diameter (mm)
I1	1.2214	1.2365	1.2415	1.233133±0.010464
I2	1.2801	1.2956	1.2865	1.2874±0.007789
I3	1.3254	1.3664	1.3452	1.345667±0.020504
I4	1.2845	1.2748	1.2896	1.282967±0.007518
I5	1.1315	1.1325	1.1369	1.133633±0.002879
I6	1.1452	1.1556	1.1654	1.1554±0.010101

It was clearly observed that the formulation batch containing high concentration of alginate polymer obtained larger beads compared to the batches containing lower concentration of polymer. This occurred due to the high viscosity of higher concentration of polymer leading to bigger droplet size from same needle [169]. Higher concentration of crosslinking agent also contributes to size increase of the beads, as they tend to adhere to the surface and increase its bulk [170].

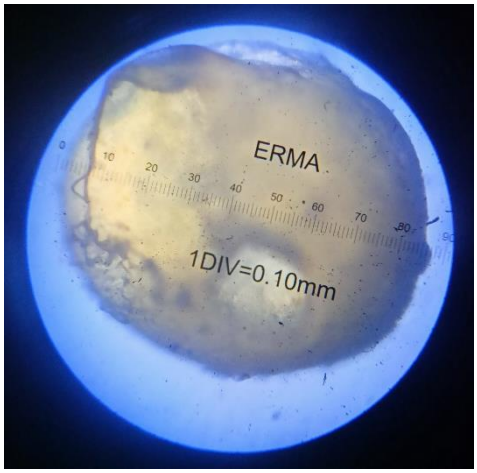

Fig 39- Microscopic image (10X) of a drug

5.4.2. Drug entrapment efficiency:

Drug entrapment efficiency or %DEE is a key parameter that ensures that drugs are properly trapped in the formulations. Required amount of beads were kept in 100ml of 7.4pH phosphate buffer for 4 hours. After the beads were swelled completely, they were crushed in a mortar and pestle, then the solution was filtered, diluted 10 times and checked for its absorbance. The observed absorbance was divided by the slope of the respective drug and the practical yield was calculated. It was then divided by the theoretical yield to get %DEE. It is calculated using the following equation:

$$\%Drug\ entrapment\ efficiency = \frac{practical\ amount\ of drug}{theoritical\ amount\ of\ drug} \times 100$$

Table 11- Drug entrapment efficiency of beads containing amoxicillin trihydrate

Batch code	Sodium Alginate (%)	Calcium chloride (%)	Amoxicillin trihydrate (mg)	% Yield	% Drug entrapment Efficiency (228nm)
A1	2%	1%	100	96%	84.417%
A2	2.5%	1%	100	98.852%	90.908%
A3	3%	1%	100	99%	87.065%
A4	2.5%	1%	60	89.231%	69.339%
A5	2.5%	1%	140	79.875%	67.426%
A6	2.5%	2%	100	103.454%	70.258%

Table 12- Drug entrapment efficiency of beads containing acetaminophen

Batch code	Sodium Alginate (%)	Calcium chloride (%)	Acetaminophen (mg)	% Yield	% Drug entrapment Efficiency (243nm)
E1	2%	1%	100	96%	83.253%
E2	2.5%	1%	100	98.33%	91.741%
E3	3%	1%	100	93.652%	85.235%
E4	2.5%	1%	60	84.745%	81.005%
E5	2.5%	1%	140	77.659%	69.185%
E6	2.5%	2%	100	99.998%	70.159%

Table 13- Drug entrapment efficiency of beads containing amoxicillin trihydrate (AMOX) and Acetaminophen (PCM)

Batch code	Sodium Alginate (%)	Calcium chloride (%)	AMOX (mg)	PCM (mg)	% Yield	% Drug entrapment Efficiency for AMOX (228nm)	% Drug entrapment Efficiency for PCM (243nm)	% Drug entrapment Efficiency For Isoabsorptive point (243nm)
I1	2%	1%	100	60	95%	84.454%	77.790%	80.082%
I2	2.5%	1%	100	60	97%	92.736%	89.522%	91.251%
I3	3%	1%	100	60	90.71 %	82.866%	79.790%	80.849%
I4	2.5%	1%	100	100	98.48 %	77.233%	68.965%	74.872%
I5	2.5%	1.5%	100	60	99.23 %	88.455%	83.298%	85.123%
I6	2.5%	2%	100	60	102.3 %	85.396%	79.860%	83.278%

From the above-mentioned tables, it was clearly observed that batches with 2.5% sodium alginate and 1% calcium chloride containing 100mg drugs have the optimum drug entrapment efficiency (table-11,12,13). Both of the drugs- amoxicillin trihydrate and acetaminophen belongs to BCS class I, i.e. high solubility and high permeability, which is why the entrapment of both the drugs is relatively low and if not, careful it may cause huge loss of the drugs in the crosslinking solution.

The batches with 2% calcium chloride have higher yield values but they do not increase the %DEE. Batches with higher drug concentrations leads more leaching of drug from the beads to the crosslinking solution leading to decreased %yield and %DEE. Also, high crosslinking density can lead to decreased elasticity of polymeric structure and might decrease the drug entrapment.

Table 14- Drug loaded calcium alginate beads with 30min curing time.

Batch code	Sodium Alginate (%)	Calcium chloride (%)	Drug (mg)	% Yield	% Drug entrapment Efficiency (243nm)	% Drug entrapment Efficiency (228nm)	% Drug entrapment Efficiency (232nm)
F1	2.5%	1%	100mg PCM	89.285%	12.484%		
F2	2.5%	1%	100mg AMX	91.855%		18.171%	
F3	2.5%	1%	100mg AMX+PCM	90.211%	11.765%	10.411%	11.903%

Table 15- Drug loaded calcium alginate beads with 10min curing time

Batch code	Sodium Alginate (%)	Calcium chloride (%)	Drug (mg)	% Yield	% Drug entrapment Efficiency (243nm)	% Drug entrapment Efficiency (228nm)	% Drug entrapment Efficiency (232nm)
F1	2.5%	1%	100mg PCM	87.365%	37.454%		
F2	2.5%	1%	100mg AMX	89.365%		35.571%	
F3	2.5%	1%	100mg AMX+PCM	90.051%	38.765%	36.761%	34.563%

When the curing time of the beads are increased- 10min (table-15) and 30min (table-14), the highly water-soluble drugs- paracetamol and amoxicillin trihydrate, readily leach out from the beads to the crosslinking solutions, leading poor entrapment of the drugs into the beads. So, the optimum curing time of beads are 5mins, where maximum drug entrapment efficiency is obtained.

5.4.3. Swelling study:

One of the most important characteristics of drug carriers is their swelling behaviour, which ensures that fluid will enter the polymer matrix and release the medication as a result. The pH of the environment strongly influenced the swelling behaviour of beads [79]. Swelling study was carried out in pH 1.2 for first 2 hours and then in pH 7.4 buffer using a tea bag. Swelling index of the beads were calculated using the following equation-

$$\%swelling\ index = \frac{weight\ of\ swollen\ beads - initial\ weight\ of\ beads}{initial\ weight\ of\ beads}$$

Table 16- Swelling index of the beads containing Amoxicillin trihydrate and Acetaminophen-

Batch code	Swelling index (%) with respect to time (minutes)					
	15 min	30 min	45 min	60 min	120 min	180 min (pH7.4)
I1	20%	35%	50%	70%	80%	170%
I2	15%	30%	40%	55%	70%	130%
I3	10%	20%	35%	40%	60%	118%
I4	25%	30%	45%	60%	75%	125%
I5	20%	30%	40%	55%	70%	110%
I6	25%	35%	45%	60%	65%	115%

The swelling profile of hydrogel beads prepared from sodium alginate could not be obtained properly as it was swelled very fast and eroded within 10 minutes after introduction into pH 7.4 buffer solution (table-16). However, the swelling profile of prepared alginate beads were carried out in pH 1.2 for 2 hours and then it was continued in pH 7.4 buffer solutions are shown in the above table. Such profiles were evident in both test media exhibiting higher swelling in 7.4 buffer than in 1.2 acid solution. This increased % swelling of sodium alginate beads in pH 7.4 may be due to the presence of carboxylate anion group in sodium alginate network. Strong electrostatic repulsive force between negative charge of carboxylate anion of sodium alginate molecule resulted in longer intermolecular distance that could be reason for higher % swelling index of sodium alginate beads in pH 7.4. But in acidic medium, there is formation of strong hydrogen bonding between carboxyl group and hydroxyl group of sodium alginate beads that leads to formation of compacted sodium alginate molecule. As a result, less amount of water can penetrate into the hydrogel beads in pH 1.2 and consequently the reduced %SI was observed [171].

5.4.4. In vitro drug release study:

In vitro release studies of prepared microbeads were carried out using USP type 2 dissolution (paddle method) apparatus at 75 rpm [172]. The release studies were performed in both stomach and intestinal environment. The dissolution was conducted at 37±0.5 ºC with 75 rpm speed. Accurately weighed quantity of hydrogel beads were added to 750ml pH 1.2 hydrochloric acid buffer for first 2 hours. Then 250ml of tri-sodium orthophosphate dodecahydrate was added to the basket to obtain 1000ml of pH 7.4 buffer for next 6 hours in a continuous dissolution process according to IP (2018, vol-1, page-306) [83].

5.4.4.1. Effect of polymer concentration:

Hydrogel beads were prepared by taking different concentrations of sodium alginate (2%, 2.5%, 3% w/v). Beads containing 2% w/v polymer concentration showed less sustained release effect and beads containing 3% w/v polymer had more sustained effect in drug release (fig-40). Higher concentration of polymer results in higher viscosity of the dispersion, which led to an increase in the diffusional resistance to the drug molecules moving from the organic phase to the aqueous phase, thereby increasing the amount of drug molecules entrapped into the polymer matrix of nanoparticles. This leads to the higher sustained effect of releasing drug from the hydrogel beads.

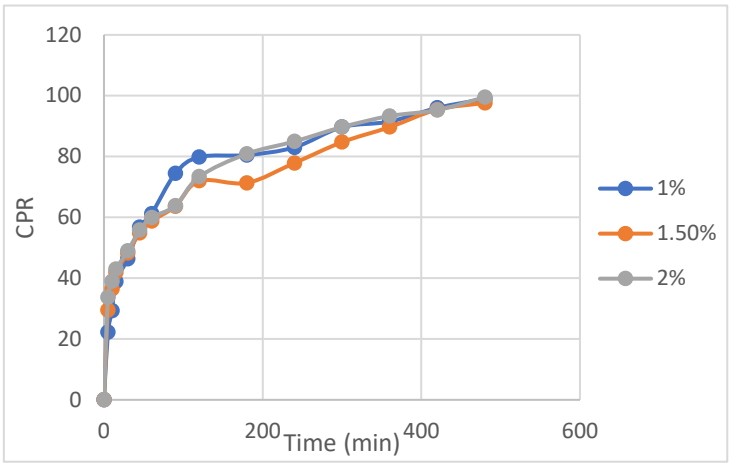

Fig 40: Effect of sodium alginate concentration

5.4.4.2. Effect of crosslinking agent:

Drug loaded beads were prepared by ionotropic gelation by crosslinking using $CaCl_2$ as crosslinking agent. 1%, 1.5%, 2% w/v concentrations were taken for crosslinking of the beads. 1.5% w/v calcium chloride has shown better sustained effect of drug release (fig-41). Although no significant changes in the results can be observed.

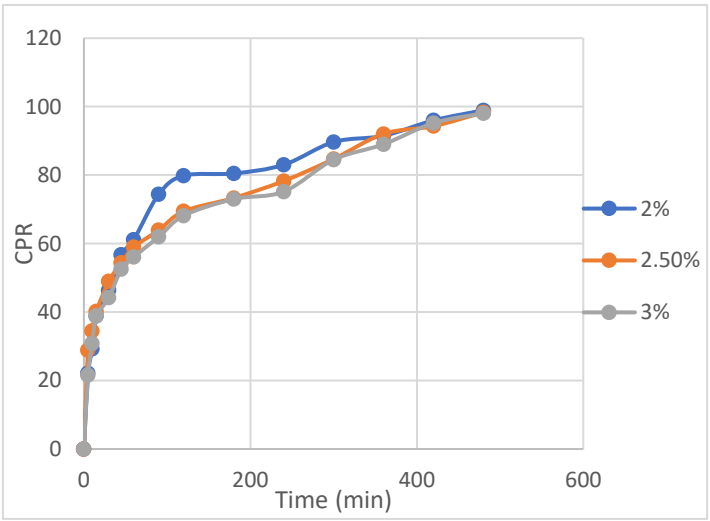

Fig 41- Effect of polymer concentration

5.4.4.3. Effect of drug amount-

Drug loaded beads were prepared by taking two amounts of amoxicillin trihydrate and paracetamol- 5:3 and 1:1 ratio. 5:3 ratio showed more entrapment and more sustained effect of the drug release, whereas when 1:1 ratio was taken it shoed lesser entrapment as well as decreased sustained effect. It was found that drug releases within the 1st hour were indicative of a burst effect (42). This could be attributed to the highly water soluble nature of the drugs [81].

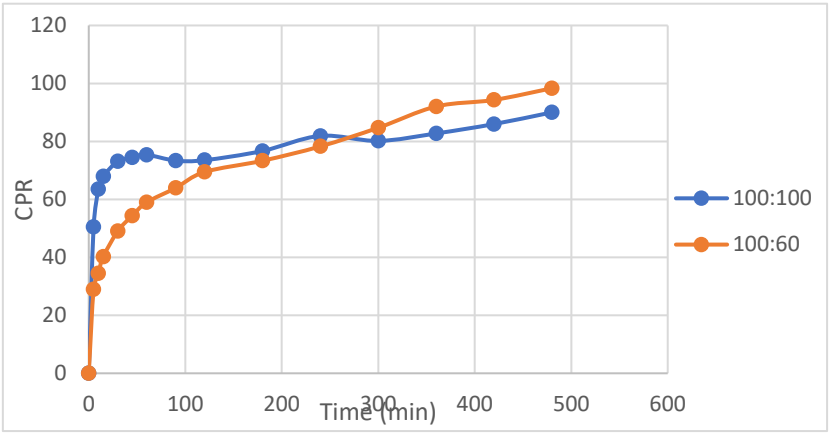

Fig 42- Effect of drug amount

5.4.5. In vitro antimicrobial activity assessment:

The developed hydrogels were screened for antibacterial activity by the well diffusion test in Mueller-Hinton agar plates. Gram-positive bacteria ***Staphylococcus aureus*** (ATCC 29737) and gram-negative bacteria ***Escherichia coli*** (ATCC 25922) were used. Then the zone of inhibition of unloaded beads (blank) Amoxicillin trihydrate (API) taken as standard and prepared hydrogel beads containing Amoxicillin trihydrate and another batch containing amoxicillin trihydrate and paracetamol was taken as test samples here (beads were taken in powder form). Zone of inhibitions were measured against above mentioned bacterial strain using slide callipers (RS PRO, China).

The mean ZOI for *S. aureus* for blank was- 0, for test – 1.63cm, samples containing Sodium alginate and amoxicillin trihydrate- 1.61cm, and samples containing Sodium alginate and amoxicillin trihydrate and paracetamol- 1.51cm (fig-43).

The mean ZOI for *E. coli* for blank was- 0, for test - 2.33cm, samples containing Sodium alginate and amoxicillin trihydrate- 1.41cm, and samples containing Sodium alginate and amoxicillin trihydrate and paracetamol- 1.33cm (fig-43).

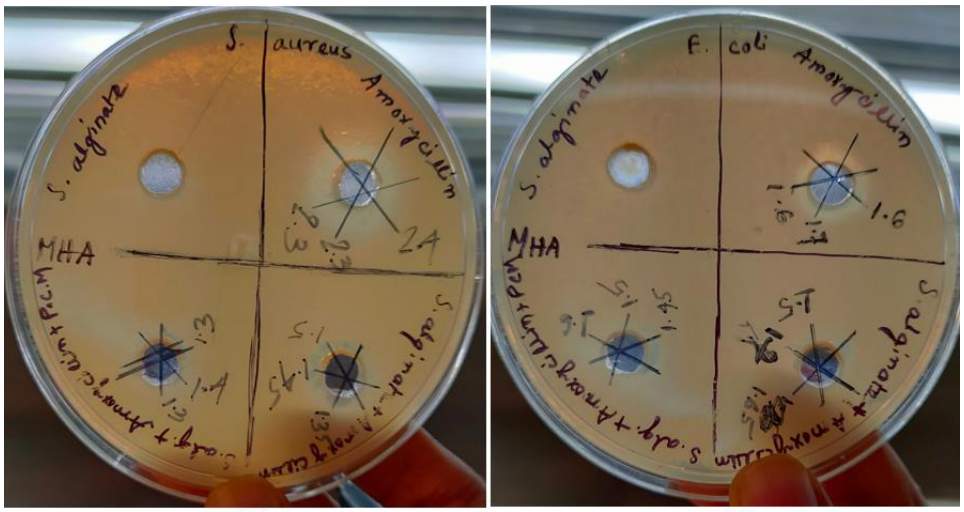

(A) (B)

Fig 43- Antimicrobial assessment for Zone of inhibition in (A) S. aureus and (B) E. coli.

The effect of prepared formulation (sodium alginate and amoxicillin trihydrate) showed comparatively less inhibitory effect as compared to the Amoxicillin trihydrate standard API mentioned in table 17. This maybe occurred due to the excessive hydrophilic nature of the drug which leads to leach out of drug from the formulation, causing drug loss and reduce its activity. Although in case of gram-negative bacteria E. coli, the test and samples has almost similar activities, compared to gram-positive S. aureus where slight reduction of zone is observed.

Table 17- Antibacterial activity of the formulation against *S. aureus* and *E. coli* in terms of zone of inhibition -

For S. aureus-

Samples	Diameter A (cm)	Diameter B (cm)	Diameter C (cm)	Average diameter of the zone (cm)
Sodium alginate	0	0	0	0
Amoxicillin trihydrate	2.4	2.3	2.3	2.33
Sodium alginate and amoxicillin trihydrate	1.5	1.35	1.45	1.41
Sodium alginate and amoxicillin trihydrate and paracetamol	1.3	1.4	1.3	1.33

For E. coli-

Samples	Diameter A (cm)	Diameter B (cm)	Diameter C (cm)	Average diameter of the zone (cm)
Sodium alginate	0	0	0	0
Amoxicillin trihydrate	1.6	1.7	1.6	1.63
Sodium alginate and amoxicillin trihydrate	1.5	1.7	1.65	1.61
Sodium alginate and amoxicillin trihydrate and paracetamol	1.45	1.5	1.6	1.51

5.4.6. Thermogravimetry Differential Thermal Analysis (TG/DTA)–

Thermogravimetry Differential Thermal Analysis is a thermal analysis technique in which the mass of a sample is measured over time as the temperature changes. TG and DSC analysis are widespread approaches in characterization of multicomponent systems such as inclusion compounds in the solid state. Therefore, the thermal properties of amoxicillin trihydrate, acetaminophen and both drugs loaded beads were investigated.

The thermogram (fig-44) shows that pure Paracetamol (A) and Amoxicillin trihydrate (B) gave only one sharp endothermic melting peak at 192.80 ℃ and 124.70 ℃ respectively which is similar to the reported data. Amoxicillin trihydrate and acetaminophen thermally decomposes several times showing several endothermic peaks. Meanwhile the hydrogel formulation containing both the drugs shows the complete disappearance of any peaks between 100-300℃ and gave only one sharp melting peak at 76.79℃, which is significantly lower than the any of the loaded drugs.

The reduced endotherm of beads formulation indicates that the crystallinity of the drug decreased in the formulation and tends to the formation of amorphous nature and also the moisture content of the formulation got increased also suggests decomposition of the sample, result that is in agreement with the DTG/TGA data obtained from DTG and TGA analyses [173], [174]. Although no standard sample was bought and tested to confirm the thermal decomposition of alginate beads containing amoxicillin trihydrate and acetaminophen.

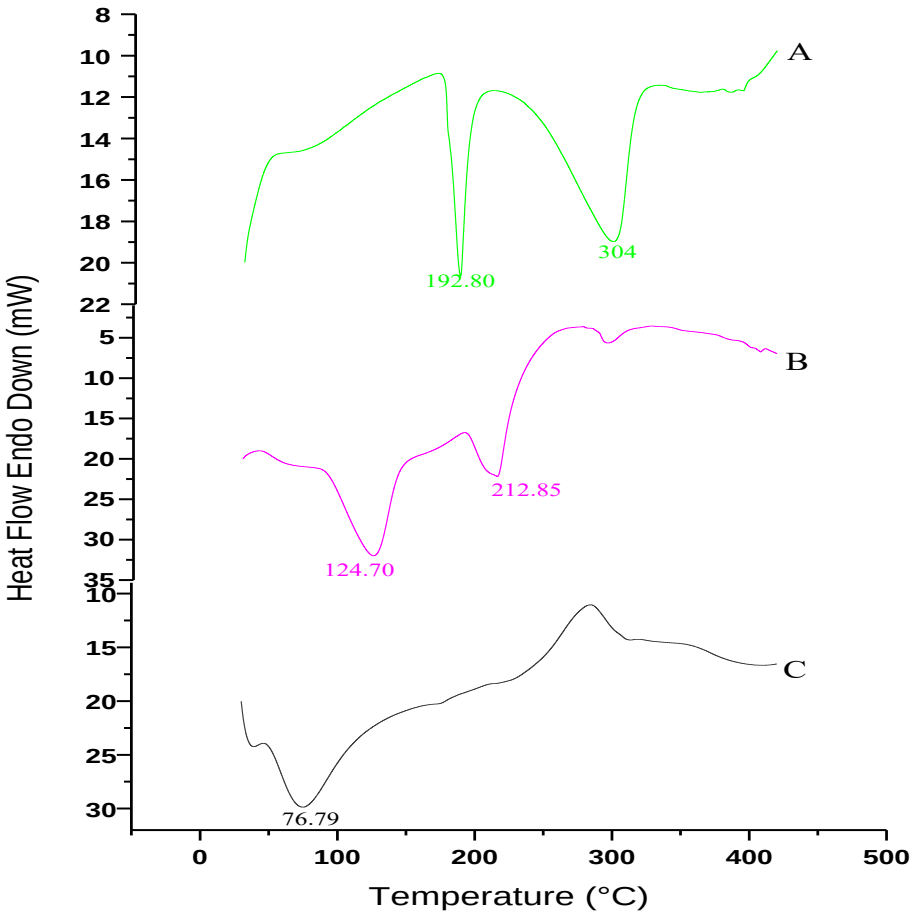

Fig 44- TG/DTA Thermogram of (A) acetaminophen (B) Amoxicillin trihydrate (C) formulation containing both the drugs

5.4.7. X-Ray diffraction method (XRD)-

XRD studies of the beads were performed to determine the physical form (amorphous or crystalline) of the drug incorporated within the beads. XRD analysis of different films, indicated varying results depending on the percentage drug loading. Figure 2(a) shows the XRD pattern of paracetamol pure drug. The main peaks for paracetamol, in particular the expected peak at 2θ of 15.60°, 18.18°, 23.48°, 24.51°, 26.69° were clearly shown indicating the presence of excess recrystallised paracetamol [175]. Figure 2(b) shows the XRD pattern for pure amoxicillin trihydrate drug with main peaks were observed at 2θ of 12.1°, 15.07°, 17.94°, 28.76° [176]. This is very interesting and can give an indication of how much of the loaded drug was molecularly dispersed. Figure 2(c) is the XRD pattern for films containing 92.73% amoxicillin trihydrate and 89.522% paracetamol, which clearly indicates that the drug was amorphous or molecularly dispersed within the beads matrix. The peak intensities of both the

paracetamol and amoxicillin trihydrate in hydrogel formulation were significantly weaker than the pure paracetamol and amoxicillin trihydrate. These weak intensities, suggesting a lower degree of crystallinity of drug in formulation than that of the individual drug. It indicated that the crystallinity of both drugs got reduced in the formulation and became amorphous in nature though retain a little bit crystallinity. This clearly indicated that changes in the crystalline state of the drug occurred during the preparation of the beads by this ionotropic gelation method. The similar diffractograms confirmed that there was no physical instability in beads containing paracetamol and amoxicillin trihydrate, the drug was found to be compatible with the other ingredients of the hydrogel formulation [81].

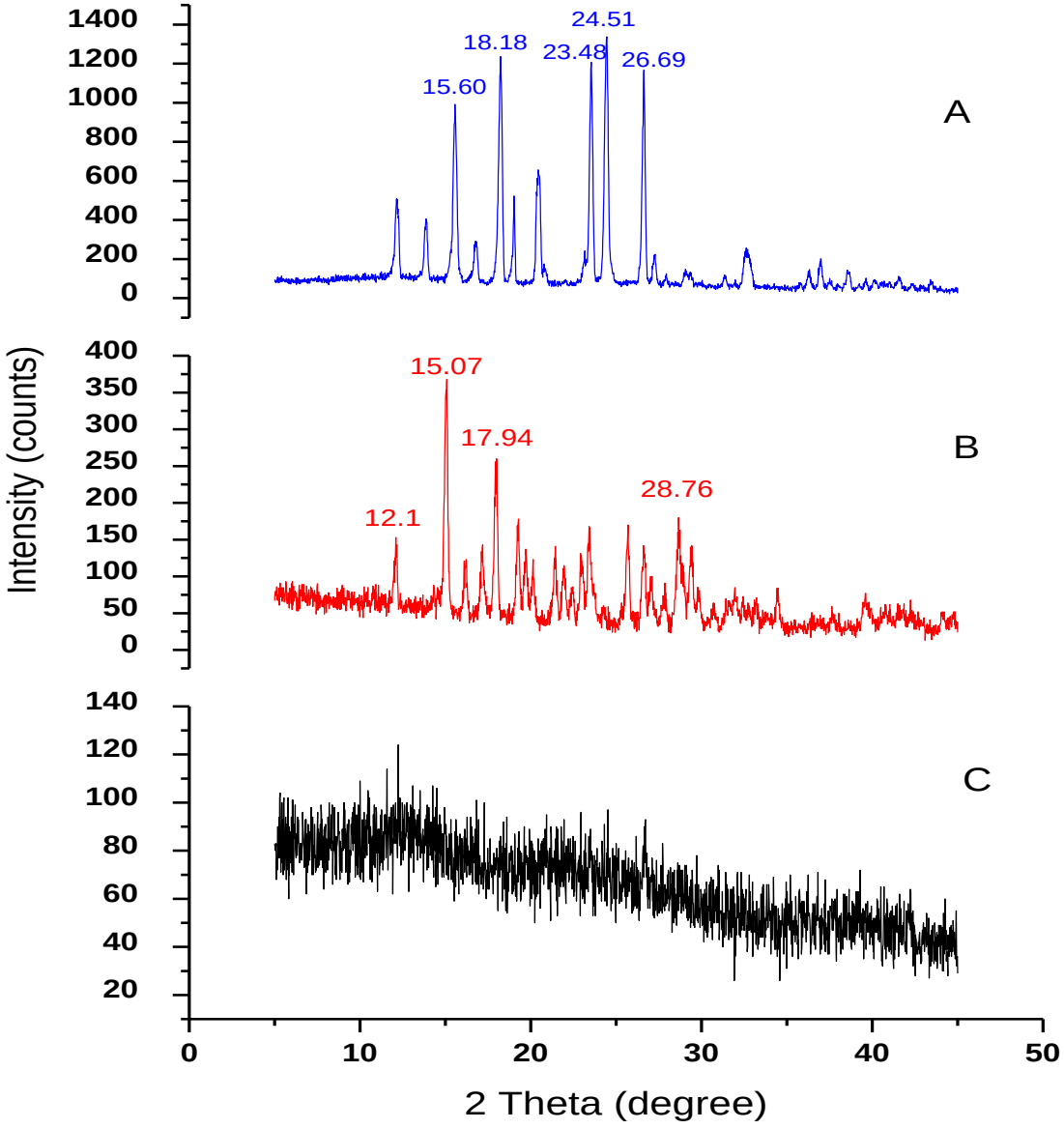

Fig 45- X-ray diffraction pattern of (A) acetaminophen (B) Amoxicillin trihydrate (C) formulation containing both the drugs

5.4.8. Scanning Electron Microscopy (SEM)-

Scanning electron microscopy was used to determine the size, shape and morphological characteristics of the bland (unloaded) and loaded hydrogel beads, prepared by 2.5% w/v sodium alginate, 1% w/v calcium chloride and amoxicillin trihydrate and paracetamol in a 5:3 ratio. The drug loaded beads had significantly different surface morphology than blank beads. In the drug loaded beads there was presence of white powder drugs on the surface of hydrogel beads.

The surface morphology of the prepared beads was studied by scanning electron microscopy (SEM) and the SEM photographs are depicted in the figure 11. SEM photographs of the blank beads compared with drug loaded beads show a difference in surface morphology. The SEM monograph of blank beads (Figure 1[A]) showed a regular smooth surface on the beads surface whereas the SEM monograph of drug loaded beads (Figure 11[B]) showed an irregular rough surface with dispersed drug particles. The surfaces of these beads were appeared to have rough with characteristic large wrinkles and cracks, as it was evident from the SEM photographs. This might be caused by partly collapsing the polymeric gel network during drying. Moreover, few polymeric debris and drug crystals were seen on the bead surface. Presence of polymeric derbies on the bead surface could be due to the simultaneous gel bead preparation and formation of the polymer-blend matrix; whereas the presence of drug crystals on the bead surface might be formed as a result of their migration along with water to the surface during drying.

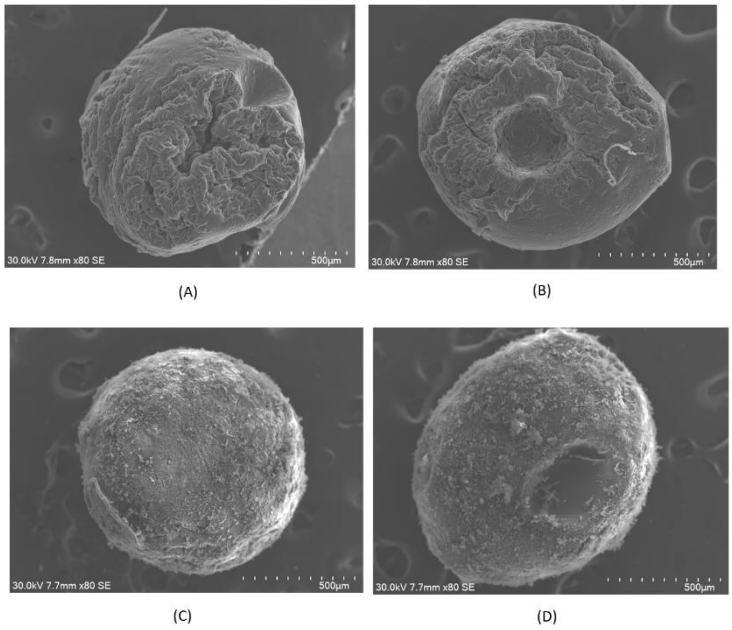

Fig 46- Scanning electron microscopic image of (A), (B) black beads, (C), (D) drug loaded beads

5.4.9. Fourier Transform Infrared Spectroscopy (FTIR)-

Infrared spectrum of amoxicillin trihydrate sample presented bands between 4000 and 400 cm^{-1}. According to Min et al. [40], two small bands at 3859 and 3739 cm^{-1} refer to crystallisation water (-OH stretch) and amide (-NH stretching), respectively, followed by bands between 3200 and 3000 cm^{-1}, characteristic of phenol (-OH stretching) and aromatic (-CH stretching), respectively. Prominent characteristic bands between 1800 and 1650 cm^{-1} (1776 and 1687 cm^{-1}) indicate carbonyl (-C=O) in beta-lactam ring and amide, respectively. 1528 cm^{-1} band is attributed to carboxylate asymmetric stretching. According to Zha et al. [22], bands in 1484 and 1120 cm^{-1} are attributed to N-C stretches of primary amine and O-C, respectively. Multiple bands in the region of 1150 and 950 cm^{-1} represented typical in-plane CH bending vibrations of aromatic compounds [177]. The major peaks for acetaminophen were observed at- 1670 cm-1, 2317 cm-1, 3727 cm-1, 3859 cm-1 for C=O stretching of amide, CH3 stretching, OH, stretching of COOH, OH, stretch of H bond of alcohol respectively[178]. Our formulation clearly shows the major and minor peaks of amoxicillin and acetaminophen which indicates the incorporation of drugs in the beads. The appearance of peaks without any vibrations also indicates the compatibility of drugs with the sodium alginate.

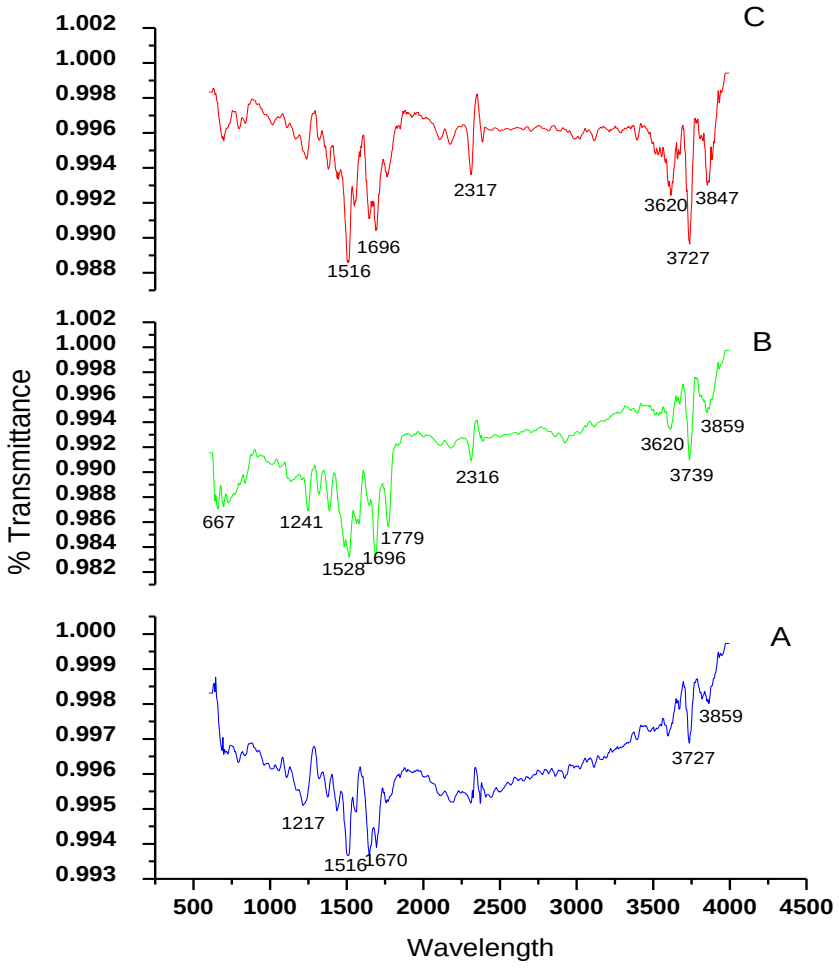

Fig 47- FTIR analysis of (A) acetaminophen (B) Amoxicillin trihydrate (C) formulation containing both the drugs

5.4.10. Drug release kinetics-

The release kinetics of a drug release study implies on the rate of drug availability inside the body with respect to time. Drug release from a formulation occurs by many methods like-diffusion, dissolution, partitioning, osmosis, swelling and erosion etc. The release of drugs follows several patterns-zero order, first order, Higuchi model, Korsmeyer-Peppas model, Hixson-Crowell model etc. It is said that whichever model's R^2 value is close to 1, tends to follow that model of release kinetics. The R^2 of the formulation batches containing both amoxicillin trihydrate and acetaminophen are listed below (table-18)-

Table 18- R^2 values of different formulation batches according to various drug release kinetics models-

Batch code	Zero order R^2	First order R^2	Higuchi model R^2	Korsmeyer-Peppas R^2
For AMOX				
I1	0.699	0.7256	0.9675	0.991
I2	0.7145	0.7456	0.9826	0.9985
I3	0.7587	0.7988	0.9921	0.9978
I4	0.7254	0.7648	0.9785	0.987
I5	0.7487	0.8123	0.9655	0.9914
I6	0.7256	0.7745	0.9458	0.9943
For PCM				
I1	0.7058	0.6393	0.892	0.9724
I2	0.7698	0.759	0.9285	0.995
I3	0.7883	0.708	0.9376	0.9802
I4	0.7564	0.723	0.9458	0.991
I5	0.7419	0.698	0.9582	0.9899
I6	0.7123	0.7245	0.9685	0.993

The 'n' value that can be obtained from the slope of a plot of log M_t/M_∞ versus log time (Korsmeyer-Peppas model) is indicative of drug release mechanism. If n is 0.45 or less, the release mechanism follows Fickian diffusion, higher values ($0.45 < n < 0.89$) for mass transfer follow a non-Fickian model (anomalous transport), where release is controlled by a combination of diffusion and polymer relaxation. When n reaches a value of 0.89 or above, the mechanism of drug release is regarded as case-II transport or super case-II transport which means the drug release rate does not change over time and involves polymer relaxation and chain disentanglement (24, 25). It is worthy note that for determination of the exponent n, only the first 60% of drug release data should be used [179]. The kinetic analysis of the in vitro release data of Amoxicillin trihydrate and Acetaminophen from the alginate beads are presented in Table 18. According to the determination coefficients (R2), the in vitro release data were in favour of Higuchi-diffusion kinetics (F2) and Korsmeyer Peppas model (F1 and F3). The values of n were >0.45 and thus it follows the Fickian diffusion method for drug release mechanism [180].

CHAPTER 6

CONCLUSION

CONCLUSION-

After performing the above experimentation, it is concluded that fabrication of sustained release hydrogel beads containing amoxicillin trihydrate and acetaminophen was successfully conducted and their evaluation tests produced desirable results. Our study was divided into two parts- method development and formulation development. A simultaneous equation method was developed for determination of amoxicillin trihydrate and acetaminophen from their combination. Amoxicillin trihydrate has amphoteric properties, conferred by its three main functional groups, COOH (pKa_1= 2.7), NH_2 (pKa_2 = 7.4) and OH (pKa = 9.6). It degrades in acidic pH (below pH-2) and forms amoxicilloic acid, by hydrolysis of the beta-lactam ring of the drug. This conversion decreases the antimicrobial activity of amoxicillin trihydrate. Our formulation with sodium alginate is used as a prevention of degradation of amoxicillin trihydrate in acidic conditions in stomach. Sodium alginate is a anionic polymer, having a COO^- group in its structure. In the presence of hydrochloric acid, the carboxyl group of sodium alginate becomes protonated and forms alginic acid, which is insoluble in water. At low pH values, this forms a gel of alginic acid. If the pH is increased, the alginic acid dissolves and returns to its original viscosity. Thus, in acidic environment of stomach sodium alginate doesn't swell much and keeps the drugs trapped inside the beads. Which leads to the less degradation of amoxicillin trihydrate in acidic pH. As the pH increases in small intestine, the beads absorb water and swells which leads to the release of drugs.

Since the last few decades mankind has been directly and indirectly dependent on antibiotics and antipyretics for control and prevention of infectious diseases with hyperthermia, starting with common cold, UTI, RTI, stomach ulcer, skin infection etc. During the outbreak of COVID-19, the world faced a terrible pandemic situation where people were directly dependent on antibiotics and antipyretic to overcome and cure the symptoms of coronavirus infection. The aim of our experiment was to combine an antibiotic (amoxicillin trihydrate) and an antipyretic drug (acetaminophen) and make a sustained release formulation of the combination to administer in microbial infection with hyperthermia. The ratio of amoxicillin trihydrate and acetaminophen was chosen at 5:3 in the beads were selected after checking its AUC observed by UV-spectrophotometric method. This experiment has investigated a simple, quick, cost effective and easy technique for the estimation of Acetaminophen and amoxicillin trihydrate in combination by simultaneous equation method. The method was validated by ICH guidelines Q2R2. The findings suggest that the following method is linear (R^2 values are >0.99), precise (%RSD values are lesser than 2%), accurate (%recovery falls under the range of 70-120%). These results have important implications for method validation and provide valuable insights into the simultaneous estimation of both the drugs separately as well as in a combination (at lambda max 232 nm). Moving forward, further research is warranted to explore the synergistic properties of the two drugs, acetaminophen and amoxicillin trihydrate combined in a single dosage form, can be administered in bacterial infections accompanying fever like- urinary tract infection, stomach ulcer, skin infections, lower respiratory tract infection, which is not yet available in the market. Overall, this study contributes to the understanding of simultaneous estimation of amoxicillin in presence of acetaminophen in pure drug form, combination and marketed dosage form.

The formulation development was done by fabricating sodium alginate beads crosslinked with calcium chloride salt by dropping gel method (ionotropic gelation). The drugs were incorporated in the alginate solution for incorporation into the beads. The resulted beads were evaluated based on various parameters. The entrapment efficiency of both the drugs were above 90% in our optimum batch (code-I3; SA-2.5%, $CaCl_2$-1%, Amox-100mg, PCM-60mg). The beads show a burst release in the first 60mins which acts as the loading dose and then it is sustained upto 8hours (release upto 99%). The swelling study concludes upto 60% (code-I3; ; SA-2.5%, $CaCl_2$-1%, Amox-100mg, PCM-60mg) swelling index in acidic pH, which is the least sweeling index. The TG/DTA studies shows decrease in temperate of formulation than pure drug which indicates incorporation of drugs in the formulation causes changes in the thermogram of the drugs. The XRD pattern confirms that drug crystallinity changes to amorphous when formulated with alginate, as there is no sharp peak observed. The SEM image shows clear incorporation of drugs in the beads. FTIR analysis confirms that both the drugs are distinctly present in the formulation and their compatibility of the drug with the excipients. The antimicrobial study obtains zone of inhibitions which indicate the antimicrobial activity of amoxicillin trihydrate is still present after formulating with acetaminophen and alginate. With the obtained results of the research work it was concluded that this formulation is suitable for sustaining the drug release from the hydrogel beads which may prevent degradation of amoxicillin trihydrate in the acidic environment of stomach, and increase patient compliance.

Due to the limited time several studies regarding this experiment are yet to be conducted. Pre-clinical animal study is needed to prove its synergistic activity as an antibiotic and antipyretic agent. The continuation of the work will include stability testing of amoxicillin trihydrate and acetaminophen in the longer run, animal study for their combined effect and antimicrobial effect of any specific microorganism.

CHAPTER 7

REFERENCES

REFERENCES-

[1] A. Procopio *et al.*, "Recent Fabrication Methods to Produce Polymer-Based Drug Delivery Matrices (Experimental and In Silico Approaches).," *Pharmaceutics*, vol. 14, no. 4, Apr. 2022, doi: 10.3390/pharmaceutics14040872.

[2] S. V. Patil, S. S. Shelake, and S. S. Patil, "Polymeric materials for targeted delivery of bioactive agents and drugs," *Fundam. Biomater. Polym.*, pp. 249–266, Jan. 2018, doi: 10.1016/B978-0-08-102194-1.00011-6.

[3] E. Saldívar-Guerra and E. Vivaldo-Lima, "Introduction to Polymers and Polymer Types," *Handb. Polym. Synth. Charact. Process.*, pp. 1–14, 2013, doi: 10.1002/9781118480793.ch1.

[4] J. Anzano, R. Lasheras, B. Bonilla, and J. Casas, "Classification of polymers by determining of C1:C2:CN:H:N:O ratios by laser-induced plasma spectroscopy (LIPS)," *Polym. Test.*, vol. 27, pp. 705–710, Sep. 2008, doi: 10.1016/j.polymertesting.2008.05.012.

[5] W. L. Adair, "Carbohydrates," *xPharm Compr. Pharmacol. Ref.*, pp. 1–12, 2007, doi: 10.1016/B978-008055232-3.60056-X.

[6] S. R. Montoro, S. de F. Medeiros, and G. M. Alves, "Nanostructured Hydrogels," *Nanostructured Polym. Blends*, pp. 325–355, 2013, doi: 10.1016/B978-1-4557-3159-6.00010-9.

[7] R. F. T. Stepto, "Fundamentals of the Formation, Structure and Properties of Polymer Networks," *Compr. Polym. Sci. Suppl.*, pp. 199–226, 1989, doi: 10.1016/B978-0-08-096701-1.00228-7.

[8] Z. J. He, K. Chen, Z. H. Liu, B. Z. Li, and Y. J. Yuan, "Valorizing renewable cellulose from lignocellulosic biomass toward functional products," *J. Clean. Prod.*, vol. 414, Aug. 2023, doi: 10.1016/j.jclepro.2023.137708.

[9] A. Aho, T. Salmi, and D. Y. Murzin, "Catalytic Pyrolysis of Lignocellulosic Biomass," *Role Catal. Sustain. Prod. Bio-Fuels Bio-Chemicals*, pp. 137–159, Mar. 2013, doi: 10.1016/B978-0-444-56330-9.00005-X.

[10] J. P. Carbone and K. H. Reinert, "Synthetic Polymers☆," *Ref. Modul. Earth Syst. Environ. Sci.*, 2015, doi: 10.1016/B978-0-12-409548-9.00802-2.

[11] A. Rudin and P. Choi, "Step-Growth Polymerizations," *Elem. Polym. Sci. Eng.*, pp. 305–339, 2013, doi: 10.1016/B978-0-12-382178-2.00007-9.

[12] E. Peters, "Plastics: Thermoplastics, Thermosets, and Elastomers," 2007, pp. 335–355. doi: 10.1002/9780470172551.ch11.

[13] G. Mensitieri, "Ongoing research and future research challenges," *Supercrit. Fluid Sci. Technol.*, vol. 9, pp. 433–459, Jan. 2021, doi: 10.1016/B978-0-444-63724-6.00014-7.

[14] E. A. MacGregor, "Biopolymers," *Encycl. Phys. Sci. Technol.*, pp. 207–245, 2003, doi: 10.1016/B0-12-227410-5/00064-8.

[15] "Plastic pipe systems," *Stand. News*, vol. 30, no. 4, p. 15, Apr. 2002, doi: 10.1016/B978-185617496-1/50002-1.

[16] A. Shrivastava, "Introduction to Plastics Engineering," *Introd. to Plast. Eng.*, pp. 1–16,

Jan. 2018, doi: 10.1016/B978-0-323-39500-7.00001-0.

[17] L. M. Abrantes and A. I. Melato, "Coatings including carboxylates for the preservation of metallic heritage artefacts," *Corros. Conserv. Cult. Herit. Met. Artefacts*, pp. 518–539, 2013, doi: 10.1533/9781782421573.5.518.

[18] A. Sorrentino, G. Gorrasi, and V. Vittoria, "Potential perspectives of bio-nanocomposites for food packaging applications," *Trends Food Sci. Technol.*, vol. 18, no. 2, pp. 84–95, Feb. 2007, doi: 10.1016/j.tifs.2006.09.004.

[19] L. Wu, N. Farzadnia, C. Shi, Z. Zhang, and H. Wang, "Autogenous shrinkage of high performance concrete: A review," *Constr. Build. Mater.*, vol. 149, pp. 62–75, Sep. 2017, doi: 10.1016/j.conbuildmat.2017.05.064.

[20] S. A. Varghese, S. M. Rangappa, S. Siengchin, and J. Parameswaranpillai, "Natural polymers and the hydrogels prepared from them," *Hydrogels Based Nat. Polym.*, pp. 17–47, Jan. 2019, doi: 10.1016/B978-0-12-816421-1.00002-1.

[21] A. C. Q. Silva, A. J. D. Silvestre, C. Vilela, and C. S. R. Freire, "Natural Polymers-Based Materials: A Contribution to a Greener Future.," *Molecules*, vol. 27, no. 1, Dec. 2021, doi: 10.3390/molecules27010094.

[22] H. Chen *et al.*, "Cellulose-based separators for lithium batteries: Source, preparation and performance," *Chem. Eng. J.*, vol. 471, Sep. 2023, doi: 10.1016/j.cej.2023.144593.

[23] L. A. Loureiro dos Santos, "Natural Polymeric Biomaterials: Processing and Properties," *Ref. Modul. Mater. Sci. Mater. Eng.*, Jan. 2017, doi: 10.1016/B978-0-12-803581-8.02253-0.

[24] E. Davison-Kotler, W. S. Marshall, and E. García-Gareta, "Sources of Collagen for Biomaterials in Skin Wound Healing.," *Bioeng. (Basel, Switzerland)*, vol. 6, no. 3, Jun. 2019, doi: 10.3390/bioengineering6030056.

[25] A. S. A. Mohammed, M. Naveed, and N. Jost, "Polysaccharides; Classification, Chemical Properties, and Future Perspective Applications in Fields of Pharmacology and Biological Medicine (A Review of Current Applications and Upcoming Potentialities).," *J. Polym. Environ.*, vol. 29, no. 8, pp. 2359–2371, 2021, doi: 10.1007/s10924-021-02052-2.

[26] A. M. G. C. Dias, A. Hussain, A. S. Marcos, and A. C. A. Roque, "A biotechnological perspective on the application of iron oxide magnetic colloids modified with polysaccharides," *Biotechnol. Adv.*, vol. 29, no. 1, pp. 142–155, Jan. 2011, doi: 10.1016/j.biotechadv.2010.10.003.

[27] J. Wu, S. Shi, H. Wang, and S. Wang, "Mechanisms underlying the effect of polysaccharides in the treatment of type 2 diabetes: A review," *Carbohydr. Polym.*, vol. 144, pp. 474–494, Jun. 2016, doi: 10.1016/j.carbpol.2016.02.040.

[28] R. Abka-Khajouei, L. Tounsi, N. Shahabi, A. K. Patel, S. Abdelkafi, and P. Michaud, "Structures, Properties and Applications of Alginates.," *Mar. Drugs*, vol. 20, no. 6, May 2022, doi: 10.3390/md20060364.

[29] K. Y. Lee and D. J. Mooney, "Alginate: properties and biomedical applications.," *Prog. Polym. Sci.*, vol. 37, no. 1, pp. 106–126, Jan. 2012, doi: 10.1016/j.progpolymsci.2011.06.003.

[30] T. Silva, J. Martins, M. Silva, M. Gimenes, and M. Vieira, "Alginate and Sericin: Environmental and Pharmaceutical Applications," 2017. doi: 10.5772/65257.

[31] A. Shalapy *et al.*, "Adsorption of Deoxynivalenol (DON) from Corn Steep Liquor (CSL) by the Microsphere Adsorbent SA/CMC Loaded with Calcium," *Toxins (Basel).*, vol. 12, Mar. 2020, doi: 10.3390/toxins12040208.

[32] L. Stanciu and S. Diaz-Amaya, "Composite biomaterials," *Introd. Biomater.*, pp. 149–169, 2022, doi: 10.1016/B978-0-12-809263-7.00007-X.

[33] Y. Deng *et al.*, "Stimuli-Responsive nanocellulose Hydrogels: An overview," *Eur. Polym. J.*, vol. 180, Nov. 2022, doi: 10.1016/j.eurpolymj.2022.111591.

[34] S. Bashir *et al.*, "Fundamental Concepts of Hydrogels: Synthesis, Properties, and Their Applications.," *Polymers (Basel).*, vol. 12, no. 11, Nov. 2020, doi: 10.3390/polym12112702.

[35] X. Sun, S. Agate, K. S. Salem, L. Lucia, and L. Pal, "Hydrogel-Based Sensor Networks: Compositions, Properties, and Applications—A Review," *ACS Appl. Bio Mater.*, vol. 4, no. 1, pp. 140–162, Jan. 2021, doi: 10.1021/acsabm.0c01011.

[36] E. M. Ahmed, "Hydrogel: Preparation, characterization, and applications: A review," *J. Adv. Res.*, vol. 6, no. 2, pp. 105–121, Mar. 2015, doi: 10.1016/J.JARE.2013.07.006.

[37] Y. Cao *et al.*, "Mechanoactive wound dressing using poly(N-isopropyl acrylamide) based hydrogels," *Eur. Polym. J.*, vol. 202, Jan. 2024, doi: 10.1016/j.eurpolymj.2023.112645.

[38] U. K. Singh and P. Sudheer, "Hydrogel Beads-A Versatile Dimension in Controlled Oral Delivery," *Int. J. Drug Deliv. Technol.*, vol. 12, no. 3, pp. 1453–1464, 2022, doi: 10.25258/ijddt.12.3.88.

[39] M. Amiri, P. Khazaeli, A. Salehabadi, and M. Salavati-Niasari, "Hydrogel beads-based nanocomposites in novel drug delivery platforms: Recent trends and developments," *Adv. Colloid Interface Sci.*, vol. 288, p. 102316, Feb. 2021, doi: 10.1016/J.CIS.2020.102316.

[40] M. N. Saqib, B. M. Khaled, F. Liu, and F. Zhong, "Hydrogel beads for designing future foods: Structures, mechanisms, applications, and challenges," *Food Hydrocoll. Heal.*, vol. 2, p. 100073, Dec. 2022, doi: 10.1016/J.FHFH.2022.100073.

[41] P. Hegger *et al.*, "Charge Matters: Modulating Secondary Interactions in Hyaluronan Hydrogels," *ChemistrySelect*, vol. 2, pp. 7701–7705, Aug. 2017, doi: 10.1002/slct.201701908.

[42] M. Bustamante-Torres, D. Romero-Fierro, B. Arcentales-Vera, K. Palomino, H. Magaña, and E. Bucio, "Hydrogels Classification According to the Physical or Chemical Interactions and as Stimuli-Sensitive Materials.," *Gels (Basel, Switzerland)*, vol. 7, no. 4, Oct. 2021, doi: 10.3390/gels7040182.

[43] J. Li, "Polymeric Hydrogels," pp. 7-1-7–18, 2004, doi: 10.1142/9789812562227_0007.

[44] S. Parveen, R. Misra, and S. K. Sahoo, "Nanoparticles: a boon to drug delivery, therapeutics, diagnostics and imaging," *Nanomedicine Nanotechnology, Biol. Med.*, vol. 8, no. 2, pp. 147–166, Feb. 2012, doi: 10.1016/J.NANO.2011.05.016.

[45] S. Adepu and S. Ramakrishna, “Controlled Drug Delivery Systems: Current Status and Future Directions.,” *Molecules*, vol. 26, no. 19, Sep. 2021, doi: 10.3390/molecules26195905.

[46] K. P. Sampath, D. Bhowmik, and S. Srivastava, “Sustained Release Drug Delivery System Potential,” *Pharma Innov.*, vol. 1, no. 2, pp. 48–60, 2012.

[47] J. Xing, M. Zhang, X. Liu, C. Wang, N. Xu, and D. Xing, “Multi-material electrospinning: from methods to biomedical applications,” *Mater. Today Bio*, vol. 21, Aug. 2023, doi: 10.1016/j.mtbio.2023.100710.

[48] L. Lei, Y. Bai, X. Qin, J. Liu, W. Huang, and Q. Lv, “Current Understanding of Hydrogel for Drug Release and Tissue Engineering.,” *Gels (Basel, Switzerland)*, vol. 8, no. 5, May 2022, doi: 10.3390/gels8050301.

[49] Y. Zhang, T. Yu, L. Peng, Q. Sun, Y. Wei, and B. Han, “Advancements in Hydrogel-Based Drug Sustained Release Systems for Bone Tissue Engineering,” *Front. Pharmacol.*, vol. 11, no. May, pp. 1–13, 2020, doi: 10.3389/fphar.2020.00622.

[50] A. Shukla, M. Kumar, R. Bishnoi, V. Kachawa, and C. Jain, “Dosage from design of sustained release drug delivery systems: An overview,” pp. 1–7, Jan. 2017.

[51] G. M. Jantzen and J. R. Robinson, “Sustained-and Controlled-Release Drug-Delivery Systems,” in *Modern Pharmaceutics, Fourth Edition, Revised and Expanded*, 2002, pp. 747–789. doi: 10.1201/9780824744694.ch15.

[52] B. Shrivastava, *Medical Microbiology*. 2011.

[53] U. Das, A. Bala, R. Molla, and S. Mandal, “Nanomedicine in infectious disease challenges and regulatory concerns,” *Nanostructured Drug Deliv. Syst. Infect. Dis. Treat.*, pp. 237–259, Jan. 2024, doi: 10.1016/B978-0-443-13337-4.00012-4.

[54] H. P. Gurushankara, “Pandemics of the 21st century: Lessons and future perspectives,” *Pandemic Outbreaks 21st Century Epidemiol. Pathog. Prev. Treat.*, pp. 139–158, Jan. 2021, doi: 10.1016/B978-0-323-85662-1.00011-2.

[55] C. Ellis, “Advances in infectious diseases.,” *Clin. Med.*, vol. 9, no. 3, pp. 254–255, Jun. 2009, doi: 10.7861/clinmedicine.9-3-254.

[56] Y. Srivastav, M. Mansoori, A. Hameed, A. Hashmi, and M. Ahmad, “Condensed Statement: Critical Framework of the Diagnosis along with Management of Peptic Ulcer Disease (PUD),” 2024, pp. 90–111. doi: 10.9734/bpi/acpr/v8/8357E.

[57] T. F. Malik, K. Gnanapandithan, and K. Singh, “Peptic Ulcer Disease.,” Treasure Island (FL), 2024.

[58] S. Sapkota, S. Sen Oli, M. Karki, P. S. Rokaha, and A. Aryal, “Peptic Ulcer Disease among Patients Undergoing Upper Gastrointestinal Endoscopy in a Tertiary Care Centre: A Descriptive Cross-sectional Study.,” Apr. 2024. doi: 10.31729/jnma.8527.

[59] I. Al-Naji *et al.*, “Chitosan/ Alginate/ Gelucire in-situ Gelling System for Oral Sustained Delivery of Paracetamol for Dysphagic Patients,” *Jordan J. Pharm. Sci.*, vol. 17, no. 2, pp. 292–306, 2024, doi: 10.35516/jjps.v17i2.1702.

[60] R. Kulsoom *et al.*, “Synthesis of calcium carbonate-quince bio-composite for programmed and on-demand drug release of paracetamol at target site: a green chemistry

approach," *Polym. Bull.*, vol. 80, no. 6, pp. 6965–6988, 2023, doi: 10.1007/s00289-022-04400-1.

[61] B. Naiel, G. El-Subruiti, R. Khalifa, A. Eltaweil, and A. Omer, "Construction of gastroretentive aminated chitosan coated (sunflower oil /alginate / i-carrageenan) floatable polymeric beads for prolonged release of Amoxicillin trihydrate," vol. 84, p. 104534, Jun. 2023, doi: 10.1016/j.jddst.2023.104534.

[62] S. H. Almurisi, A. A. Doolaanea, K. A. Al-Japairai, B. Chatterjee, and M. Z. I. Sarker, "Development and Validation of UV Spectrophotometric Method for Determination of Paracetamol in Chitosan Coated Alginate Beads and Dissolution Studies," *Pharm. Chem. J.*, vol. 56, no. 7, pp. 1011–1016, 2022, doi: 10.1007/s11094-022-02742-8.

[63] F. L. Aranda, B. L. Rivas, F. L. Aranda, and B. L. Rivas, "REMOVAL OF AMOXICILLIN THROUGH DIFFERENT METHODS, EMPHASIZING REMOVAL BY BIOPOLYMERS AND ITS DERIVATIVES. AN OVERVIEW," *J. Chil. Chem. Soc.*, vol. 67, no. 3, pp. 5643–5655, Sep. 2022, doi: 10.4067/S0717-97072022000305643.

[64] T. P. de Araújo *et al.*, "Acetaminophen removal by calcium alginate/activated hydrochar composite beads: Batch and fixed-bed studies.," *Int. J. Biol. Macromol.*, vol. 203, pp. 553–562, Apr. 2022, doi: 10.1016/j.ijbiomac.2022.01.177.

[65] N. N. Idris, T. Hamidon, N. S. Abdullah, L. Suryanegara, and M. H. Hussin, "Potential of oil palm frond cellulose nanocrystals-activated carbon hydrogel beads for the removal of paracetamol from aqueous media," *Cellulose*, vol. 29, Feb. 2022, doi: 10.1007/s10570-021-04379-4.

[66] S. Almurisi, A. A. Doolaanea, M. E. Akkawi, B. Chatterjee, and M. Sarker, "Taste masking of paracetamol encapsulated in chitosan-coated alginate beads," *J. Drug Deliv. Sci. Technol.*, vol. 56, p. 101520, Apr. 2020, doi: 10.1016/j.jddst.2020.101520.

[67] S. H. Almurisi, A. A. Doolaanea, M. E. Akkawi, B. Chatterjee, K. Ahmed Saeed Aljapairai, and M. Z. Islam Sarker, "Formulation development of paracetamol instant jelly for pediatric use.," *Drug Dev. Ind. Pharm.*, vol. 46, no. 8, pp. 1373–1383, Aug. 2020, doi: 10.1080/03639045.2020.1791165.

[68] S. Sharma, G. Sarkar, B. Srestha, D. Chattopadhyay, and M. Bhowmik, "In-situ fast gelling formulation for oral sustained drug delivery of paracetamol to dysphagic patients.," *Int. J. Biol. Macromol.*, vol. 134, pp. 864–868, Aug. 2019, doi: 10.1016/j.ijbiomac.2019.05.092.

[69] T. Guo, N. Zhang, J. Huang, Y. Pei, F. Wang, and K. Tang, "A facile fabrication of core–shell sodium alginate/gelatin beads for drug delivery systems," *Polym. Bull.*, vol. 76, pp. 1–16, Jan. 2019, doi: 10.1007/s00289-018-2377-z.

[70] A. J. Sami *et al.*, "Formulation of novel chitosan guargum based hydrogels for sustained drug release of paracetamol.," *Int. J. Biol. Macromol.*, vol. 108, pp. 324–332, Mar. 2018, doi: 10.1016/j.ijbiomac.2017.12.008.

[71] S. Hamed, F. Ayob, M. Alfatama, and A. A. Doolaanea, "Enhancement of the immediate release of paracetamol from alginate beads," *Int. J. Appl. Pharm.*, vol. 9, pp. 47–51, Mar. 2017, doi: 10.22159/ijap.2017v9i2.15672.

[72] P. Treenate and P. Monvisade, "In vitro drug release profiles of pH-sensitive

hydroxyethylacryl chitosan/sodium alginate hydrogels using paracetamol as a soluble model drug," *Int. J. Biol. Macromol.*, vol. 99, pp. 71–78, 2017, doi: 10.1016/j.ijbiomac.2017.02.061.

[73] N. Ramalingam, "Formulation and Evaluation of Paracetamol Loaded Mucoadhesive Microspheres," *Int. J. Pharm. Pharmacol.*, vol. 1, no. 2, 2017, doi: 10.31531/2581-3080.1000106.

[74] O. Abdallah, N. Rashed, A. El-Olemy, and A. Eldin, "UV Spectrophotometric Determination of Paracetamol in Presence of Drotaverine Hydrochloride," *J. Adv. Pharm. Res.*, vol. 1, pp. 89–95, Apr. 2017, doi: 10.21608/aprh.2017.1977.

[75] S. Wadher, K. Tukaram, L. Sima, K. Supriya, and S. Shivpuje, *DEVELOPMENT AND VALIDATION OF STABILITY INDICATING UV SPECTROPHOTOMETRIC METHOD FOR SIMULTANEOUS ESTIMATION OF AMOXICILLIN TRIHYDRATE AND METRONIDAZOLE IN BULK AND IN-HOUSE TABLET*. 2017.

[76] S. K. Dey *et al.*, "Floating mucoadhesive alginate beads of amoxicillin trihydrate: A facile approach for H. pylori eradication.," *Int. J. Biol. Macromol.*, vol. 89, pp. 622–631, Aug. 2016, doi: 10.1016/j.ijbiomac.2016.05.027.

[77] N. Patel, D. Lalwani, S. Gollmer, E. Injeti, Y. Sari, and J. Nesamony, "Development and evaluation of a calcium alginate based oral ceftriaxone sodium formulation.," *Prog. Biomater.*, vol. 5, pp. 117–133, 2016, doi: 10.1007/s40204-016-0051-9.

[78] D. S. Seeli, S. Dhivya, N. Selvamurugan, and M. Prabaharan, "Guar gum succinate-sodium alginate beads as a pH-sensitive carrier for colon-specific drug delivery.," *Int. J. Biol. Macromol.*, vol. 91, pp. 45–50, Oct. 2016, doi: 10.1016/j.ijbiomac.2016.05.057.

[79] S. K. Bajpai and N. Kirar, "Swelling and drug release behavior of calcium alginate/poly (sodium acrylate) hydrogel beads," *Des. Monomers Polym.*, vol. 19, no. 1, pp. 89–98, 2016, doi: 10.1080/15685551.2015.1092016.

[80] R. Poojari and R. Srivastava, "Composite alginate microspheres as the next-generation egg-box carriers for biomacromolecules delivery.," *Expert Opin. Drug Deliv.*, vol. 10, no. 8, pp. 1061–1076, Aug. 2013, doi: 10.1517/17425247.2013.796361.

[81] S. Mandal, S. Kumar, B. Krishnamoorthy, and S. Basu, "Development and evaluation of calcium alginate beads prepared by sequential and simultaneous methods," *Brazilian J. Pharm. Sci.*, vol. 46, pp. 785–793, Dec. 2010, doi: 10.1590/S1984-82502010000400021.

[82] R. A. H. Ishak, G. A. S. Awad, N. D. Mortada, and S. A. K. Nour, "Preparation, in vitro and in vivo evaluation of stomach-specific metronidazole-loaded alginate beads as local anti-Helicobacter pylori therapy.," *J. Control. release Off. J. Control. Release Soc.*, vol. 119, no. 2, pp. 207–214, Jun. 2007, doi: 10.1016/j.jconrel.2007.02.012.

[83] M. of H. Government of India, *Indian Pharmacopoeia 2018*, vol. I. Delhi: Manager of Publications, 2018., 2018.

[84] V. Pawar, R. Awasthi, G. Garg, and G. Kulkarni, "Development and Validation of a Simple UV Method for In Vitro Determination of Amoxicillin Trihydrate in New Gastroretentive Dosage Form," *Int. J. Pure Appl. Chem.*, vol. 5, pp. 329–333, Jan. 2010.

[85] Z. Al-Obaidi, A. Ani, A. Hussein, and A. Al-Juhaishi, "A comparative study for the quantification of paracetamol in multicomponent oral solution employing standard

addition method utilized in UV-Visible spectroscopy and RP-HPLC," *J. Pharm. Sci. Res.*, vol. 11, pp. 339–342, Feb. 2019.

[86] B. Manu, S. Mahamood, V. Hari, and S. Surathkal, "A novel catalytic route to degrade paracetamol by Fenton process," *Int. J. Res. Chem. Environ.*, vol. 1, pp. 157–164, Jul. 2011.

[87] M. Haeseker, T. Havenith, L. Stolk, C. Neef, C. Bruggeman, and A. Verbon, "Is the standard dose of amoxicillin-clavulanic acid sufficient?," *BMC Pharmacol. Toxicol.*, vol. 15, no. 1, p. 38, 2014, doi: 10.1186/2050-6511-15-38.

[88] D. W. G. Harron, "Technical Requirements for Registration of Pharmaceuticals for Human Use: The ICH Process," *Textb. Pharm. Med.*, vol. 1994, no. November 1996, pp. 447–460, 2013, doi: 10.1002/9781118532331.ch23.

[89] P. O. Erah, A. F. Goddard, D. A. Barrett, P. N. Shaw, and R. C. Spiller, "The stability of amoxycillin, clarithromycin and metronidazole in gastric juice: relevance to the treatment of Helicobacter pylori infection.," *J. Antimicrob. Chemother.*, vol. 39, no. 1, pp. 5–12, Jan. 1997, doi: 10.1093/jac/39.1.5.

[90] D. Dimitrakopoulou, I. Rethemiotaki, Z. Frontistis, N. P. Xekoukoulotakis, D. Venieri, and D. Mantzavinos, "Degradation, mineralization and antibiotic inactivation of amoxicillin by UV-A/TiO_2 photocatalysis.," *J. Environ. Manage.*, vol. 98, pp. 168–174, May 2012, doi: 10.1016/j.jenvman.2012.01.010.

[91] E. Elmolla and M. Chaudhuri, "Photocatalytic Degradation of Amoxicillin, Ampicillin and Cloxacillin Antibiotics in Aqueous Solution Using UV/TiO2 and UV/H2O2/TiO2 Photocatalysis," *Desalination*, vol. 252, pp. 46–52, Mar. 2010, doi: 10.1016/j.desal.2009.11.003.

[92] H. Çağlar Yılmaz, E. Akgeyik, S. Bougarrani, M. el Azzouzi, and S. Erdemoglu, "Photocatalytic degradation of amoxicillin using Co-doped TiO 2 synthesized by reflux method and monitoring of degradation products by LC–MS/MS," *J. Dispers. Sci. Technol.*, vol. 41, pp. 1–12, Mar. 2019, doi: 10.1080/01932691.2019.1583576.

[93] T. Reyns, M. Cherlet, S. De Baere, P. De Backer, and S. Croubels, "Rapid method for the quantification of amoxicillin and its major metabolites in pig tissues by liquid chromatography-tandem mass spectrometry with emphasis on stability issues.," *J. Chromatogr. B, Anal. Technol. Biomed. life Sci.*, vol. 861, no. 1, pp. 108–116, Jan. 2008, doi: 10.1016/j.jchromb.2007.11.007.

[94] S. Baere, P. Wassink, S. Croubels, S. De Boever, K. Baert, and P. Backer, "Quantitative liquid chromatographic–mass spectrometric analysis of amoxycillin in broiler edible tissues," *Anal. Chim. Acta*, vol. 529, pp. 221–227, Jan. 2005, doi: 10.1016/j.aca.2004.09.069.

[95] A. Freitas, J. Barbosa, and F. Ramos, "Determination of Amoxicillin Stability in Chicken Meat by Liquid Chromatography–Tandem Mass Spectrometry," *Food Anal. Methods*, vol. 5, Jun. 2012, doi: 10.1007/s12161-011-9267-4.

[96] A. Jerzsele and G. Nagy, "The stability of amoxicillin trihydrate and potassium clavulanate combination in aqueous solutions.," *Acta Vet. Hung.*, vol. 57, no. 4, pp. 485–493, Dec. 2009, doi: 10.1556/AVet.57.2009.4.3.

[97] S. S. Ayoub, "Paracetamol (acetaminophen): A familiar drug with an unexplained

mechanism of action.," *Temp. (Austin, Tex.)*, vol. 8, no. 4, pp. 351–371, 2021, doi: 10.1080/23328940.2021.1886392.

[98] N. Bednarčuk *et al.*, "Antibiotic Utilization during COVID-19: Are We Over-Prescribing?," *Antibiot. (Basel, Switzerland)*, vol. 12, no. 2, Feb. 2023, doi: 10.3390/antibiotics12020308.

[99] B. Conti, "Prostaglandin E2 that triggers fever is synthesized through an endocannabinoid- dependent pathway.," *Temp. (Austin, Tex.)*, vol. 3, no. 1, pp. 25–27, 2016, doi: 10.1080/23328940.2015.1130520.

[100] S. Balli, K. R. Shumway, and S. Sharan, "Physiology, Fever.," Treasure Island (FL), 2024.

[101] F. David S. Wald, MD, Malcolm Law, FRCP, Joan K. Morris, PhD, Jonathan P. Bestwick, MSc, Nicholas J. Wald, "Combination Therapy Versus Monotherapy in Reducing Blood," *J. Control. Release*, vol. 91, no. 3, pp. 375–384, 2003, [Online]. Available: http://dx.doi.org/10.1163/156856209X404514%0Ahttp://dx.doi.org/10.1016/j.ijbiomac.2015.01.045%0Ahttp://www.bmj.com/cgi/doi/10.1136/bmj.b1665%0Ahttp://dx.doi.org/10.1016/j.amjmed.2008.09.038%0Ahttp://www.clinicalhypertension.com/content/22/1/7

[102] L. F. Prescott, "Kinetics and metabolism of paracetamol and phenacetin.," *Br. J. Clin. Pharmacol.*, vol. 10 Suppl 2, no. Suppl 2, pp. 291S-298S, Oct. 1980, doi: 10.1111/j.1365-2125.1980.tb01812.x.

[103] B. J. Akhavan, N. R. Khanna, and P. Vijhani, "Amoxicillin.," Treasure Island (FL), 2024.

[104] H. Abbas, I. Hussein, and A. Abed, "The Tolerability and Degradation Rate of Amoxicillin Alone and with Clavulanic Acid in the Acidic and Alkaline Medium," *J. Glob. Pharma Technol.*, vol. 11, pp. 656–661, Nov. 2019.

[105] F. Aranda and B. Rivas, "REMOVAL OF AMOXICILLIN THROUGH DIFFERENT METHODS, EMPHASIZING REMOVAL BY BIOPOLYMERS AND ITS DERIVATIVES. AN OVERVIEW," *J. Chil. Chem. Soc.*, vol. 67, pp. 5643–5655, Sep. 2022, doi: 10.4067/S0717-97072022000305643.

[106] S. Beg, A. Nayak, K. Kohli, S. K. Swain, and M. Saquib, "Antimicrobial activity assessment of time-dependent release bilayer tablets of amoxicillin trihydrate," *Brazilian J. Pharm. Sci.*, vol. 48, pp. 265–272, Apr. 2012, doi: 10.1590/S1984-82502012000200010.

[107] M. Douša and R. Hosmanová, "Rapid determination of amoxicillin in premixes by HPLC," *J. Pharm. Biomed. Anal.*, vol. 37, pp. 373–377, Mar. 2005, doi: 10.1016/j.jpba.2004.10.010.

[108] K. Hirte, B. Seiwert, G. Schüürmann, and T. Reemtsma, "New hydrolysis products of the beta-lactam antibiotic amoxicillin, their pH-dependent formation and search in municipal wastewater.," *Water Res.*, vol. 88, pp. 880–888, Jan. 2016, doi: 10.1016/j.watres.2015.11.028.

[109] A. Kotwani and K. Holloway, "Trends in antibiotic use among outpatients in New Delhi, India.," *BMC Infect. Dis.*, vol. 11, p. 99, Apr. 2011, doi: 10.1186/1471-2334-11-99.

[110] G. L. Marlière, M. B. Ferraz, and J. Q. dos Santos, “Antibiotic consumption patterns and drug leftovers in 6000 Brazilian households.,” *Adv. Ther.*, vol. 17, no. 1, pp. 32–44, 2000, doi: 10.1007/BF02868029.

[111] A. Arancibia, J. Guttmann, G. González, and C. González, “Absorption and disposition kinetics of amoxicillin in normal human subjects.,” *Antimicrob. Agents Chemother.*, vol. 17, no. 2, pp. 199–202, Feb. 1980, doi: 10.1128/AAC.17.2.199.

[112] C. Gordon, C. Regamey, and W. M. Kirby, “Comparative clinical pharmacology of amoxicillin and ampicillin administered orally.,” *Antimicrob. Agents Chemother.*, vol. 1, no. 6, pp. 504–507, Jun. 1972, doi: 10.1128/AAC.1.6.504.

[113] R. Andreozzi, M. Canterino, R. Marotta, and N. Paxeus, “Antibiotic removal from wastewaters: the ozonation of amoxicillin.,” *J. Hazard. Mater.*, vol. 122, no. 3, pp. 243–250, Jul. 2005, doi: 10.1016/j.jhazmat.2005.03.004.

[114] P. MUTIYAR and A. Mittal, “Occurrences and fate of an antibiotic amoxicillin in extended aeration-based sewage treatment plant in Delhi, India: A case study of emerging pollutant,” *Desalin. water Treat.*, vol. 51, pp. 6158–6164, Mar. 2013, doi: 10.1080/19443994.2013.770199.

[115] E. Aydin and I. Talinli, “Analysis, occurrence and fate of commonly used pharmaceuticals and hormones in the Buyukcekmece Watershed, Turkey.,” *Chemosphere*, vol. 90, no. 6, pp. 2004–2012, Feb. 2013, doi: 10.1016/j.chemosphere.2012.10.074.

[116] C. Foti and O. Giuffrè, “Interaction of Ampicillin and Amoxicillin with Mn(2+): A Speciation Study in Aqueous Solution.,” *Molecules*, vol. 25, no. 14, Jul. 2020, doi: 10.3390/molecules25143110.

[117] P. Proctor, N. Gensmantel, and M. Page, “The chemical reactivity of penicillins and other ?-lactam antibiotics,” *J. Chem. Soc. Trans. 2 - J CHEM SOC PERKIN TRANS 2*, vol. 2, Jan. 1982, doi: 10.1039/p29820001185.

[118] J.-E. Hugonnet *et al.*, “Factors essential for L,D-transpeptidase-mediated peptidoglycan cross-linking and β-lactam resistance in Escherichia coli.,” *Elife*, vol. 5, Oct. 2016, doi: 10.7554/eLife.19469.

[119] G. W. Przybyła, K. A. Szychowski, and J. Gmiński, “Paracetamol – An old drug with new mechanisms of action,” *Clin. Exp. Pharmacol. Physiol.*, vol. 48, no. 1, pp. 3–19, 2021, doi: 10.1111/1440-1681.13392.

[120] J. A. Forrest, J. A. Clements, and L. F. Prescott, “Clinical pharmacokinetics of paracetamol.,” *Clin. Pharmacokinet.*, vol. 7, no. 2, pp. 93–107, 1982, doi: 10.2165/00003088-198207020-00001.

[121] R. B. Raffa *et al.*, “Pharmacokinetics of Oral and Intravenous Paracetamol (Acetaminophen) When Co-Administered with Intravenous Morphine in Healthy Adult Subjects.,” *Clin. Drug Investig.*, vol. 38, no. 3, pp. 259–268, Mar. 2018, doi: 10.1007/s40261-017-0610-4.

[122] P. Katakam, P. Raju, K. Kumari, and M. Narasu, “Spectrophotometric Estimation of Amoxicillin Trihydrate in Bulk and Pharmaceutical Dosage Form,” *E-Journal Chem.*, vol. 5, pp. 1114–1116, Nov. 2008, doi: 10.1155/2008/350646.

[123] D. M. Patel, M. Sardhara, D. Thumbadiya, and C. Patel, “Development and validation

of spectrophotometric method for simultaneous estimation of paracetamol and lornoxicam in different dissolution media," *Pharm. Methods*, vol. 3, pp. 98–101, Jul. 2012, doi: 10.4103/2229-4708.103885.

[124] M. Sendanyoye, "Validation of HPLC-UV method for determination of amoxicillin Trihydrate in capsule," *Ann. Adv. Chem.*, pp. 055–072, 2018, doi: 10.29328/journal.aac.1001014.

[125] D. S. Nikam, C. G. Bonde, S. J. Surana, G. Venkateshwarlu, and P. G. Dekate, "Development and validation of RP-HPLC method for simultaneous estimation of Amoxicillin trihydrate and Flucloxacillin sodium in capsule dosage form," *Int. J. PharmTech Res.*, vol. 1, no. 3, pp. 935–939, 2009.

[126] K. Bialik-Was, K. N. Raftopoulos, and K. Pielichowski, "Alginate Hydrogels with Aloe vera: The Effects of Reaction Temperature on Morphology and Thermal Properties," *Materials (Basel).*, vol. 15, no. 3, 2022, doi: 10.3390/ma15030748.

[127] W. Krasaekoopt, B. Bhandari, and H. Deeth, "The influence of coating materials on some properties of alginate beads and survivability of microencapsulated probiotic bacteria," *Int. Dairy J.*, vol. 14, no. 8, pp. 737–743, 2004, doi: 10.1016/j.idairyj.2004.01.004.

[128] W. P. Voo, C. W. Ooi, A. Islam, B. T. Tey, and E. S. Chan, "Calcium alginate hydrogel beads with high stiffness and extended dissolution behaviour," *Eur. Polym. J.*, vol. 75, pp. 343–353, 2016, doi: 10.1016/j.eurpolymj.2015.12.029.

[129] N. Obradovic *et al.*, "Influence of Chitosan Coating on Mechanical Stability of Biopolymer Carriers with Probiotic Starter Culture in Fermented Whey Beverages," *Int. J. Polym. Sci.*, vol. 2015, pp. 1–8, Oct. 2015, doi: 10.1155/2015/732858.

[130] K. Narra *et al.*, "Effect of formulation variables on rifampicin loaded alginate beads.," *Iran. J. Pharm. Res. IJPR*, vol. 11, no. 3, pp. 715–721, 2012.

[131] S. J. Kim, K. J. Lee, and S. I. Kim, "Thermo-sensitive Swelling Behavior of Poly(2-Ethyl-2-oxazoline)/Poly(Vinyl Alcohol) Interpenetrating Polymer Network Hydrogels," *J. Macromol. Sci. Part A*, vol. 41, no. 3, pp. 267–274, Dec. 2004, doi: 10.1081/MA-120028206.

[132] A. Mohanan and B. Vishalakshi, "Swelling and Diffusion Characteristics of Interpenetrating Network Films Composed of Sodium Alginate and Gelatin: Transport of Azure B," *Int. J. Polym. Mater. Polym. Biomater.*, vol. 58, no. 11, pp. 561–580, Aug. 2009, doi: 10.1080/00914030903035469.

[133] M. F. Aldawsari, M. M. Ahmed, F. Fatima, M. K. Anwer, P. Katakam, and A. Khan, "Development and characterization of calcium-alginate beads of apigenin: In vitro antitumor, antibacterial, and antioxidant activities," *Mar. Drugs*, vol. 19, no. 8, 2021, doi: 10.3390/md19080467.

[134] S. Takka and A. Gürel, "Evaluation of chitosan/alginate beads using experimental design: Formulation and in vitro characterization," *AAPS PharmSciTech*, vol. 11, no. 1, pp. 460–466, 2010, doi: 10.1208/s12249-010-9406-z.

[135] S. Magaldi *et al.*, "Well diffusion for antifungal susceptibility testing.," *Int. J. Infect. Dis. IJID Off. Publ. Int. Soc. Infect. Dis.*, vol. 8, no. 1, pp. 39–45, Jan. 2004, doi: 10.1016/j.ijid.2003.03.002.

[136] C. Valgas, S. M. De Souza, E. F. A. Smânia, and A. Smânia, “Screening methods to determine antibacterial activity of natural products,” *Brazilian J. Microbiol.*, vol. 38, no. 2, pp. 369–380, 2007, doi: 10.1590/S1517-83822007000200034.

[137] M. Balouiri, M. Sadiki, and S. K. Ibnsouda, “Methods for in vitro evaluating antimicrobial activity: A review.,” *J. Pharm. Anal.*, vol. 6, no. 2, pp. 71–79, Apr. 2016, doi: 10.1016/j.jpha.2015.11.005.

[138] K. Mukherjee, P. Dutta, and T. K. Giri, “Al3+/Ca2+ cross-linked hydrogel matrix tablet of etherified tara gum for sustained delivery of tramadol hydrochloride in gastrointestinal milieu,” *Int. J. Biol. Macromol.*, vol. 232, no. December 2022, p. 123448, 2023, doi: 10.1016/j.ijbiomac.2023.123448.

[139] O. Sreekanth Reddy, M. C. S. Subha, T. Jithendra, C. Madhavi, and K. Chowdoji Rao, “Curcumin encapsulated dual cross linked sodium alginate/montmorillonite polymeric composite beads for controlled drug delivery,” *J. Pharm. Anal.*, vol. 11, no. 2, pp. 191–199, 2021, doi: 10.1016/j.jpha.2020.07.002.

[140] M. A. Morales *et al.*, “In situ synthesis and magnetic studies of iron oxide nanoparticles in calcium-alginate matrix for biomedical applications,” *Mater. Sci. Eng. C*, vol. 28, no. 2, pp. 253–257, 2008, doi: 10.1016/j.msec.2006.12.016.

[141] T. H. Peroxide and S. Ability, “Alginate-Mediated Synthesis of Hetero-Shaped Silver,” *Molecules*, vol. 25, no. M, p. 435, 2020.

[142] S. Kumar, “Immobilization and Biochemical Properties of Purifi ed Xylanase from Bacillus amyloliquefaciens SK-3 and Its Application in Kraft Pulp Biobleaching,” *J. Clin. Microbiol. Biochem. Technol.*, vol. 2016, pp. 26–34, Dec. 2016.

[143] J. Lei, J.-H. Kim, and Y. Jeon, “Preparation and properties of alginate/polyaspartate composite hydrogels,” *Macromol. Res. - MACROMOL RES*, vol. 16, pp. 45–50, Nov. 2008, doi: 10.1007/BF03218959.

[144] T. Mk, S. Patil, H. Shettigar, K. Bairwa, and S. Jana, “Effect of Biofield Treatment on Spectral Properties of Paracetamol and Piroxicam,” no. July 2015, 2016, doi: 10.4172/2150-3494.100098.

[145] I. Nugrahani, S. N. Soewandhi, and S. Ibrahim, “SOLID STATE INTERACTION BETWEEN AMOXICILLIN TRIHYDRATE AND,” no. January, 2007.

[146] D. Wójcik-Pastuszka, J. Krzak, B. Macikowski, R. Berkowski, B. Osiński, and W. Musiał, “Evaluation of the release kinetics of a pharmacologically active substance from model intra-articular implants replacing the cruciate ligaments of the knee,” *Materials (Basel).*, vol. 12, no. 8, 2019, doi: 10.3390/ma12081202.

[147] S. Stein, T. Auel, W. Kempin, M. Bogdahn, W. Weitschies, and A. Seidlitz, “Influence of the test method on in vitro drug release from intravitreal model implants containing dexamethasone or fluorescein sodium in poly (d,l-lactide-co-glycolide) or polycaprolactone.,” *Eur. J. Pharm. Biopharm. Off. J. Arbeitsgemeinschaft fur Pharm. Verfahrenstechnik e.V*, vol. 127, pp. 270–278, Jun. 2018, doi: 10.1016/j.ejpb.2018.02.034.

[148] J. Siepmann and N. A. Peppas, “Higuchi equation: derivation, applications, use and misuse.,” *Int. J. Pharm.*, vol. 418, no. 1, pp. 6–12, Oct. 2011, doi: 10.1016/j.ijpharm.2011.03.051.

[149] T. HIGUCHI, "MECHANISM OF SUSTAINED-ACTION MEDICATION. THEORETICAL ANALYSIS OF RATE OF RELEASE OF SOLID DRUGS DISPERSED IN SOLID MATRICES.," *J. Pharm. Sci.*, vol. 52, pp. 1145–1149, Dec. 1963, doi: 10.1002/jps.2600521210.

[150] N. A. Peppas, "Analysis of Fickian and non-Fickian drug release from polymers.," *Pharm. Acta Helv.*, vol. 60, no. 4, pp. 110–111, 1985.

[151] R. W. Korsmeyer, R. Gurny, E. Doelker, P. Buri, and N. A. Peppas, "Mechanisms of solute release from porous hydrophilic polymers," *Int. J. Pharm.*, vol. 15, no. 1, pp. 25–35, 1983, doi: 10.1016/0378-5173(83)90064-9.

[152] S. Dash, P. N. Murthy, L. Nath, and P. Chowdhury, "Kinetic modeling on drug release from controlled drug delivery systems," *Acta Pol. Pharm. - Drug Res.*, vol. 67, no. 3, pp. 217–223, 2010.

[153] A. Jain and S. K. Jain, "IN VITRO RELEASE KINETICS MODEL FITTING OF LIPOSOMES: AN INSIGHT.," *Chem. Phys. Lipids*, Oct. 2016, doi: 10.1016/j.chemphyslip.2016.10.005.

[154] M. N. Freitas and J. M. Marchetti, "Nimesulide PLA microspheres as a potential sustained release system for the treatment of inflammatory diseases," *Int. J. Pharm.*, vol. 295, no. 1–2, pp. 201–211, 2005, doi: 10.1016/j.ijpharm.2005.03.003.

[155] L. V. Allen, *Modern Pharmaceutics 4th Edition, Revised and Expanded*, vol. 37, no. 12. 1980.

[156] S. A. Bravo, M. C. Lamas, and C. J. Salamón, "In-vitro studies of diclofenac sodium controlled-release from biopolymeric hydrophilic matrices.," *J. Pharm. Pharm. Sci. a Publ. Can. Soc. Pharm. Sci. Soc. Can. des Sci. Pharm.*, vol. 5, no. 3, pp. 213–219, 2002.

[157] M. Grassi and G. Grassi, "Mathematical modelling and controlled drug delivery: matrix systems.," *Curr. Drug Deliv.*, vol. 2, no. 1, pp. 97–116, Jan. 2005, doi: 10.2174/1567201052772906.

[158] M. H. Shoaib, J. Tazeen, H. A. Merchant, and R. I. Yousuf, "Evaluation of drug release kinetics from ibuprofen matrix tablets using HPMC.," *Pak. J. Pharm. Sci.*, vol. 19, no. 2, pp. 119–124, Apr. 2006.

[159] P. L. Ritger and N. A. Peppas, "A simple equation for description of solute release II. Fickian and anomalous release from swellable devices," *J. Control. Release*, vol. 5, no. 1, pp. 37–42, 1987, doi: 10.1016/0168-3659(87)90035-6.

[160] M. Gülfen, Y. Canbaz, and A. Özdemir, "Simultaneous Determination of Amoxicillin, Lansoprazole, and Levofloxacin in Pharmaceuticals by HPLC with UV–Vis Detector," *J. Anal. Test.*, vol. 4, Mar. 2020, doi: 10.1007/s41664-020-00121-4.

[161] R. Faqeer, R. Bakain, M. Rasheed, and A. Makahleh, "Development of Novel HPLC Method for Analysing Drugs Used in H-Pylori Treatment," *Asian J. Pharm. Sci.*, vol. 14, p. 2021, Oct. 2021.

[162] N. Tavakoli, J. Varshosaz, F. Dorkoosh, and M. Zargarzadeh, "Development and validation of a simple HPLC method for simultaneous in vitro determination of amoxicillin and metronidazole at single wavelength," *J. Pharm. Biomed. Anal.*, vol. 43, pp. 325–329, Feb. 2007, doi: 10.1016/j.jpba.2006.06.002.

[163] L. Jeeboi and S. Boddu, “UV spectrophotometric method for simultaneous estimation of tramadol hydrochloride and aceclofenac in bulk and tablet dosage form,” vol. 8, pp. 334–340, Jan. 2016.

[164] Wrushali A. Panchale, Chaitanya A. Gulhane, Jagdish V. Manwar, and R. L. Bakal, “Simultaneous estimation of salbutamol sulphate and ambroxol HCl from their combined dosage form by UV-VIS spectroscopy using simultaneous equation method,” *GSC Biol. Pharm. Sci.*, vol. 13, no. 3, pp. 127–134, 2020, doi: 10.30574/gscbps.2020.13.3.0397.

[165] I. Bulduk, “HPLC-UV method for quantification of favipiravir in pharmaceutical formulations,” *Acta Chromatogr.*, Sep. 2020, doi: 10.1556/1326.2020.00828.

[166] C. V. Sharma and V. Mehta, “Paracetamol: Mechanisms and updates,” *Contin. Educ. Anaesthesia, Crit. Care Pain*, vol. 14, no. 4, pp. 153–158, 2014, doi: 10.1093/bjaceaccp/mkt049.

[167] V. Prajapati, G. Jani, T. Khutliwala, and B. Zala, “Raft forming system—An upcoming approach of gastroretentive drug delivery system,” *J. Control. Release*, vol. 168, Mar. 2013, doi: 10.1016/j.jconrel.2013.02.028.

[168] B. -. Lee, P. Ravindra, and E. Chan, “Size and Shape of Calcium Alginate Beads Produced by Extrusion Dripping,” *Chem. Eng. Technol.*, vol. 36, Sep. 2013, doi: 10.1002/ceat.201300230.

[169] A. Mehregan Nikoo, R. Kadkhodaee, B. Ghorani, H. Razzaq, and N. Tucker, “Controlling the morphology and material characteristics of electrospray generated calcium alginate microhydrogels,” *J. Microencapsul.*, vol. 33, no. 7, pp. 605–612, Oct. 2016, doi: 10.1080/02652048.2016.1228707.

[170] A. Partovinia and E. Vatankhah, “Experimental investigation into size and sphericity of alginate micro-beads produced by electrospraying technique: Operational condition optimization,” *Carbohydr. Polym.*, vol. 209, no. January, pp. 389–399, 2019, doi: 10.1016/j.carbpol.2019.01.019.

[171] K. Guruviah, P. Kumar, and K. Kumar, “Green synthesis of novel silver nanocomposite hydrogel based on sodium alginate as an efficient biosorbent for the dye wastewater treatment: prediction of isotherm and kinetic parameters,” *Desalin. Water Treat.*, vol. 57, pp. 1–14, May 2016, doi: 10.1080/19443994.2016.1178178.

[172] M. F. Aldawsari, M. M. Ahmed, F. Fatima, M. K. Anwer, P. Katakam, and A. Khan, “Development and Characterization of Calcium-Alginate Beads of Apigenin: In Vitro Antitumor, Antibacterial, and Antioxidant Activities.,” *Mar. Drugs*, vol. 19, no. 8, Aug. 2021, doi: 10.3390/md19080467.

[173] H. Maswadeh, “Incompatibility of Paracetamol with Pediatric Suspensions Containing Amoxicillin, Azithromycin and Cefuroxime Axetil,” *Pharmacol. & Pharm.*, vol. 08, no. 11, pp. 355–368, 2017, doi: 10.4236/pp.2017.811026.

[174] G. G. G. de Oliveira, A. Feitosa, K. Loureiro, A. R. Fernandes, E. B. Souto, and P. Severino, “Compatibility study of paracetamol, chlorpheniramine maleate and phenylephrine hydrochloride in physical mixtures,” *Saudi Pharm. J.*, vol. 25, no. 1, pp. 99–103, 2017, doi: 10.1016/j.jsps.2016.05.001.

[175] I. Jendrzejewska, T. Goryczka, E. Pietrasik, J. Klimontko, and J. Jampilek, “X-ray and

Thermal Analysis of Selected Drugs Containing Acetaminophen," *Molecules*, vol. 25, no. 24, 2020, doi: 10.3390/MOLECULES25245909.

[176] M. Narkar, P. Sher, and A. Pawar, "Stomach-specific controlled release gellan beads of acid-soluble drug prepared by ionotropic gelation method," *AAPS PharmSciTech*, vol. 11, no. 1, pp. 267–277, 2010, doi: 10.1208/s12249-010-9384-1.

[177] B. D. L. Novo, F. Arruda, and N. Gomes, "Amoxicillin Trihydrate Characterization and investigative adsorption using a Brazilian montmorillonite Amoxicillin Trihydrate Characterization and investigative adsorption using a Brazilian montmorillonite," no. August, 2022, doi: 10.1590/1517-7076-rmat-2022-0109.

[178] F. Zapata, A. López-Fernández, F. Ortega-Ojeda, G. Quintanilla, C. García-Ruiz, and G. Montalvo, "Introducing ATR-FTIR Spectroscopy through Analysis of Acetaminophen Drugs: Practical Lessons for Interdisciplinary and Progressive Learning for Undergraduate Students," *J. Chem. Educ.*, vol. 98, no. 8, pp. 2675–2686, Aug. 2021, doi: 10.1021/acs.jchemed.0c01231.

[179] R. W. Korsmeyer, R. Gurny, E. Doelker, P. Buri, and N. A. Peppas, "Mechanisms of solute release from porous hydrophilic polymers," *Int. J. Pharm.*, vol. 15, no. 1, pp. 25–35, May 1983, doi: 10.1016/0378-5173(83)90064-9.

[180] O. A. A. Ahmed, S. M. Badr-Eldin, and T. A. Ahmed, "Kinetic study of the in vitro release and stability of theophylline floating beads," *Int. J. Pharm. Pharm. Sci.*, vol. 5, no. 1, pp. 179–184, 2013.

CHAPTER 8

PUBLICATIONS

A Review on Applications of Biosynthesised Silver Nanoparticles

Aditi Bala [1], Rahul Molla [1], Sangita Panja [2], Sanchita Mandal [1*].

[1] Department of Pharmaceutical Technology, Jadavpur University,

Kolkata- 700032

[2] Bengal School of Technology, MAKAUT, West Bengal.

[*] Corresponding author.

Address- Department of Pharmaceutical Technology, Jadavpur

University, Kolkata 700032

A Review on Applications of Biosynthesized Silver Nanoparticles

ABSTRACT-

In modern era nanotechnology and nanoparticles are being emerged very quickly, and have attracted remarkable attention due to their biomedical and industrial activities. Nowadays, biosynthesis of silver nanoparticles (AgNPs) has gained so much attention in developed countries due to the demand of eco-friendly technology for material synthesis. The use of green chemistry is environmentally friendly, less-toxic, and cost effective. The chemical synthesis of nanoparticles increases the adverse effects on the ecosystem and living organisms. One possible way to reduce these adverse effects is the biological-mediated synthesis of nanoparticles with new biological sources like plants and microorganisms. The silver nanoparticles produced by plants or other microorganisms have various applications such as antibacterial, antifungal, antivirus, anticancer drugs, in waste water treatment, animal and fish farms etc. In recent days strategies for improving the efficacy of antibiotics is done by combining them with AgNPs. They control the microbial infections as by the damaging microbial deoxyribonucleic acid (DNA). This review describes the synthesis of the AgNPs from green sources, and their prominent impact on their applications.

KEYWORDS-

Biosynthesis, nanoparticles, silver nanoparticles, drug delivery, anticancer, antifungal, antibacterial.

INTRODUCTION-

The synthesis and use of various noble metal nanoparticles has been increasingly developed worldwide. As physical and chemical methods of preparation of nanoparticles are quite time consuming, costly, non-environmentally friendly and toxic, scientists have opted for green chemistry for synthesis of nanoparticles. “BIO SYNTHESIS” is an environmentally friendly

process in chemical technology that are used to produce compounds using biological sources like different constituents of plants and other microbes as reducing agent to produce silver nanoparticles. The other terms for this are “GREEN SYNTHESIS” (by plants) or “BIOGENIC SYNTHESIS”. They are very much needed as there are many problems associated with environmental concerns with other methods.

Nano technology is the branch of science that deals with the synthesis, characterization and application of particles in nano scale which is from 1 to 100nm [1]. Nano technology are used profusely in medical and pharmaceutical fields these days. As nanoparticles are extremely small in size and have higher surface area they can bind to various functional groups and can be used in different formulations as well as in medical devices. The physical, chemical, and biological characteristics of the particles vary from those of their bulk counterparts as the particle size decreases, in addition to the ratio of surface area to volume increasing. Despite the fact that there are many different types of metals in nature, only a limited few, like gold, silver, palladium, and platinum, are extensively produced in nanostructured form. Silver nanoparticles have drawn the most attention among the aforementioned metals due to their special characteristics for use in a variety of applications, including pharmaceutics, agriculture, water detoxification, air filtration, textile industries, as a catalyst in oxidation reactions. Additionally, they have strong antibacterial activity against a variety of microorganisms without being toxic to animal cells. So, they are being used against multi-drug resistance microorganisms. Nanoparticles are generally synthesized by using physical and chemical procedures. Chemically prepared nanoparticles have some limitations like hazardous chemicals binding on their surface and for that they are not appropriate for medical usage. Furthermore, by-products produced in chemical routes are environmentally toxic. These techniques are expensive and demand a lot of energy and space. Using biological systems such as microorganisms, plants, viruses and animal cell cultures is an alternative procedure for preparation of nanoparticles [2].

Silver nanoparticles possess unique attributes which are breakthrough myriad applications such as antimicrobial, anticancer, larvicidal, catalytic, and wound healing activities. The biosynthesis of silver nanoparticles has been proposed as a cheap and environmentally friendly alternative to the chemical and physical methods. A large number of microbes such as bacteria, fungus, yeasts, and plants either intra or extracellular, are of higher crop yields and lower expenses have been discovered to be capable of synthesizing nanoparticles [3].

BIOSYNTHESIS OF SILVER NANOPARTICLES-

We know that plants are rich in different phytochemicals like tannins, flavonoids, terpenoids, saponins, enzymes etc. These work as a reducing agent for synthesis of silver nanoparticles (usually from $AgNO_3$). They also help to stabilize the Ag+ ion in the nanoparticles. Fungi and other microorganisms are also some ideal candidates in the synthesis of metal nanoparticles with different sizes, because they can secrete large number of enzymes which act as reducing agents for AgNPs.

APPLICATIONS OF SILVER NANO PARTICLES-

Several researchers in science and industry have focused their attention on the multidisciplinary topic of nanotechnology. Nanotechnology offers the flexible and easy synthesis of metal-based biocompatible nano-materials that can be applied to a wide range of potential applications in medical and biological sciences, including medical diagnosis, medicine, bio sensing, health care, drug delivery [4], coating and conservation [5], wound healing, the food industry, cosmetics and environmental remediation (water purification) [6]. Figure 1 shows the different applications of AgNPs which are discussed in this review.

As AgNPs have very small particle size they have play a vital role in the applied sciences. The application of silver nano-materials is very diverse because of their unique properties. The AgNPs can be applied in both of the micro level and macro level. The nanoparticles which are biosynthesized have been used in a variety of applications including targeted drug delivery, treatment of cancer, gene therapy, antibacterial antifungal agents etc.

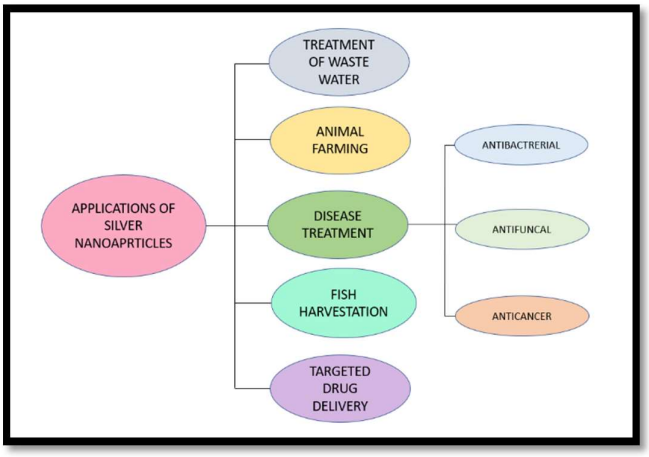

FIGURE 1

IN THE TREATMENT OF WASTE WATER-

Pollution in drinking water is a worldwide concern global problem as it causes irreversible damage to plants, humans, and animals and spreads numerous epidemics and chronic disease [7]. Wastewater contains a high concentration of metals, herbicides, pesticides, and toxic industrial effluents that can disrupt various biochemical processes in animals and human beings and could cause various diseases and even genetic disorders by altering in enzymatic activities/pathways.

Over a billion people having lack of access to drinking pure and clean water. Many death ratios have been noticed due to waterborne disease [8]. For these issues, silver nanomaterial is an emerging material regarding in purification of wastewater treatment [9]. A laboratory-scale study concluded that 1 mg AgNPs in 1 L water could inhibit the growth of microbes by 80% [10], and due to their specific properties, the wastewater can be reduced [11].

IN ANIMAL FARMING-

Animal welfare, particularly that of domestic cattle and small ruminants, has a big impact on food production and economic development in developing nations. The world is concerned about bacterial and fungal infections in animal husbandry. Numerous compounds are secreted by bacterial and fungal species, contaminating the environment and animal feed. Animals and poultry acquire serious infections as a result of contaminated feed. Therefore, nanotechnology has the potential to cure many diseases related to animal health [12]. In African countries, rabbit industries are at their peak regarding their production, housing management, economic growth, and nutrition [13]. Nanotechnology is being applied to this issue, and nanoparticles are being provided as dietary supplements in place of salt and other minerals. These nanoparticles have many great properties in animal farming such as growth, maintaining health, and disease [14].

Concerning their medicinal value, nanoparticles are being used as a source of drug delivery in animal husbandry [15]. Disease spreading from food in animals is one of the important among all animal diseases. Animal feed contamination is significantly influenced by fungi. There are numerous mycotoxins known to infect animal feed. A promising strategy to prevent this contamination is silver nanoparticles.

A study was conducted by Gangadoo et al. [16] regarding the nanoparticles and their use in broiler feed. Nanoparticles were supplemented in the feed. The results have concluded that the dose of the nanoparticle improved the dietary supplements and showed no toxicity. Some studies have revealed their results and concluded that nanomaterials could improve reproduction in poultry, livestock, and fisheries [17].

IN HARVESTING FISHES-

Fish, a crucial agricultural product, increases the value of rural incomes by promoting employment, generating income, and maintaining the safety of the world's food supply. Fishery generates more profitable financial gain than any other aquaculture farming operation, even only through catch and collecting. This industry is also vulnerable to a number of issues, such as overexploitation, pollution, climate change, and illnesses, which can stunt growth and cause significant financial loss. In aquaculture production, different diseases have developed into one of the major limiting factors [18]. *Pseudomonas* and *Aeromonas sp.* are one of the widely known fish pathogens [19].

Among a large number of aquatic pathogens, the gm(-ve) "*Aeromonas hydrophila*" has been recovered from a wide variety of freshwater fishes and possesses the ability to grow in both aerobic and anaerobic conditions and encourages the spread of several fish diseases, including haemorrhagic septicaemia, ulcers, fin-rot, and tail-rot. Their infection enhances environmental pollution, the elevation of water temperature, and the addition of stressors in the aquatic medium [20]. To prevent these diseases antibiotics are used. However, a study on *A. hydrophila* from various fish tissues have revealed that the pathogen had developed resistance to many antibiotics like amoxicillin, ampicillin, lincomycin, novobiocin, oxacillin, penicillin,

rifampicin, and tetracycline [21], and thus researchers have attempted to find the alternative of these antibiotics [22]. In this situation, biologically produced AgNPs' ability to inhibit *A. hydrophila* growth was compared to that of antibiotics.

The biologically produced AgNPs were used in this work to treat fish pathogens such as *Vibrio harveyii, Vibrio parahaemolyticus, Vibrio alginolyticus,* and *Vibrio anguillarum* for bacterial infections [23]. The result revealed that the highest anti-microbial activity of AgNPs was found against the pathogens *Vibrio harveyii* and *Vibrio parahaemolyticus.*

SILVER NANOPARTICLES IN DISEASE TREATMENT-

The research community is in the continuous search of novel opportunities for improving disease diagnosis, drug designing, drug delivery proper treatments with lesser side effects, therefore, nano biotechnology is an important field with many novel applications [24]. Since ancient times, metals and especially silver were known for their antibacterial effects, but these days available methodologies allow the further exploitation like Anti-Cancer, Anti-Fungal, Anti-Viral activity even Targeted Delivery of AgNPS.

AgNPs are a very important inhibitory material for different diseases even known as a good antimicrobial agent against pathogenic bacterial species [25]. Silver nanoparticles can react with the thiol group of proteins in bacterial cells, which leads to the inactivation of the cell. It also can stop oxidative phosphorylation and DNA replication [26]. The inhibitory process takes place by DNA replication, reactive oxygen species, and direct damage of the microbial cell [27]. A researcher Reidy et al. [28] has revealed that the nanoparticles first stick to the cell wall, secondly, the nanoparticles penetrate the parasite cell, and third, it starts DNA damage by damaging the thiol group of protein. For this reason, AgNPs are being used to cure a wide range of diseases, for example malaria [29].

A new era of antimalarial approach is being emerged by using nanoparticles alone or in combination with commonly used drugs and maybe an innovative therapeutic approach for malaria treatment [30]. A study was conducted to check the anti-plasmodial activity AgNPs. The results were highly encouraging since growth inhibition was obtained with LC50 values of 3.75 g/ml (amylase product AgNPs) and 8 g/ml (Ashoka produced AgNPs), and 30 g/ml (Neem produced AgNPs), whereas plant extract or amylase alone did not show any activity even up to 40 g/ml [31].

AS ANTIBACTERIAL AND ANTIFUNGAL AGENT-

The development of new therapeutic drugs with broad-spectrum antibacterial action is crucial since bacterial resistance is a major health concern. The marketed antibacterial agents are having several drawbacks, such as high toxicity, high cost, low solubility, and side effects. Therefore, conducting studies on effective and secure anti-bacterial components is very important and of high interest [32].

It has been widely discussed that AgNPs have the best antimicrobial effect with the lowest ecotoxicity in the environment [33]. Comparatively the antimicrobial effect of AgNPs is different against Gram-positive and Gram-negative bacterial species [34]. It has been disclosed by Rafique et al. [35] that Gram-positive bacteria are less sensitive to AgNPs as compared to Gram-negative bacteria. As an example, the biosynthesis of AgNPs revealed that *Staphylococcus aureus* is more active than *Escherichia coli*. Another study evaluated the antibacterial activity of AgNPs synthesized using aqueous plant extracts of *Pimpinella anisum* seeds, against several bacterial isolates including *Klebsiella pneumoniae*, *Acinetobacter baumannii, Streptococcus pyogenes, Pseudomonas aeruginosa*, and *Salmonella typhi*. They also used in vitro growth and proliferation assays and cell viability tests to evaluate the harmful effects of AgNPs on HT115 and hSSC cells. *P. anisum*-produced AgNPs revealed remarkable antibacterial activity against a variety of microbes as well as cytotoxicity against HT115s and hSSCs.

There is a growing interest in the identification of new and novel antimicrobial agents due to the increase of the antimicrobial resistance globally threat to the public [36]. The best antibacterial agent is AgNPs since producing smaller nanoparticles can magnify silver's negative effects on microbial cells. Jebril et al., [37] reported that plant induced AgNPs are the most promising antimicrobial sources against certain kinds of fungal isolates. *Verticillium dahalia's* growth was significantly inhibited by the presence of AgNPs at a concentration of 60 ppm, according to the findings of the plant-mediated AgNPs study. Guerra et al., (2020) reported that 55-60% of broth fungal cell growth was decreased after the application of AgNPs [38].

Silver nanomaterials enter the bacterial cell wall, afterward breach it, and finally cause changes in the cell membrane, which leads to bacterial cell death [39]. The AgNPs create small pores on the cell surface and the cell becomes porous, therefore the accumulation of AgNPs occurs on the surface of the cell [40]. A free radical formation might be considered another mechanism of action when AgNPs formed a cluster of radicals inside the bacterial cell, which also leads to cell death [39]. When in contact with bacterial cells, AgNPs produce clusters of free radicals that can destroy the cells and make them permeable, which causes the cells to automatically die, according to a study done using electron spin resonance spectroscopy [41]. AgNPs are being employed for eliminating microorganisms in medical devices, implants and hospital masks. They are also used in hospitals as antibiotic supplements or for preventing infection.

AS ANTICANCER AGENT-

Silver nanoparticles have been used as good sensitizers to cure radio resistant glioblastoma malignant tumor [42]. In recent studies biogenic silver nanoparticles showed inhibition of proliferation of human colon cancer cell line HCT15 by arresting growth phase, decreasing DNA synthesis and prompting apoptosis [43]. Dependence on anticancer activity of AgNPs on human cancer cell lines has been found, for the synthesis of NPs as well as on the type of the cell lines [44]. Fruit, leaf, seed, and root extracts of *Citrullus colocynthis* produced AgNPs with various size and altered ID50 on various cell lines. *Ulva lactuca*, a type of seaweed, was used in the toxicity test of biologically produced AgNPs to demonstrate their potential cytotoxicity

against tumours. It showed human colon cancer, HT-29 cell lines' ID50 was 49 g/ml while human liver cancer Hep G-2 cell lines' ID50 was 12.5 g/ml [45].

USE OF AgNP IN TARGETED DRUG DELIVERY-

AgNPs can provide passive or active targeting to tumor tissue this is why they are used as a novel drug delivery system. In in-vivo study efficacy of anticancer therapy is increased by accumulation of drug at desired site of action. Cellular uptake of drugs is facilitated by receptor mediated endocytosis. These active targeting depends on molecular recognition. Surface functionalization with specific targeted molecules or coating with biocompatible and biodegradable polymers are suggested methods for improving the properties of biogenic AgNPs [46,47]. For instance, doxorubicin (DOX) and daunorubicin (DNR), two hydrophilic anticancer medications, were loaded onto AgNPs produced by using different amounts of *Setaria verticillata* seed extract. The capacity (40.25%) and significant loading (80.50%) efficiency of DOX-AgNPs and DNR-AgNPs made them potential new DDSs in the future. [48].

Drug delivery inside the cells depends on the size of NPs as it is done by endocytosis. Spherical AgNPs were synthesized from *Aerva javanica* plant and was combined with the anti-cancer drug gefitinib. The average size of AgNPs were 5.7nm was determined by Scanning transmission electron microscopy (STEM). Gefitinib-AgNPs and gefitinib by itself were tested for apoptotic potential. Significantly reduction of breast cancer cell viability was seen after treatment with conjugated gefitinib-AgNPs. Gefitinib is delivered with AgNPs to maximize its efficacy and minimize its adverse effects [49]. Numerous green synthetic AgNPs with anticancer potential present novel therapeutic possibilities. The development of DDSs with distinctive capabilities and a biocompatible profile is facilitated by their unique properties as nanocarriers [45].

OTHER APPLICATIONS OF BIO-GENIC SILVER NANOPARTICLES-

Earlier reports cite the use of microorganism such as algae, bacteria, fungi and also plants are used for the biosynthesis of AgNPs. Recently, several plant extracts have been emerged as novel resources for their ability to produce safe and non-toxic silver nanoparticles. In fact, biosynthesis results in low-energy use and have better environmental impact, with respect to conventional chemical synthesis methods. The ability to effectively manage AgNPs size and structure, which must be done in order to maximise uses, may be made possible by the great specificity of biomolecules involved in the biosynthesis process. The use of plants as sustainable and renewable resources in the synthesis of AgNPs is more advantageous over microorganisms, which need expensive methodologies for maintaining microbial cultures and more time for synthesis.

Benefits of synthesis of AgNPs using plant extracts are that it is economical, energy efficient, cost-effective; provide healthier work places and communities; and protect human health and environment leading to lesser waste and safer products [50].

Waste products that resulted from the microbial-based method is likely to be more harmful to the environment depending on the type of microbes involved in the synthesis. Hence, plant-mediated synthesis brings less pollution and so reducing the harmful impact on the environment. With all the aforementioned advantages and outstanding features over other methods, the biosynthetic method employing plant extracts has viable technique as well as a good alternative to conventional chemical and physical nanoparticle preparation methods, and even microbial methods [51].

CONCLUSIONS AND FUTURE DIRECTIONS OF SILVER NANOPARYICLES-

An increasing concern towards green chemistry and use of green route for synthesis of silver nanoparticles leads to the desire to develop environmentally friendly techniques. In this review, we learned about the biological sources for AgNP synthesis, as well as their most promising applications in daily lives and other environmental processes. Use of microorganisms and plants for bio synthesis of AgNPs is an emerging and exciting area of nanotechnology and may have significant impact on further advances in nano-science. It is expected that the applications for AgNPs will continue to grow, but there are more concepts that we need to understand with respect to their accumulation in the environment and their potential long-term effects on humans and animals. I strongly believe that biosynthesized silver nanoparticles will open a new direction towards various biomedical applications as “nano-drugs” in near future. There are also hope to that AgNPs can be used as nano-weapon against phyto-pathogens and as surface plasma resonance enhancers. Also, these AgNPs would provide a potential solution for the present energy crisis by finding their use as energy-producing devices. Further studies are still needed to understand the precise molecular mechanism leading to the formation of silver nanoparticles by microorganisms and plants in order to have a better control over their size, shape and effects [52].

REFERENCE-

[1] Rautela A, Rani J. Green synthesis of silver nanoparticles from Tectona grandis seeds extract: characterization and mechanism of antimicrobial action on different microorganisms. Journal of Analytical Science and Technology. 2019 Dec; 10(1):1-0.

[2] Pirtarighat S, Ghannadnia M, Baghshahi S. Green synthesis of silver nanoparticles using the plant extract of Salvia spinosa grown in vitro and their antibacterial activity assessment. Journal of Nanostructure in Chemistry. 2019 Mar; 9(1):1-9.

[3] Abdelghany TM, Al-Rajhi AM, Al Abboud MA, Alawlaqi MM, Ganash Magdah A, Helmy EA, Mabrouk AS. Recent advances in green synthesis of silver nanoparticles and their applications: about future directions. A review. BioNanoScience. 2018 Mar; 8(1):5-16.

[4] Mathur P, Jha S, Ramteke S, Jain NK. Pharmaceutical aspects of silver nanoparticles. Artificial cells, nanomedicine, and biotechnology. 2018 Oct 31;46(sup1):115-26.

[5] Sierra-Fernández A, Gómez Villalba LS, Rabanal ME, Fort González R. New nanomaterials for applications in conservation and restoration of stony materials: A review.

[6] Singh J, Dutta T, Kim KH, Rawat M, Samddar P, Kumar P. 'Green'synthesis of metals and their oxide nanoparticles: applications for environmental remediation. Journal of nanobiotechnology. 2018 Dec;16(1):1-24.

[7] Ahmad IZ, Ahmad A, Tabassum H, Kuddus M. Applications of Nanoparticles in the Treatment of Wastewater. Handb. Ecomater., Springer, Cham. 2017:1-25.

[8] Albukhari SM, Ismail M, Akhtar K, Danish EY. Catalytic reduction of nitrophenols and dyes using silver nanoparticles@ cellulose polymer paper for the resolution of waste water treatment challenges. Colloids and Surfaces A: Physicochemical and Engineering Aspects. 2019 Sep 20;577:548-61.

[9] Brown J. Impact of silver nanoparticles on wastewater treatment. In Nanotechnologies for environmental remediation 2017 (pp. 255-267). Springer, Cham.

[10] Choi O, Hu Z. Size dependent and reactive oxygen species related nanosilver toxicity to nitrifying bacteria. Environmental science & technology. 2008 Jun 15;42(12):4583-8.

[11] Kühr S, Schneider S, Meisterjahn B, Schlich K, Hund-Rinke K, Schlechtriem C. Silver nanoparticles in sewage treatment plant effluents: chronic effects and accumulation of silver in the freshwater amphipod Hyalella azteca. Environmental Sciences Europe. 2018 Dec;30(1):1-1.

[12] Tatli Seven P, Seven I, Gul Baykalir B, Iflazoglu Mutlu S, Salem AZ. Nanotechnology and nano-propolis in animal production and health: An overview. Italian Journal of Animal Science. 2018 Oct 2;17(4):921-30.

[13] Al-Sagheer AA, Daader AH, Gabr HA, El-Moniem A, Elham A. Palliative effects of extra virgin olive oil, gallic acid, and lemongrass oil dietary supplementation on growth performance, digestibility, carcass traits, and antioxidant status of heat-stressed growing New Zealand White rabbits. Environmental Science and Pollution Research. 2017 Mar;24(7):6807-18.

[14] Mohapatra P, Swain RK, Mishra SK, Behera T, Swain P, Behura NC, Sahoo G, Sethy K, Bhol BP, Dhama K. Effects of dietary nano-selenium supplementation on the performance of layer grower birds. Asian Journal of Animal and Veterinary Advances. 2014;9(10):641-52.

[15] Yang J, Luo M, Tan Z, Dai M, Xie M, Lin J, Hua H, Ma Q, Zhao J, Liu A. Oral administration of nano-titanium dioxide particle disrupts hepatic metabolic functions in a mouse model. Environmental Toxicology and Pharmacology. 2017 Jan 1;49:112-8.

[16] Gangadoo S, Dinev I, Willson NL, Moore RJ, Chapman J, Stanley D. Nanoparticles of selenium as high bioavailable and non-toxic supplement alternatives for broiler chickens. Environmental Science and Pollution Research. 2020 May;27(14):16159-66.

[17] Swain PS, Rajendran D, Rao SB, Dominic G. Preparation and effects of nano mineral particle feeding in livestock: A review. Veterinary World. 2015 Jul;8(7):888.

[18] Hofherr J, Natale F, Trujillo P. Is lack of space a limiting factor for the development of aquaculture in EU coastal areas?. Ocean & Coastal Management. 2015 Nov 1;116:27-36.

[19] Paniagua CA, Rivero OC, Anguita JU, Naharro GE. Pathogenicity factors and virulence for rainbow trout (Salmo gairdneri) of motile Aeromonas spp. isolated from a river. Journal of Clinical Microbiology. 1990 Feb;28(2):350-5.

[20] Mahanty A, Mishra S, Bosu R, Maurya UK, Netam SP, Sarkar B. Phytoextracts-synthesized silver nanoparticles inhibit bacterial fish pathogen Aeromonas hydrophila. Indian journal of microbiology. 2013 Dec;53(4):438-46.

[21] Belém-Costa A, Cyrino JE. Antibiotic resistence of Aeromonas hydrophila isolated from Piaractus mesopotamicus (Holmberg, 1887) and Oreochromis niloticus (Linnaeus, 1758). Scientia Agricola. 2006;63:281-4.

[22] Das BK, Samal SK, Samantaray BR, Sethi S, Pattnaik P, Mishra BK. Antagonistic activity of cellular components of Pseudomonas species against Aeromonas hydrophila. Aquaculture. 2006 Mar 31;253(1-4):17-24.

[23] Fatima R, Priya M, Indurthi L, Radhakrishnan V, Sudhakaran R. Biosynthesis of silver nanoparticles using red algae Portieria hornemannii and its antibacterial activity against fish pathogens. Microbial Pathogenesis. 2020 Jan 1;138:103780.

[24] Jain KK. Advances in the field of nano-oncology. BMC medicine. 2010 Dec;8(1):1-1.

[25] Durán N, Durán M, De Jesus MB, Seabra AB, Fávaro WJ, Nakazato G. Silver nanoparticles: A new view on mechanistic aspects on antimicrobial activity. Nanomedicine: nanotechnology, biology and medicine. 2016 Apr 1;12(3):789-99.

[26] Durán N, Marcato PD, Conti RD, Alves OL, Costa F, Brocchi M. Potential use of silver nanoparticles on pathogenic bacteria, their toxicity and possible mechanisms of action. Journal of the Brazilian Chemical Society. 2010;21(6):949-59.

[27] Marambio-Jones C, Hoek E. A review of the antibacterial effects of silver nano materials and potential implications for human health and the environment. Journal of nanoparticle research. 2010 Jun;12(5):1531-51.

[28] Reidy B, Haase A, Luch A, Dawson KA, Lynch I. Mechanisms of silver nanoparticle release, transformation and toxicity: a critical review of current knowledge and recommendations for future studies and applications. Materials. 2013 Jun;6(6):2295-350.

[29] Dinesh D, Murugan K, Madhiyazhagan P, Panneerselvam C, Mahesh Kumar P, Nicoletti M, Jiang W, Benelli G, Chandramohan B, Suresh U. Mosquitocidal and antibacterial activity of green-synthesized silver nanoparticles from Aloe vera extracts: towards an effective tool against the malaria vector Anopheles stephensi?. Parasitology research. 2015 Apr;114(4):1519-29.

[30] Rai M, Ingle AP, Paralikar P, Gupta I, Medici S, Santos CA. Recent advances in use of silver nanoparticles as antimalarial agents. International Journal of Pharmaceutics. 2017 Jun 30;526(1-2):254-70.

[31] Mishra A, Kaushik NK, Sardar M, Sahal D. Evaluation of antiplasmodial activity of green synthesized silver nanoparticles. Colloids and Surfaces B: Biointerfaces. 2013 Nov 1;111:713-8.

[32] Kakakhel MA, Sajjad W, Wu F, Bibi N, Shah K, Yali Z, Wang W. Green synthesis of silver nanoparticles and their shortcomings, animal blood a potential source for silver nanoparticles: A review. Journal of Hazardous Materials Advances. 2021 Sep 1;1:100005.

[33] Qais FA, Shafiq A, Khan HM, Husain FM, Khan RA, Alenazi B, Alsalme A, Ahmad I. Antibacterial effect of silver nanoparticles synthesized using Murraya koenigii (L.) against multidrug-resistant pathogens. Bioinorganic chemistry and applications. 2019 Oct;2019.

[34] Rajeshkumar S, Bharath LV. Mechanism of plant-mediated synthesis of silver nanoparticles–a review on biomolecules involved, characterisation and antibacterial activity. Chemico-biological interactions. 2017 Aug 1;273:219-27.

[35] Rafique M, Sadaf I, Tahir MB, Rafique MS, Nabi G, Iqbal T, Sughra K. Novel and facile synthesis of silver nanoparticles using Albizia procera leaf extract for dye degradation and antibacterial applications. Materials Science and Engineering: C. 2019 Jun 1;99:1313-24.

[36] Yilmaz MT, İspirli H, Taylan O, Dertli E. Synthesis and characterisation of alternan-stabilised silver nanoparticles and determination of their antibacterial and antifungal activities against foodborne pathogens and fungi. LWT. 2020 Jun 1;128:109497.

[37] Jebril S, Jenana RK, Dridi C. Green synthesis of silver nanoparticles using Melia azedarach leaf extract and their antifungal activities: In vitro and in vivo. Materials Chemistry and Physics. 2020 Jul 1;248:122898.

[38] Guerra JD, Sandoval G, Avalos-Borja M, Pestryakov A, Garibo D, Susarrey-Arce A, Bogdanchikova N. Selective antifungal activity of silver nanoparticles: A comparative study between Candida tropicalis and Saccharomyces boulardii. Colloid and Interface Science Communications. 2020 Jul 1;37:100280.

[39] Prabhu S, Poulose EK. Silver nanoparticles: mechanism of antimicrobial action, synthesis, medical applications, and toxicity effects. Int Nano Lett. 2012; 2: 32. Search in. 2012.

[40] Sondi I, Salopek-Sondi B. Silver nanopartiklar som antimikrobiellt medel: En fallstudie på E. coli som modell för gramnegativa bakterier. J Colloid Interface Sci. 2004;275(1):177-82.

[41] Danilczuk M, Lund A, Sadlo J, Yamada H, Michalik J. Conduction electron spin resonance of small silver particles. Spectrochimica Acta Part A: Molecular and Biomolecular Spectroscopy. 2006 Jan 1;63(1):189-91.

[42] Xu R, Ma J, Sun X, Chen Z, Jiang X, Guo Z, Huang L, Li Y, Wang M, Wang C, Liu J. Ag nanoparticles sensitize IR-induced killing of cancer cells. Cell research. 2009 Aug;19(8):1031-4.

[43] Prabhu D, Arulvasu C, Babu G, Manikandan R, Srinivasan P. Biologically synthesized green silver nanoparticles from leaf extract of Vitex negundo L. induce growth-inhibitory effect on human colon cancer cell line HCT15. Process Biochemistry. 2013 Feb 1;48(2):317-24.

[44] Singh J, Singh T, Rawat M. Green synthesis of silver nanoparticles via various plant extracts for anti-cancer applications. Nanomedicine. 2017;7(3):1-4.

[45] Ivanova N, Gugleva V, Dobreva M, Pehlivanov I, Stefanov S, Andonova V. Silver nanoparticles as multi-functional drug delivery systems. London, UK: IntechOpen; 2018 Nov 5.

[46] Jeyaraj M, Rajesh M, Arun R, MubarakAli D, Sathishkumar G, Sivanandhan G, Dev GK, Manickavasagam M, Premkumar K, Thajuddin N, Ganapathi A. An investigation

on the cytotoxicity and caspase-mediated apoptotic effect of biologically synthesized silver nanoparticles using Podophyllum hexandrum on human cervical carcinoma cells. Colloids and Surfaces B: Biointerfaces. 2013 Feb 1;102:708-17.

[47] Blanco MD, Teijón C, Olmo RM, Teijón JM. Targeted nanoparticles for cancer therapy. In Recent advances in novel drug carrier systems 2012 Oct 31. IntechOpen.

[48] Naz M, Nasiri N, Ikram M, Nafees M, Qureshi MZ, Ali S, Tricoli A. Eco-friendly biosynthesis, anticancer drug loading and cytotoxic effect of capped Ag-nanoparticles against breast cancer. Applied Nanoscience. 2017 Nov;7(8):793-802.

[49] Khalid S. Hanif R. Green biosynthesis of silver nanoparticles conjugated to gefitinib as delivery vehicle. Int J Adv Sci Eng Technol. 2017;5(2):59-63.

[50] Ahmed S, Ahmad M, Swami BL, Ikram S. A review on plants extract mediated synthesis of silver nanoparticles for antimicrobial applications: a green expertise. Journal of advanced research. 2016 Jan 1;7(1):17-28.

[51] Keat CL, Aziz A, Eid AM, Elmarzugi NA. Biosynthesis of nanoparticles and silver nanoparticles. Bioresources and Bioprocessing. 2015 Dec;2(1):1-1.

[52] Abdelghany TM, Al-Rajhi AM, Al Abboud MA, Alawlaqi MM, Ganash Magdah A, Helmy EA, Mabrouk AS. Recent advances in green synthesis of silver nanoparticles and their applications: about future directions. A review. BioNanoScience. 2018 Mar; 8(1):5-16.

International Journal of Pharmaceutical Science Invention
ISSN (Online): 2319-6718, ISSN (Print): 2319- 670X
www.ijpsi.org Volume 12 Issue 5 ǁ Sep. –Oct., 2023 ǁ PP. 30-40

A Detailed Discussion on Mucoadhesive Drug Delivery System

Rahul Molla[1], Aditi Bala[1], Gouranga Baidya[1], Sanchita Mandal[1*]
[1] Department of Pharmaceutical Technology, Jadavpur University
Kolakata- 700032

[*]Corresponding Author
Address- Department of Pharmaceutical Technology, Jadavpur University
Kolakata- 700032

Abstract: *Two surfaces that cling to one another—a mucous membrane being one of them—are said to exhibit mucoadhesion. In the pharmaceutical sciences, this has been of interest to improve the distribution of drugs locally or to introduce challenging molecules (such as proteins and oligonucleotides) into the bloodstream. The carbomers and chitosans are two well-known examples of mucoadhesive materials, which are hydrophilic macromolecules with several hydrogen bond-forming groups. It has been suggested that there are two steps to the mechanism underlying mucoadhesion: the contact (wetting) stage and the consolidation stage (the formation of sticky contacts). Every application is different when it comes to the proportional relevance of each step. Adsorption, for instance, is a crucial step if the dosage form cannot be applied directly to the target mucosa, and consolidation is a crucial step if the formulation is subjected to high dislodging forces. Overhydration of a dose form, mucus turnover, or epithelia will all eventually lead to adhesive joint failure. Present research is yielding new mucoadhesive materials with ideal adhesive qualities, which should expand the technology's possible uses. The mucosal membrane, mucoadhesion mechanism, hypotheses, factors influencing mucoadhesion, dosage forms for mucoadhesive, evaluation techniques, and their application are all covered in this review.*

Key words*: mucoadhesion, mucus layer, mechanism, theories, mucoadhesive dosage forms*

Date of Submission: 28-10-2023 Date of acceptance: 17-11-2023

I. Introduction:

The oral drug delivery system is the most widely used route of administration because ofease of administration of drugs and higher patients'compliance. The bioavailability of orallyadministered drugs is subjective by various factors. One of the most significant parameters is residence time (RT) of the dosage as most of the conventional dosage forms have limits relating to fast gastric emptying time. Mucoadhesive dosage form is a type of novel drug delivery system which can stay in contact of the mucosal lining for a prolong period of time due to its bio adhesive property and improve the residence time of the drugs. Mucoadhesive drug delivery system helps to improve the bioavailability of drugs at the site of action for prolongperiod of time at a controlled manner of drug releases(Boddupalli et al. 2010).

To maintain drug concentration in the therapeutically effective range at the site of action by conventional drug delivery system, the drugs need to be administered numerous times a day, which is incompatible to patients and may lead to appearance of drug toxicity. To overcome the above limitation of conventional drug delivery system, mucoadhesive drug delivery system is an emerging tool in the field of novel drug delivery system.

Many problems are arising during the preparation of controlled drug delivery system for better absorption and enhanced bioavailability. The process of drug absorption from GIT is complex and is subjected to several factors. It is recognized that the extent of GIT drug absorption is correlated to residence time at the intestinal mucosa region(Pant, Badola, and Division 2016). Mucoadhesive drug delivery system can persist in the GI region for many hours and therefore significantly improved the residence time of the drugs at mucosal region(Ugwoke et al. 2005).Extended gastric retention increases bioavailability, decrease drug waste and increases the solubility of drugs which are less soluble in high pH environment.

Many techniques, such as the hydrodynamically balanced system (HBS), floating drug delivery system, low density system, raft system with alginate gels, mucoadhesive or bio-adhesive system, high density system, super porous hydrogel, and magnetic system, are currently used to prepare a successful specific drug delivery system(Tripathi et al. 2019).Modern technological advancements have made it possible to create dosage forms

that can be administered orally, topically, parenterally, rectally, nasally, ocularly, vaginally, etc. Out of all these routes, oral route is considered as the best preferred and practiced way of drug delivery due to

- Ease of administration
- Ease of production
- More flexibility in designing
- Low cost

Drugs taken orally are absorbed mostly through the gastrointestinal tract (GIT), primarily from the stomach and intestine. Medications that enter the stomach and have a localized effect ought to remain there for an extended period of time(Kharia et al. 2011), which is hard to happen in case of available conventional dosage forms like tablets, capsules etc due to gastric emptying(Sarawade, Ratnaparkhi, and Chaudhari 2014).Many factors, such as temperature, meal viscosity, volume, and composition, emotional state, pH of the stomach area, posture, and so on, affect how quickly dosage forms are gastric emptied. (Bhardwaj, Kumar Sharma, and Malviya 2011).

The distribution of medication to moist cavities, such as the bladder, vagina, and mouth lining, is known as mucosal drug delivery. This makes it possible to treat diseases locally with high medication concentrations and fewer systemic negative effects.(Davis et al. 2005).These are the systems in which formulation interact with mucosal layer and increase the residential time of formulation at the site of administration for better absorption(Smart 2005). These systems are designed to provide Controlled/Sustained Release of drug at the site of administration.

1.1 Mucosal membrane:

Mucus membranes are moist surface lining of the wall of most of the body cavities such as gastrointestinal tract and respiratory tract. They consist of connective tissue layer (the lamina propria), an epithelial layer, and mucus layer. The epithelial layer may be singled layer (stomach, small and large intestine, bronchi) or multi layered /stratified (oesophagus cornea, vagina,). It also contains goblets cell which secretes mucus directly onto the surface of epithelial tissue layer. Mucus layer contains specialised secretory glands such as salivary glands which secretes mucus directly onto the epithelial layer(Hooda, Tripathi, and Kapoor 2012). Mucus is a translucent and viscid secretion which forms a thin, continuous gel blanket adherent to the mucosal epithelial surface. The average thickness of this layer varies from about 50 to 450 µm in human(Ahuja, Khar, and Ali 1997). Mucus is present as either gel layer adherent to mucosal surface or luminal soluble or suspended form(Khanvilkar, Donovan, and Flanagan 2001). Mucus is usually consisting of following components

- Water (95%)
- Mucin glycoproteins and lipid (0.5-5%)
- Mineral salts (1%)
- Free proteins (0.5-1%) (12)

Mucus glycoproteins are high molecular proteins and is attached with oligosaccharides units (8 to 10 monosaccharides residues)(Strous and Dekker 1992).

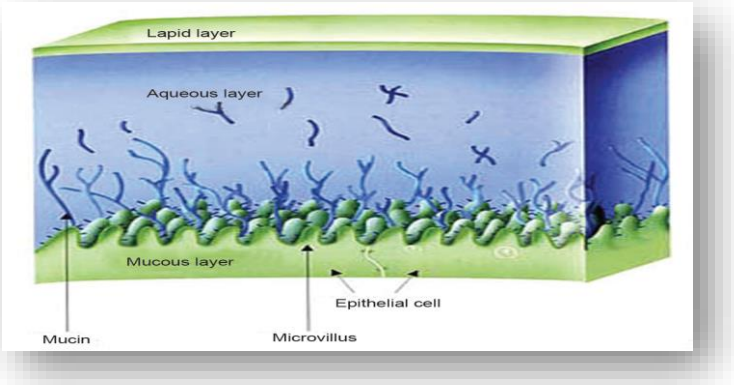

Figure1: Structure of mucus layer

Mucosal drug delivery system can be delivered via different routes:

- Oral route
- Buccal route
- Nasal route

- Vaginal route
- Rectal route

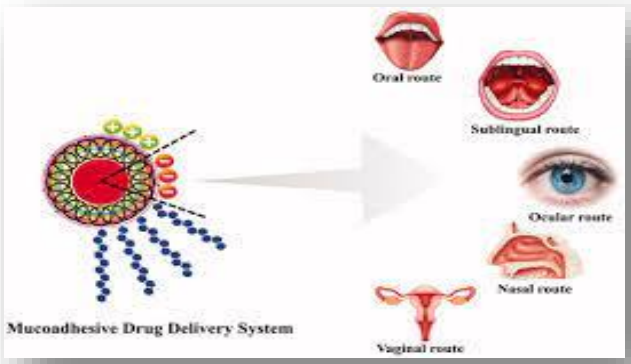

Figure 2 : Routes of administration

1.2 Advantages: Mucoadhesive drug delivery system provides several advantages over other controlled drug delivery system

- Enhances the residential time of the drug at the site of drug absorption and improve the drugs absorption
- Painless and ease of drug administration
- Enhance the bioavailability of the drug
- Lowers the frequency of drug administration
- Provides site specific drug delivery and reduces the side effect
- Protect the drug from degradation due to pH sensitive environment
- Improve the therapeutic performance of drug
- Low enzymatic activity and first pass metabolism was avoided
- Non-invasive method of drug administration

1.3 Disadvantages:

- If MDDS are adhere too tightly then it will be difficult to remove and injury of mucosal lining may happen
- Patient may suffer from unpleasant feeling
- Eating and drinking may be restricted
- Expensive as compared to other formulation

1.4 Ideal characteristics of mucoadhesive polymers:

• The polymer and its degradation products should be nontoxic and should be non-absorbable from the GI tract.

- It should be non-irritant to the mucus membrane.
- It should preferably form a strong non covalent bond with the mucin–epithelial cell surfaces.
- It should adhere quickly to most tissue and should possess some site specificity.
- It should allow easy incorporation of the drug and should offer no hindrance to its release.
- The polymers must not decompose on storage or during the shelf life of the dosage 0form.
- The cost of polymer should not be high so that the prepared dosage form remains competitive.
- Strong hydrogen bonding groups (-OH, -COOH).
- Strong anionic charges.
- Sufficient flexibility to penetrate the mucus network or tissue crevices.
- Surface tension characteristics suitable for wetting mucus/mucosal tissue surface.
- High molecular weigh

II. Mechanism of mucoadhesion:

The process by which specific macromolecules adhere to the mucous layer surface is still poorly understood. To enhance surface contact and create intimate contact, mucoadhesive must spread throughout the substrate, which will aid in the mucus's chain's diffusion. A strong mucoadhesion requires the dominance of the attractive force over the repulsive force.(Carvalho et al. 2010). The mechanism of mucoadhesion is generally divided into two steps:

- The contact stages
- The Consolidation stages

During the contact stage, the mucoadhesive and mucus membrane come into contact, and the formulation begins to spread and swell to make contact with the mucus layer. Mucoadhesive compounds are activated by moisture during the consolidation stage.(Boddupalli et al. 2010). The system becomes more malleable when there is moisture present, which enables the mucoadhesive molecules to separate and form weak hydrogen and van der Waals bonds. The mucoadhesive molecules and the mucus's glycoproteins interact with one another through chain penetration and the formation of secondary bonds, according to the diffusion theory. The mucoadhesive device contains properties that promote both chemical and mechanical interactions in order for this to happen. For instance, molecules with high molecular weight, flexible chains, anionic surface charge, hydrogen bond building groups (-OH, -COOH), and surface-active characteristics that aid in spreading throughout the mucus layer(Carvalho et al. 2010), can present mucoadhesive properties. Essentially there are theories to explain the mucoadhesion mechanism

1. Contact stages
2. Consolidation stages

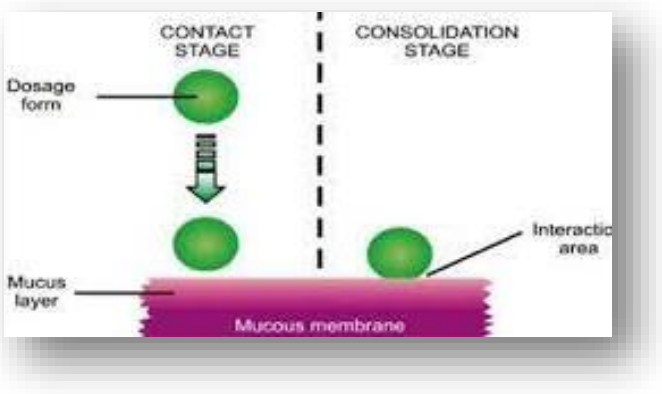

Figure 3: Mechanism of mucoadhasion

III. Theories of mucoadhesion:

Since mucoadhesive drug delivery is being studied for a long period of time since the 1980s, an overall knowledge has been procured. Till date a various number of mechanisms taking place at drug delivery system – mucus interface and the factors affecting the mechanistic pathways have been investigated by scientist. The different theories involved in mucoadhesion have been explained below-

3.1Wettability theory: The wetting theory is primarily involved in liquid or low viscous mucoadhesive system. It describes the ability of any mucoadhesive system to spread over the biological surface thus it gives an accountability of "spreadability" of the drug delivery system. The spread ability over the surface can be found by measuring the contact angle. This states that, lower the contact angle, greater the ability to spread over the surface. The contact angle should be zero or close to zero for adequate spreading over the surface(Boddupalli et al. 2010). The spreadability coefficient, *SAB*, can be calculated from the difference between thesurface energies γB and γA the interfacial energy γAB, as indicated in the equation given below(Eq-1)

$SAB = \gamma B - \gamma A - \gamma AB$ ----------1

3.2Adsorption theory: Adhesion is the result of interactions (primary and secondary bonding) between the adhesive polymer and mucus substrate. Primary bonds due to chemisorption's result in adhesion due to ionic, covalent and metallic bonding(Andrews, Laverty, and Jones 2009), which is generally undesirable due to their permanency. Secondary bonds are generally formed due to van der Waals forces, hydrophobic interactions and hydrogen bonding.

3.3. Diffusion theory: This theory describes the interpenetration of both the mucoadhesive polymer and mucin chain to a sufficient depth to form a semi-permanent adhesive bond. It is believed that the adhesive force is directly proportional to degree of penetration of polymer chain. This penetration rate depends on the diffusion coefficient, flexibility and nature

of the mucoadhesive chains, mobility and contact time(Sedley 2009). According to the literature, the depth of interpenetration required to produce an efficient bioadhesive bond lies in the range 0.2–0.5 μm. The required time (t) for the highest degree of adhesion during interpenetration among two substrates can be calculated using L (interpenetration depth) and Db (the coefficient of diffusion). (Eq: 2)
t=L2/Db …….2

3.4 Fracture theory: Fracture theory attempts to relate the difficulty of separation of two surfaces after adhesion. Fracture theory equivalent to adhesive strength is given by: (Eq: 3)

G = (E€/L) ½ ……3

where E is the Young's modulus of elasticity, € is the fracture energy, and L is the critical crack length when two surfaces are separated(Ahuja, Khar, and Ali 1997) .

3.5 Electronic theory: This theory suggests that electron transfer occurs upon contact of mucoadhesive surfaces due to differences in their electronic structure. This is proposed to result in the formation of an electrical double layer at the interface, with subsequent adhesion due to attractive forces(Smart 2005).

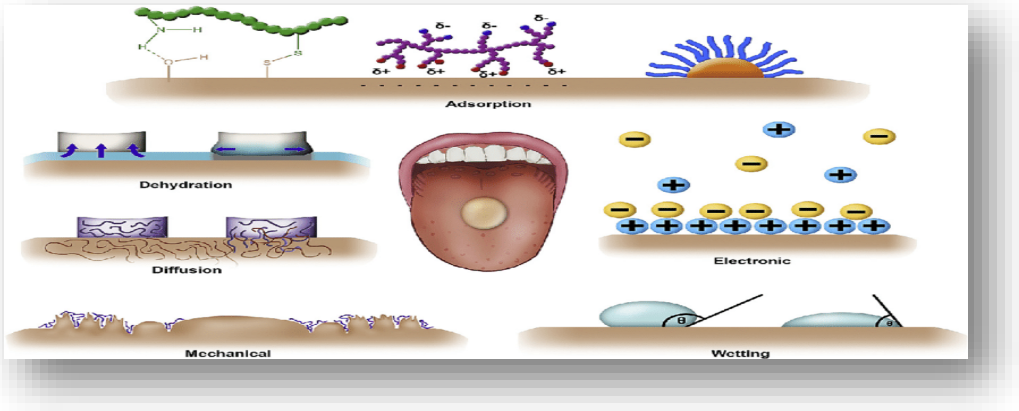

Figure 4 Theories of mucoadhesion

IV. Factors affecting mucoadhesive drug delivery system:

4.1 Polymers related factors:

a. **Molecular weight:**The mucoadhesive strength of a polymer increases with molecular weights above 100,000. Direct correlationbetween the mucoadhesive strength of polyoxymethylene polymers and their molecular weights lies in the range of 200,000–7,000,000(Mukhopadhyay et al. 2018). The interpenetration of polymer molecule is favourable for low molecular weight and polymer with lower molecular weight will form weak gels and readily dissolve whereas entanglement is favour for higher molecular weight polymers(Leitner, Marschütz, and Bernkop-Schnürch 2003).

b. **Flexibility of polymer chain:** Mucoadhesion starts with the diffusion of polymer chain in the interfacial region. To achieve desire entanglement with the mucus, polymer chain should contain a substantial degree of flexibility. this parameter is believed to be important for interpenetration and entanglement, allowing binding groups to come together as water soluble polymers become crosslinked and mobility of the chain get reduced.

c. **Concentration of polymer:** The importance of this factor lies in the formation of strong bond between bio adhesive polymer and the mucus. This can be explained by available polymer chain length for penetration into the mucus membrane. When the concentration of polymer is too low, then the number of penetrating polymers is less and the interaction between the polymer and mucus is unstable. In general, the number of penetrating polymer and strength of bio adhesion is directly proportional the concentration of polymer. However, for each polymer, there is a critical concentration, above which the polymer produces an "unperturbed" state due to a significantly coiled structure(Salamat-Miller, Chittchang, and Johnston 2005).

d. **Cross linking density:**The average pore size, the number and average molecular weight of the cross-linked polymers, and the density of cross-linking are three important and inter-related structural parameters of a polymer network. Therefore, it seems reasonable that with increasing density of crosslinking, diffusion of water into the polymer network occurs at a lower rate which, in turn, causes an insufficient swelling of the polymer and a decreased rate of interpenetration between polymer and mucin(Andrews, Laverty, and Jones 2009).

e. **Hydrogen bonding capacity:**Another crucial element for a polymer's mucoadhesion is hydrogen bonding. Desired polymers need to have functional groups that can create hydrogen bonds in order for mucoadhesion to happen. The existence of (COOH, OH etc.) is what allows for the formation of hydrogen bonds. To increase the polymer's capacity for hydrogen bonding, it must be flexible. Good hydrogen bonding ability is exhibited by polymers such polyvinyl alcohol, hydroxylated methacrylate, poly (methacrylic acid), and all of their co-polymers.

4.2 Physiological factors

a. **Mucin turnover:**High mucin turnover is not beneficial for mucoadhesive property because of following reason: the high mucin turnover limits theresidence time of mucoadhesive drug delivery system as it detaches from mucin layer, even though it has good bio adhesive property(Saraswathi, Balaji, and Umashankar 2013). High mucin turnover may produce soluble mucin molecule; thus, molecule interact with polymer before they interact with mucin layer. hence there will not besufficient mucoadhesion.

b. **Diseases state:** The physicochemical property of mucus may alter during some disease state, such as common cold, gastric ulcers, ulcerative colitis, bacterial and fungal infections etc. Thus, alteration in the physiological state may affect the bio adhesive property.

c. **Rate of renewal of mucosal cells:** Rate of renewal of mucosal cells varies extensively from different types of mucosa. It limits the persistence of bioadhesive systems on mucosal surfaces.

d. **Tissue movement:**When food and liquids are consumed, tissue moves around in the GIT during peristalsis, which impacts the mucoadhesive system, particularly when a gastro-retentive dosage form is used.

4.3 Biological environment related factors:

a. **pH of polymer-substrate interface:**The charge on the surface of polymers and mucus is influenced by pH. Because of variations in the dissociation of functional groups on the carbohydrate moiety and the amino acids of the polypeptide backbone, mucus will have a varied charge density depending on pH, which may have an impact on adherence. The degree of hydration of cross-linked polycyclic acid is dependent on the medium's pH; it progressively increases from pH 4 to pH 7, then decreases as alkalinity or ionic strength rises. Nevertheless, the carboxylate anions' electrostatic repulsion causes the chain to fully expand at higher pH values.

b. **Applied strength:**To ensure a good bio adhesive property, the appropriate strength should be given while putting a buccal mucoadhesive drug delivery system. Pressure initially supplied to the mucoadhesive tissue contact site can impact the depth of interpenetration even when there are no attractive forces between the polymer and mucus. This is because strong pressure applied for a sufficient amount of time causes the polymer to become bioadhesive with mucus.

c. **Initial contact time:**The amount of swelling and interpenetration of the bioadhesive polymer chains is determined by the contact time between the mucus layer and the bioadhesive. Furthermore, the bioadhesive strength rises with an increase in the initial contact time. Even yet, the system's performance is severely impacted by the initial pressure and initial contact time.

d. **Moistening:**To enhance the mobility of polymer chains, the mucoadhesive polymer needs to be moistened in order for it to spread across the surface and form a large enough macromolecular network for the interpenetration of mucin molecules and polymer. But for mucoadhesive polymers, which exhibit optimal swelling and bioadhesion, there is a threshold hydration level..

V. Mucoadhesive dosage formulations

5.1. Tablet: Tablets have an oval shape, are flat, and have a diameter of about 5 to 8 mm. Mucoadhesive tablets, in contrast to traditional tablets, don't cause significant discomfort when speaking or drinking. They become softer, stick to the mucosa, and stay there until the release or disintegration process is finished. The coupling of mucoadhesive properties to tablets has additional benefits, such as efficient absorption and enhanced drug bioavailability due to a high surface to volume ratio and facilitated much more intimate contact with the mucus layer. Mucoadhesive tablets, in general, have the potential to be used for controlled release drug delivery. Because mucoadhesive tablets can be made to stick to any mucosal tissue, including the stomach mucosa, they provide the opportunity for both localized and systemic control drug release.Mucoadhesive tablets are applied to the gastric epithelium's mucosal tissues in order to administer medications with a localized effect. Because they extend the medicine's release, decrease the frequency of drug administration, and increase patient compliance, mucoadhesive tablets are frequently utilized. Mucoadhesive tablets' primary flaw is their lack of physical flexibility, which makes it difficult for patients to comply with repeated, long-term use.

5.2 Patches: Bio adhesive patches may range from simple erodible and nonerodable adhesive disks to laminated systems in the size range of 1-16cm2. These can be designed to provide either unidirectional or bidirectionalrelease of the drug. Adhesive patches are prepared using two techniques: solvent casting and direct

milling. Using the solvent casting process, the drug and polymer solution is cast onto a backing layer sheet, and the solvent(s) are then allowed to evaporate to create the intermediate sheet from which patches are punched. The direct milling method involves mixing formulation ingredients uniformly, compressing them to the required thickness, and then cutting or punching out patches of a predefined size and shape. To regulate the direction of medication release, stop drug loss, and reduce device deformation and disintegration throughout the application time, an impermeable backing layer may also be used.

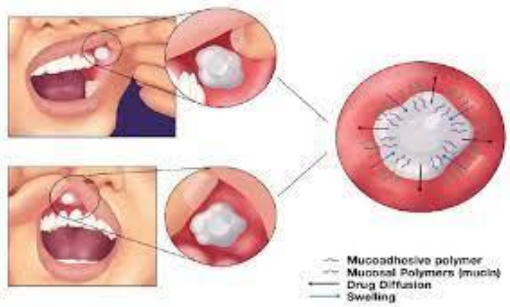

Figure 5: Mucoadhesive tablet

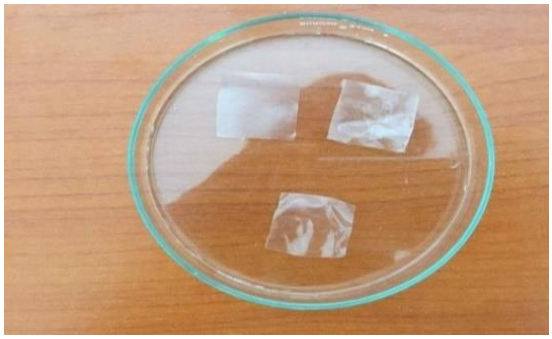

Figure 6: Mucoadhesive patch

5.3 Films: Due of their greater flexibility and comfort, mucoadhesive films are favored over mucoadhesive tablets. Additionally, they can avoid oral gels' brief duration of residence on the mucosa, as saliva readily washes and removes them. Additionally, films aid in wound protection during local drug delivery for oral disorders, hence lessening discomfort and improving disease treatment outcomes. In addition to being soft, elastic, and flexible, the perfect film should also be sturdy enough to resist breaking from the pressure of mouth movements. For the intended duration of action, it must also have strong mucoadhesive properties to stay in the mouth.

Figure 7: Mucoadhesive film

Figure 8: mucoadhesive gel

5.4 Gel and ointments: Ointments and gels, which are semi-solid dosage forms, have the advantage of being easily distributed throughout the mouth mucosa, vagina, or eye. Even while the accuracy of medication dosing with semi-solid dose forms may not match that of patches, tablets, or films, By employing particular mucoadhesive polymers, such as sodium carboxy-methyl-cellulose, Carbopol, and xanthan gum, low retention of the gels at the site of administration has been overcome. These polymers experience a phase shift from liquid to semi-solid. This alteration increases the viscosity, resulting in a steady and regulated release of the medication.

VI. Evaluation of mucoadhesive drug delivery system:

6.1Surface pH: The created mucoadhesive film is placed on a Petri plate that has previously held 4 mL of distilled water. It is then allowed to swell for one hour at room temperature (25 ± 1°C). Subsequently, the film's pH is determined by placing the pH meter's terminal electrode on its enlarged surface.

6.2 Flatness:A distinct-sized (1 cm2) sheet of mucoadhesive film is placed up against a plane surface, sliced into many vertical pieces (strips), and its length is then measured. The formula below is used to compute percent constriction. A zero-percentage restriction implies 100% flatness.

Constriction (%) = {(L1 −L2)/L1} * 100 …….4

Here, L1 represents the initial length of the film and L2 represents the final length of the strip.

Flatness (%) = 100−constriction (%).

6.3 Drug content: Using a magnetic stirrer, little bits of mucoadhesive films are dissolved in 100 mL of 0.1 N NaOH. At that stage, a 0.45 µm syringe filter is used to filter the mixture. A sample with a concentration of 10 µg/mL is obtained from the prepared stock solution, and it is scanned using an ultraviolet–vis spectrophotometer. Usually, placebo mucoadhesive films are employed as a blank control. The absorbance is used to calculate the drug's content(Tangri, Khurana, and Satheesh Madhav 2011).

6.4 Swelling properties: Buccal adhesive dose forms were weighed one at a time (w1) and arranged independently in Petri dishes with 4 millilitres of pH 6.6 phosphate buffer. The dose forms were taken out of the Petri plates at regular intervals of 5, 1, 2, 3, 4, 5, and 6 hours, and any extra surface water was wiped off using filter paper (W2). After reweighing the dose form, the swelling index (SI) was computed as follows, (Eq: 5)

$$SI= (W2-W1)/W1 \quad \ldots\ldots\ldots 5$$

6.5 Measuring the force of attachment:

One of the established techniques for determining the force of adherence of different bioadhesive dose forms is the Wilhelmy plate method. A micro tensiometer and a microbalance are used in the process, which measures the dynamic contact angles. For this, the CAHN dynamic contact angle analyser is employed.(Vasir, Tambwekar, and Garg 2003). The bioadhesive force between the polymer or dosage form suspended in a micro tensiometer and attached to a metal wire is measured using the Wilhelmy plate method. The tissue chamber, which is elevated to allow for contact between the tissue and the test substance, is filled with mucosal tissue, often rat jejunum. The stage is lowered and the force of adhesion is measured after a predetermined amount of time—seven minutes for microspheres.

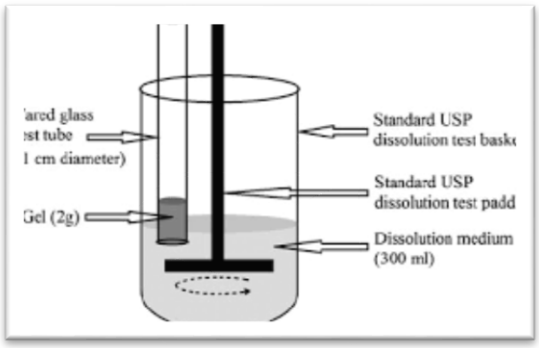

Figure 3 : USP apparatus

Figure 9: Wilhelmy plate

6.6 In vitro residence time determination*:* The duration of in vitro residence is estimated using a USP disintegration device. Eight hundred milliliters of isotonic phosphate buffer (IPB), maintained at 37°C and with a pH of 6.75, make up the disintegration medium. A segment of rabbit intestinal mucosa, measuring 3 cm in length, is adhered vertically to the glass section surface of the apparatus. The mucoadhesive film is hydrated using a pH of 6.75 and an IPB of 15 µl. The glass slab is placed vertically against the mechanical assembly and allowed to move simultaneously up and down to fully submerge the film in the buffer solution at the lowest position and remove it again at the highest point. The duration required for the film to fully separate from the mucosal surface is noted (average of three trials). Again, the in vitro residence duration is determined by regulating the substrate type, pH, temperature, and composition of the media. The in vitro residence time estimation provides information to improve the formulation, but it does not disclose the true strength of the mucoadhesive bond. The maximum force required to remove the film from the substrate is used to determine the strength of mucoadhesion.

6.7.Tensile strength: The aqueous dispersion sample of a mucoadhesive polymer was sandwiched between two polyoxymethylene discs. While the lower end disc is fixed and rests on a machine frame, the upper disc is adjustable. Tensile strength is the amount of force extracted from the buccal mucosa of a recently removed cow. In this test, the stress is evenly distributed across the mucoadhesive joint. Pig mucous membrane that connects the top moveable disc to the big intestine. Thus, it can be concluded that the tensile strength depends on both the type of polymer and concentration used after calculating the maximum force and work for detachment.
Tensile strength = (Force at failure/Cross-sectional area of the film)

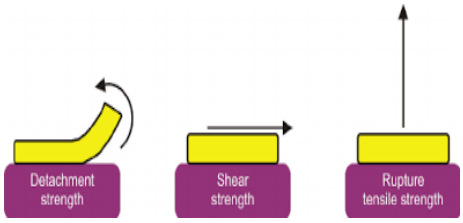

Figure 4 : Tensile strength determination

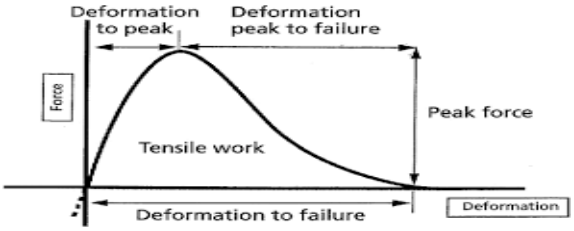

Figure 5: Graph of deformation of mucoadhesive dosage

VII. Application of mucoadhesive dosage formulations:

Mucoadhesive drug delivery system can be applied to deliver the drug via various routes of administration for the treatment of associated diseases. Routes and associated application of mucoadhesive dosage form are described below.

7.1. Nasal routes: This section examines specific applications of mucoadhesive compounds with respect to nasal administration of small organic molecules, antibiotics, vaccines, DNA, proteins and other macromolecules.

7.1.1Antibiotic: Parenteral administration is still the only way that many antibiotics are now given. Mucoadhesive polymers have been used in a few recent studies to investigate the nasal route's potential for systemic antibiotic administration. Lim et al. developed and assessed mucoadhesive microspheres of hyaluronic acid and chitosan for nasal administration of gentamicin and other medications in a preliminary investigation.(Ugwoke et al. 2005).

7.1.2 Small organic molecule: The preferred medication for treating Parkinson's disease patients with on/off phenomenon is apomorphine. After being administered via nasal delivery, the compound's aqueous solution has a relative bioavailability of 45% and is absorbed rather effectively. Other small molecular weight drugs that have been characterized for nasal administration with mucoadhesive agents, in addition to apomorphine, are budesonide, caffeine, ketorolac, metoprolol, midazolam, morphine-6-glucoronate, nicotine, oxprenolol, oxymetazoline, and pentazocine.(Ugwoke et al. 2005).

7.1.3Vaccine and DNA: Pathogens enter the body through mucosal contact, which leads to pathogenic infections in disease states as influenza, pertussis, meningitis, measles, etc. Since neutralizing antibodies and particular cellular responses might occur at these locations of pathogen entry, these diseases make excellent candidates for nasal vaccination. Given the remarkable efficiency of the live polio vaccine when administered at birth, mucosal immunization may be safer and more effective in young children when maternal antibodies are present.(Ugwoke et al. 2005).

7.1.4 Proteins: It has been proposed that mucoadhesive polymers can increase the uptake of big molecules across the nasal mucosa and prolong their residence duration. According to Garcia et al., cyanocobalamin's bioavailability in rabbits was significantly increased by incorporating it into microcrystalline cellulose, dextran microspheres, and crospovidone as opposed to only using basic nasal solutions.

7.2 Buccal route: Many medications that have poor bioavailability and are quickly broken down when taken orally can benefit from oral mucoadhesive drug delivery, which has the advantages of low enzymatic activity and high accessibility. In the past, periodontal disorders were treated using hydrophilic polymers such as SCMC, HPC, and polycarbophil; however, the current tendency is to effectively exploit these systems for the delivery of peptides, proteins, and polysaccharides. A first-generation mucoadhesive paste called Orabase has been utilized as a barrier for oral ulcers. This is typically how buccostem, an adhesive antiemetic pill containing prochlorperazine, is delivered.(Tangri, Khurana, and Satheesh Madhav 2011).

7.3 Ocular route: Natamycin can be delivered using mucoadhesive drug delivery system to treat fungal eye infection. Palmitoyl-ethanolamide (PEA) are now a days delivered via mucoadhesive system to treat glaucoma. Ciprofloxacin is administered as PEGylated nano lipid as mucoadhesive carrier to treat bacterial conjunctivitis(Dave et al. 2021).

7.4 . Vaginal mucoadhesive drug delivery: Choi et al. created temperature-sensitive, mucoadhesive liquid suppositories with acetaminophen utilizing the mucoadhesive qualities of carboxyvinyl polymer and poloxamer, which are utilized to improve drug absorption. It was shown that HPMC mucoadhesive tablets were an appropriate method of administering benzydamine and a good substitute for conventional dosage forms for topical vaginal therapy.(Perioli et al. 2011). Clotrimazole (CT) which is an imidazole derivative having antifungal activity was also developed for treatment of human mycotic infections and plays an important role in antifungal chemotherapy.

7.5 Rectal route: It was also demonstrated that the tuberculous medication rifampicin was better absorbed when administered rectal via a mucoadhesive gel as opposed to oral solution and solid suppositories.

Table 1: Different types of mucoadhesive dosage forms and associated routes of administration:

Delivery route	Dosage forms				
	Tablets	Ointments	Gel	Patch	Film
Buccal	Theophylline, multiple polymers	Benzyl nicotinate, multiple polymers	Benzydamine, chitosan derivative	Miconazole, PVA/PVP	Femtanyl, PVP
Nasal	N/A	Mupirocin, glycerine ester	Insulin, starch	Insulin, chitosan/PGE	Chlorpromazine, chitosan/pectin
Ocular	Diclofenac, poly(acrylic) acid	Sulphadicramide, multiple polymers	Puerarin, poloxamer/ Carbopol	Ciprofloxacin, PVA/CMC	Fluorescein, HPMC
Vaginal	Metronidazole, chitosan	Terameprocol, white petroleum	Amphotericin, pluronic	ALA, PMVE/MA	SDS, multiple polymers
Rectal	Ramosetron, carbopol	Zinc oxide, petroleum	Quinine, HPMC	N/A	Theophylline, pHEMA

8. **Conclusion and future trends:** Since mucosal locations are easily accessible and have minimal enzymatic activity, they make an appealing non-invasive alternative for quick, regulated drug administration for both local and systemic application. To achieve the best possible therapeutic result, it is crucial to choose the right therapeutic agent, polymer, and drug carrier based on the pathophysiological state of the mucosa. A molecular weight of less than 400 to 500D, aqueous solubility of 1 mg/ml, a logP value in the range of 1 to 2, and a daily dose not to exceed 10 mg are the characteristics of an ideal medication candidate. The chemical makeup, surface tension, charge on the surface, molecular weight, rate of hydration, and concentration of polymers are important factors that influence how long drug delivery systems stay at the application site.

Now a days cationic, thiolated and pre-activated thiomers polymers are widely used in mucosal drug delivery system. Recent the use of nanocarriers in the mucosal drug delivery system indicated higher retention at the mucosal site, tuneable drug release behaviour and enhanced permeability for higher therapeutic outcomes. **Nanofibers** has been chosen as a special drug carrier in mucoadhesive drug delivery system due to its "unique structural and functional features". Along with superior biophysical property, nanofibers have ability to enhance the solubility of poorly soluble drug. Further electrospinning and electrospraying appear to be a versatile and simple electrostatic spinning technique capable to impart the nanofiber matrices with many desirable properties suitable for mucoadhesive systems. Degree of keratinization, mucosal thickness, low absorptive surface area, mucosal microbiome and mucosal secretion are the key challenges must be addressed for determining the acceptability of a mucosal site for optimum therapeutic response.

The effective design of innovative mucoadhesive drug delivery systems may benefit from this overview of mucoadhesive dosage forms. Mucoadhesive drug delivery systems offer a variety of uses, such as the creation of new mucoadhesive, device design, mucoadhesion processes, and improved penetration. Mucoadhesive drug delivery will become even more crucial in the delivery of these molecules as a result of the flood of new drug molecules brought out by drug discovery.

Referances:

[1]. Ahuja, Alka, Roop K. Khar, and Javed Ali. 1997. "Mucoadhesive Drug Delivery Systems." Drug Development and Industrial Pharmacy 23 (5): 489–515. https://doi.org/10.3109/03639049709148498.

[2]. Andrews, Gavin P., Thomas P. Laverty, and David S. Jones. 2009. "Mucoadhesive Polymeric Platforms for Controlled Drug Delivery." European Journal of Pharmaceutics and Biopharmaceutics 71 (3): 505–18. https://doi.org/10.1016/j.ejpb.2008.09.028.

[3]. Bhardwaj, Lovenish, Pramod Kumar Sharma, and Rishabha Malviya. 2011. "A Short Review on Gastroretentive Formulations for Stomach Specific Drug Delivery: Special Emphasis on Floating In Situ Gel Systems." African Journal of Basic and Applied Sciences 3 (6): 300–312.

[4]. Boddupalli, Bindu M., Zulkar N.K. Mohammed, Ravinder Nath A., and David Banji. 2010. "Mucoadhesive Drug Delivery System: An Overview." Journal of Advanced Pharmaceutical Technology and Research 1 (4): 381–87. https://doi.org/10.4103/0110-5558.76436.

[5]. Carvalho, Flávia Chiva, Marcos Luciano Bruschi, Raul Cesar Evangelista, and Maria Palmira Daflon Gremião. 2010. "Mucoadhesive Drug Delivery Systems." Brazilian Journal of Pharmaceutical Sciences 46 (1): 1–17. https://doi.org/10.1590/S1984-82502010000100002.

[6]. Dave, Ridhdhi S., Taylor C. Goostrey, Maya Ziolkowska, Sofia Czerny-Holownia, Todd Hoare, and Heather Sheardown. 2021. "Ocular Drug Delivery to the Anterior Segment Using Nanocarriers: A Mucoadhesive/Mucopenetrative Perspective." Journal of Controlled Release 336 (June): 71–88. https://doi.org/10.1016/j.jconrel.2021.06.011.

[7]. Davis, Stanley S, Stanley S Bob, Stanley S Davis, and Stanley S Davis. 2005. "Davis2005 (1)" 10 (4).

[8]. Hooda, Rakesh, Mohit Tripathi, and Kiran Kapoor. 2012. "A Review on Oral Mucosal Drug Delivery System." The Pharma Innovation 1 (1): 14–21. www.thepharmajournal.com.

[9]. Khanvilkar, Kavita, Maureen D. Donovan, and Douglas R. Flanagan. 2001. "Drug Transfer through Mucus." Advanced Drug Delivery Reviews 48 (2–3): 173–93. https://doi.org/10.1016/S0169-409X(01)00115-6.

[10]. Kharia, A. A., S. Hiremath, L. K. Omray, R. Yadav, and G. R. Godge. 2011. "Gastro Retentive Drug Delivery System." Indian Drugs 48 (5): 7–15.

[11]. Leitner, V. M., M. K. Marschütz, and A. Bernkop-Schnürch. 2003. "Mucoadhesive and Cohesive Properties of Poly(Acrylic Acid)-Cysteine Conjugates with Regard to Their Molecular Mass." European Journal of Pharmaceutical Sciences 18 (1): 89–96.

https://doi.org/10.1016/S0928-0987(02)00245-2.
[12]. Mukhopadhyay, Rohan, Subhajit Gain, Surajpal Verma, Bhupendra Singh, Manish Vyas, Meenu Mehta, and Anzarul Haque. 2018. "Polymers in Designing the Mucoadhesive Films: A Comprehensive Review." International Journal of Green Pharmacy 12 (2): S330–44.
[13]. Pant, Shailaja, Ashutosh Badola, and Preeti kothiyal Division. 2016. "Review Article A Review in Gastroretentive Drug Delivery System." Magazine.Pharmatutor.Org 4 (7): 29–40.
[14]. Perioli, Luana, Valeria Ambrogi, Cinzia Pagano, Elena Massetti, and Carlo Rossi. 2011. "New Solid Mucoadhesive Systems for Benzydamine Vaginal Administration." Colloids and Surfaces B: Biointerfaces 84 (2): 413–20. https://doi.org/10.1016/j.colsurfb.2011.01.035.
[15]. Salamat-Miller, Nazila, Montakarn Chittchang, and Thomas P. Johnston. 2005. "The Use of Mucoadhesive Polymers in Buccal Drug Delivery." Advanced Drug Delivery Reviews 57 (11): 1666–91. https://doi.org/10.1016/j.addr.2005.07.003.
[16]. Saraswathi, B., Anna Balaji, and M. S. Umashankar. 2013. "Polymers in Mucoadhesive Drug Delivery System-Latest Updates." International Journal of Pharmacy and Pharmaceutical Sciences 5 (SUPPL 3): 423–30.
[17]. Sarawade, Anupama, M P Ratnaparkhi, and Shilpa Chaudhari. 2014. "Available Online at Http // Www.Ijrdpl.Com Review Article FLOATING DRUG DELIVERY SYSTEM : An Overview" 3 (5): 1106–15.
[18]. Sedley, David. 2009. "Epicureanism in the Roman Republic." The Cambridge Companion to: Epicureanism 9780521873: 29–45. https://doi.org/10.1017/CCOL9780521873475.003.
[19]. Smart, John D. 2005. "The Basics and Underlying Mechanisms of Mucoadhesion." Advanced Drug Delivery Reviews 57 (11): 1556–68. https://doi.org/10.1016/j.addr.2005.07.001.
[20]. Strous, Ger J, and Jan Dekker. 1992. "Mucin-Type Glycoproteins" 27: 57–92.
[21]. Tangri, Pranshu, Shaffi Khurana, and N. V. Satheesh Madhav. 2011. "Mucoadhesive Drug Delivery: Mechanism and Methods of Evaluation." International Journal of Pharma and Bio Sciences 2 (1): 458–67.
[22]. Tripathi, Julu, Prakash Thapa, Ravi Maharjan, and Seong Hoon Jeong. 2019. "Current State and Future Perspectives on Gastroretentive Drug Delivery Systems." Pharmaceutics 11 (4). https://doi.org/10.3390/pharmaceutics11040193.
[23]. Ugwoke, Michael I., Remigius U. Agu, Norbert Verbeke, and Renaat Kinget. 2005. "Nasal Mucoadhesive Drug Delivery: Background, Applications, Trends and Future Perspectives." Advanced Drug Delivery Reviews 57 (11): 1640–65. https://doi.org/10.1016/j.addr.2005.07.009.
[24]. Vasir, Jaspreet Kaur, Kaustubh Tambwekar, and Sanjay Garg. 2003. "Bioadhesive Microspheres as a Controlled Drug Delivery System." International Journal of Pharmaceutics 255 (1–2): 13–32. https://doi.org/10.1016/S0378-5173(03)00087-5.

ScienceDirect

Nanostructured Drug Delivery Systems in Infectious Disease Treatment

2024, Pages 237-259

Chapter 11 - Nanomedicine in infectious disease challenges and regulatory concerns

Ushasi Das, Aditi Bala, Rahul Molla, Sanchita Mandal

Show more

https://doi.org/10.1016/B978-0-443-13337-4.00012-4 ↗

Get rights and content ↗

Abstract

Emerging infectious diseases are newly recognized diseases like COVID-19 or already existing diseases, including Ebola, chikungunya, avian flu, swine flu, Zika virus, and influenza, which have emerged in the last few decades, but their occurrences are rapidly increasing in some geographical range. These diseases have characteristics of emergence and re-emergence after specific time intervals due to the development of antimicrobial resistance, scarcity of target, termination of dormancy period, etc. To fight against these diseases modern scientific tools like theranostic delivery systems provide a good alternative to current treatment options which can deliver antimicrobial agents as well as diagnostic agents with the ability to target infectious microorganisms. The main problem that scientists face with infectious diseases during the development of new drugs is the lack of relevant predictive cellular or animal models of human diseases. In the last few decades, nanomaterials have emerged as a promising tool for theranostic applications attributed to their multifunctionality and unique nanometric architecture and are being explored in, the simultaneous, diagnosis and treatment of cancer, neurodegenerative disorders, cardiovascular diseases, and also in infectious diseases. Although, affordability, efficacy, reproducibility, and safety are the major concerns associated with nanotechnology-based medicines, i.e., nanomedicines, some bioinspired smartly engineered nanomaterials including functionalized dendrimers, carbon

nanotubes, nanoparticles (NPs), nanocrystals, quantum dots, liposomes, etc. are emerging as promising nanometric platform to be engineered smartly for various theranostic applications which could be extended to infectious diseases.

References (0)

Cited by (0)

SUPERCRITICAL FLUID TECHNOLOGY AND ITS APPLICATIONS IN PHARMACEUTICAL INDUSTRIES

by Aditi Bala, Sanchita Mandal*
Department of Pharmaceutical Technology, Jadavpur University.
188, Raja S.C. Mallick Rd, Kolkata 700032.

Abstract- A supercritical fluid (SCF) can be defined as a dense non condensable fluid. A fluid reaches the supercritical status when its temperature and pressure exceed the relevant critical temperature and pressure. At the critical point only, a single phase exist which has some properties typical of liquids (density) and some of gases (viscosity, compressibility, and mass diffusion coefficient). Supercritical fluid moves like a gas but dissolves things like a liquid. The critical temperature for a pure substance is the temperature above which gas cannot become liquid, regardless of applied pressure. For a pure substance the critical pressure is defined as the pressure above which liquid and gas cannot coexist at any temperature.

Supercritical fluid used in pharmaceuticals is mainly carbon di-oxide (CO_2) (used more than 98%) because of its low and easily accessible critical temperature (31.2◦ C) and pressure (7.4MPa), non-flammability, non-toxicity and inexpensiveness. This flexibility is enabling the use of SCFs for various applications in the food and pharmaceutical industries, with the drug delivery system design being a more recent addition. Solubility of materials in supercritical CO_2 can be done by few process such as rapid expansion of supercritical solution (RESS), gas anti-solvent (GAS), supercritical anti-solvent (SAS), and particle from a gas-saturated solution (PGSS).

Drug Deliver Using Supercritical Fluid Technology-

Micro Particles and Nanoparticles:

- Krukonis first used rapid expansion of supercritical fluid (RESS) to prepare 5 to 100 µm particles of an array of solutes including lovastatin, poly-hydroxy-acids, mevinolin and poly-(lactic acid) (PLA) particles of lovastatin and naproxen.
- A gas anti-solvent (GAS) process was used to produce clonidine-PLA micro particles.

RAPID EXPANSIONS OF SUPERCRITICAL SOLUTIONS

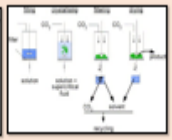

GAS ANTISOLVENT RECRYSTALIZATION

Liposomes:

- Fredereksen et al., developed a method for preparation of liposome's encapsulating a solution of FITC-dextran (hydrophilic) and using $SCCO_2$ as a solution for lipids.
- Using the SCFT process, critical fluid liposomes (CFL), encapsulating hydrophobic drugs, such as taxoids, camptothecins, doxorubicin, vincristine, and cisplatin, prepared.

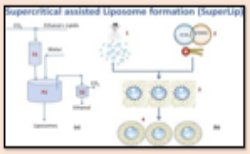

Supercritical assisted Liposome (Critical fluid Liposomes/CFL)

Solid Dispersion:

- SCF techniques are applied to prepare solvent-free solid dispersion dosage forms to enhance the solubility of poorly soluble compounds.
- A solid dispersion of carbamazepine in PEG4000 increased the rate and extent of dissolution of carbamazepine when prepared using SCFT.

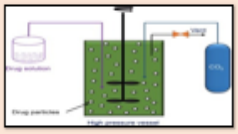

Solid Dispersion using SCFT

Coating:

- A novel SCF coating process has been developed to coat (single/multiple layer) solid particles (from 20nm to 100µm) with coating materials, such as lipids, biodegradable polyester, or polyanhydride polymers.
- An active substance (solid particle or an inert porous solid particle) can be coated and the coating is performed using a solution of a coating material in SCF, which is used at temperature and pressure conditions that do not solubilize the particles being coated.

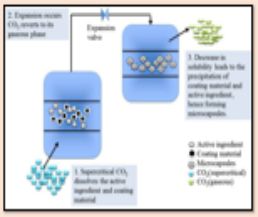

Coating of active particles using SCFT

Product Sterilization:

- It has been suggested that high-pressure CO2 exhibits microbicidal activity by penetrating into the microbes, thereby lowering their internal pH to a lethal level.

Powders of Macromolecules:

- Debenedetti et al used an antisolvent method to form micro particles of insulin and catalase. Protein solutions in hydroethanolic mixture (20:80) were allowed to enter a chamber concurrently with supercritical CO2. The SCF expanded and entrained the liquid solvent, precipitating sub micron protein particles.

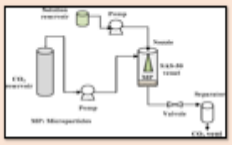

SUPERCRITICAL ANTISOLVENT METHOD

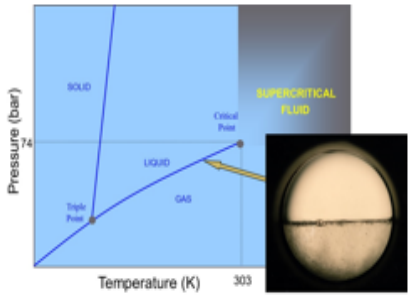

Advantages

- Solvent=CO2, leaves no traces
- No need for distillation step
- Do not alter taste/aroma/chemical composition of any products

Disadvantages

- High capital cost

Applications of Supercritical Fluid Technology in Pharmaceutical Industries-

Extraction and Purification: Supercritical fluid extraction technique are now widely used in industry as in caffeine production & isolation of Taxol from the bark of the Taxus brevifolia in which $SCCO_2$ is used. Purification via SCF technology gives a better alternative to all conventional purification methods as it is almost automated, quick, high yielding.

Media for Crystallization: SCF technology is used to generate high purity polymorphs size and shape of the polymorph can be manipulated by controlling temperature and/or pressure during processing while degree of crystallization can be improved by manipulating the rate of crystallization & high degree of crystallinity.

Extraction of Fermentation Broth: Supercritical carbon dioxide countercurrent column extraction is currently being investigated as a new process for the extraction of pharmaceutically active compounds from fermentation broths. This process offers an inexpensive method to extract and simultaneously fractionate compounds of interest without leaving organic solvent residues in the product.

Drug Extraction and Analysis: Supercritical fluid technology can be applied to extract drug from biological fluid sample for analysis as well. Sc-carbon dioxide is reported to be used to extract ibuprofen, indomethacin and flufenamic acid from plasma sample and analyzed using high performance liquid chromatography method. Apart from this, benzodiazepines are also reported to be separated from the dosage form matrix using supercritical fluid technology.

Other uses of Supercritical Fluid technology in pharmaceutical science are- Solubilizing products, medium for polymerization, as supercritical bio catalyst, micronization of products, separation of enantiomeric mixtures,

Conclusion- Supercritical fluid technology is considered an innovative and promising way to design drug delivery systems and/or to improve the formulation properties (like solubility) of many drug candidates.. Hence these technologies are expected to form a basis for the commercialization of many water-insoluble drugs in their solid-dispersion formulations in the near future.

References-

1. Frederiksen L, Anton K, Hoogevest PV, Keller HR, Leuenberger H. Preparation of liposomes encapsulating water-soluble compounds using supercritical carbon dioxide. Journal of pharmaceutical sciences. 1997 Aug;86(8):921-8.
2. Tom JW, Debenedetti PG. Particle formation with supercritical fluids—a review. Journal of Aerosol Science. 1991 Jan 1;22(5):555-84.
3. McHugh M, Krukonis V. Supercritical fluid extraction: principles and practice. Elsevier; 2013 Oct 22.
4. Wakure BS, Yadav AV, Bhatia NM, Salunke MA. Supercritical fluid technology: Nascent contrivance for pharmaceutical product development. International Journal of Pharmaceutical Sciences and Research. 2012 Jul 1;3(7):1872.
5. Thakkar FM, Soni TG, Gohel MC, Gandhi TR. Supercritical fluid technology: a promising approach to enhance the drug solubility. Journal of pharmaceutical sciences and research. 2009 Dec 1;1(4):1.

techno india university
WEST BENGAL

Certificate of Participation

A National Seminar on
"Current scenario of Pharmaceutical Technology: Academia to Industry"

This is to certify that

Prof./Dr./Mr./Ms. Aditi Bala. *from* Jadavpur University. ~~*has participated*~~ / *presented a paper in* ~~*the oral*~~ / *poster session at the National Seminar on "Current Scenario of Pharmaceutical Technology: Academia to Industry" organized by School of Pharmacy, Techno India University, West Bengal, India on 20th September 2023*

PROF. (DR.) BEDUIN MAHANTI, DIRECTOR, SCHOOL OF PHARMACY, TIU, WB	DR. LABONI DAS, CONVENOR, SCHOOL OF PHARMACY, TIU, WB	DR. SHREYASI CHAKRABORTY, CO-CONVENOR, SCHOOL OF PHARMACY, TIU, WB